ANALYTICAL STUDY
OF FLOW THROUGH
COMPRESSIBLE POROUS MEDIA

A Thesis

Presented to

the Faculty of the Department of Chemical Engineering

the University of Houston

In Partial Fulfillment

of the Requirements for the Degree

Master of Science in Chemical Engineering

by

Harrison Raymond Cooper

August 1958

ACKNOWLEDGEMENT

I wish to acknowledge the generous assistance and advice given me by my advisory committee, particularly Dean F. M. Tiller and Professor J. R. Crump.

I also wish to express my appreciation to the Alcoa Foundation for their support of the graduate program in the Department of Chemical Engineering of the University of Houston. As the first recipient of the Alcoa Fellowhip during the school year of 1956-1957, I am particularly greatful for the opportunity it gave me to continue graduate studies and research leading to this thesis.

TABLE OF CONTENTS

LIST OF TABLES

LIST OF FIGURES

CHAPTER I

THE PROBLEM

I. BASIS OF THE THEORY OF FILTRATION

Fundamental understanding of filtration is based on the theory of flow through porous media. Solids are separated from liquid suspensions with formation of porous filter cakes. Liquid flows through the cake during filtration and the filter cake is treated as a porous medium. Filter cakes consist of packed beds of solid particles whose interstices are filled with liquid. In general the porous structure of the cake is not stable but decreases in void volume due to mechanical pressure or stress generated by frictional flow of fluid through the cake. Materials exhibiting the property of continuous decrease in relative moisture content or porosity during the course of filtration are referred to as compressible. Analysis of flow through filter cakes is more complicated than treatment of flow in stable porous media because of changing mass and compressibility of cakes during filtration.

II. STATEMENT OF THE PROBLEM

Theoretical developments in filtration up to the present have not taken into account variation in moisture content of the cake due to compression. In constant pressure filtration, calculations are frequently performed assuming negligible medium resistance in addition to constant average porosity or void volume of filter cakes. These assumptions become less valid when conditions are met (a) pressure driving force of filtration becomes lower, (b) time cycles become shorter, (c) solids being filtered form cakes of greater compressibility, and (d) slurries become more concentrated. Rotary drum vacuum filtration is a widely applied method of filtration in which the described operating conditions are frequently encountered. Examination of the effect of assuming negligible medium resistance and constant porosity has never been reported in the literature for calculation of rotary drum filtration rates.

Cake pressure drop in constant pressure filtration increases from zero initially to a maximum value as a result of gradually decreasing pressure drop across the filter medium. As cake pressure drop increases, specific resistance of solids in compressible cakes also increases. The effect of solids resistance increase during constant pressure filtration has never been examined in analysis of filtrate flow rates. Compression of the solids also results in decreased cross sectional area for liquid flow with decreasing void volume or porosity. Augmentation of the volume of liquid flowing results. Calculation of rates have previously been based on assumed constant superficial liquid velocity at each instant throughout the cake cross section.

Point porosity in a filter cake varies from a maximum at the cake surface to a minimum at the medium resulting from pressure gradients due to flow of fluid through the cake. Liquid flow rate variation through a cake is dependent on the time rate of change of porosity variation at each point in the cake thickness. Experimental data in the literature have led to conflicting conclusions as to the manner in which porosity varies vs. distance from the cake surface. Examination of the factors determining porosity distribution is of interest in study of variable flow rates through filter cakes.

It has been found that treatment of filtration processes based on fundamental theory is hampered by lack of knowledge of cake properties at the interface of the cake and slurry. Evaluation of permeability of cake solids at a given pressure differential from data obtained from compression-permeability cell measurement requires extrapolation of point data taken at pressures above a minimum of one pound per square inch to zero pressure. No fundamental principle exists from which to infer the proper method for extrapolation. Because the mathematical form of the quantity in which the extrapolated values are used is a reciprocal term and the specific resistance of solids generally approaches a low magnitude as pressure becomes low, large differences in calculated results arise with use of different methods of extrapolation. A solution to the problem of evaluating surface characteristics is needed to obtain dependable prediction of rates by mathematical means.

III. SUMMARY OF CONCLUSIONS

The analytical study forming the basis of this thesis in investigating problems introduced in the previous discussion resulted in contributions to the theoretical understanding of filtration processes as described in the following outline.

Increase in Flow Rate of Liquid from Surface to Medium in Compressible Filter Cakes A partial differential equation of second degree with variable coefficients determined from compression-permeability cell measurements was derived for describing the filtration process for the general case of variable filtrate flow rate through a filter cake. The filtrate rate was eliminated as a variable in the equation with pressure being the dependent variable; time and distance or cake mass are independent variables. Boundary conditions were not established as a basis for solution of the equation. Variable flow rate of filtrate in the cake becomes a significant factor in determining filtration rates for concentrated slurries of compressible materials as is demonstrated by an illustrative calculation for filtrate volume vs. time for the extreme cases of flow into the cake from the surface and flow out of the cake at the medium. As the liquid fraction of the slurry decreases liquid flow rates at the surface layer of solids become small in comparison to the flow rates through the most compressed solids at the filter medium.

Constant Pressure Filtration of Concentrated Slurries Calculation procedures utilizing numerical methods were established to determine the effect of variable cake moisture and finite medium resistance on constant pressure rate predictions. It is shown that the effect of these two factors on filtration calculations are greatest when filtrations of concentrated compressible slurries are conducted over short time intervals at low pressure differentials. The conventional method used in analysis of constant pressure filtration data for determining resistance of the filter medium is demonstrated to be subject to error due to the effect of changing cake porosity in filtration of compressible materials.

Rotary Drum Filtration The methods for numerical evaluation of filtration rates based on the more rigorous procedure taking into consideration resistance and variability of cake moisture were applied to conditions of rotary drum filtration. In vacuum filtration the pressure differential due to the static head of slurry above the submerged drum surface is often a significant portion of the total pressure driving force, varying from zero initially as the drum enters the slurry to a maximum value and decreasing to zero as the drum emerges. The expression for rotary drum filtration rates with variable pressure due to static head was solved by trial and error approximation.

Porosity Variation Through Filter Cakes Numerical procedures using compression-permeability cell data were devised to plot the porosity of solids as a function of distance from the filter cake surface. It was determined that porosity vs. distance curves could assume various shapes as the porosity decreases from a maximum value at the cake surface to a minimum value at the filter medium. This is in contradiction to a recently published hypothesis which was supported by experimental data.[35] Numerical differentiation of experimental compression-permeability cell data for eleven materials was carried out to demonstrate that porosity gradients could be steepest at either surface or medium; and that the direction of the porosity-distance slope could change within the cake. The gradients predicted by this analysis were substantiated by calculated porosity-distance curves for several materials.

Porosity and Specific Resistance at Surface of Filter Cakes

Experimental approaches are suggested for determining values of porosity and specific resistance of surface layers of solids in filter cakes, knowledge of these properties being required to guide extrapolation of compression-permeability cell data to zero pressure for numerical evaluation of filtration rates according to the fundamental equation of filtration. It is hoped that experimental work will lead to a theoretical basis for predicting surface characteristics of filter cakes.

CHAPTER II

THE THEORY OF FILTRATION

Filtration is a process of mechanical separation of solids from a suspension, the process being carried out by forcing the suspension through a porous barrier. In filtration the solid may be deposited either on the surface or in the porous interior of the barrier. The fluid in which the solids are suspended can be either liquid or gas.

The mathematical treatment of gas filtration is complicated by changes in gas density with pressure variations occurring across the barrier and accumulated solids. The following discussion of the theory of filtration will be based on incompressible liquid suspensions.

In liquid filtration terminology, the porous barrier is called the medium or septum and the accumulation of solid is known as filter cake. Liquid from the suspension, or slurry, which passes through the cake and medium is termed filtrate.

I. INTRODUCTION

Methods of solid-liquid separation other than filtration having wide application are settling, thickening, centrifuging, and dewatering. Often a combination of these techniques is utilized when a separation is required in a process application. Economic factors based on recovery and throughput rates, equipment size and cost, and properties of the suspension determine which method or combination of methods is usable in a given process. Settling and thickening are considered particularly applicable when solid particles can be induced to settle rapidly out of the suspension by gravity. Dewatering is utilized when solids are free filtering, which usually is true with particles of large size.

Centrifugal equipment is employed in filtration and dewatering applications to achieve separation by means of induced centrifugal forces obtained through rapid spinning of a charge of slurry. The acceleration being directed toward the center of rotation, the more dense solids will be withdrawn and deposited on a collector placed in the centrifuge near the periphery of rotation. If the collector is made porous as in a suspended basket centrifuge, liquids will in turn pass through the solid cake and be conducted out of the equipment. In principle, the action of the centrifuge can be looked upon as gravity separation in a greatly magnified gravitational field.

Filtration is applied to separation problems when the particles in suspension are too fine to obtain rapid separation by gravity settling. Most filtration applications are distinguished by the use of external pressure to increase the rate of filtrate flow above that which would flow by gravity through the cake. Augmented pressure is necessary because cakes consisting of very fine particles usually offer considerable resistance to fluid flow in comparison to beds of free filtering materials. In some applications settling or thickening is used to obtain a concentrated slurry which then is filtered to separate remaining excess liquid.

When small amounts of fine solids (concentrations of 0.1% solids or less by weight) are suspended in a liquid, the filtration process removing the fines is often called clarification. Removal of fine solids by filtration usually results in plugging of filter media because fine particles reduce medium permeability by obstructing small interior pores. Clarification of dilute suspensions can be accomplished by filtering the slurry through a coating of permeable solids in a technique known as precoat filtration. The usual precoat materials, diatomaceous earths and cellulose pulps, ward off permanent damage to medium.[12] Provision can be made for renewing or replacing the precoat surface when its resistance increases because of accumulations of fines on or near the surface. In rotary drum filtrations using precoat techniques an advancing knife blade called a doctor blade is installed for scraping a thin slice of precoat material from the drum surface continuously as the drum revolves.[2] When fines are in low enough concentration advantages similar to that obtained in precoat filtration for clarifying liquid streams may be obtained by introducing materials called filter aids into the suspension before filtration. Filter aids provide a means to adsorb small particles in the suspension as well as improving the permeability of the filter cake. Fine solids adhere to the filter aid particles and filtration can be carried out at higher rates with less difficulty with medium blinding. Activated carbons in addition to the usual precoat materials, pulp and diatomaceous earth, are utilized as filter aids. Precoats and filter aids are usually employed only when the eliminated solid material is waste because of expense of further separation that would be necessary. A special process in which mixture of filter aid with separated solids has been used to advantage is filtration of metallurgical slimes using fine carbon which later acts as a reducing agent in smelting for metal recovery.

Filtration rates for suspensions of solids that are too concentrated for practical use of precoat methods are improved in many instances through use of additives which coagulate particles into form which results in more permeable cakes. Materials having the property to decrease cake resistance by altering characteristics of solids by addition to the slurry are called coagulants or flocculants.

The mechanical design of equipment for filtration is a problem dependent upon the process flow sheet as well as consideration of filteration characteristics of the slurry. Description of equipment design details and suitability are reviewed thoroughly in the literature.[7, 15, 23] Depending upon whether the process calls for continuous or batch operation, commercial designs of equipment are offered which permit a range of possible operating pressures and mechanical handling features. Rotary drum, rotary disc, rotary pan, and belt filters are examples of continuous equipment of different basic design. Commonly used types of batch filters are plate and frame presses, pressure leaf, enclosed revolving disc, and cartridge filters, each of which have design characteristics directed toward advantageous use in applications where such requirements as efficient washing, low operating labor, or ease of cleaning are needed.

Filtration characteristics of materials being processed also influence selection of filter design. Under ideal circumstances flow rates of liquid across a cake are proportional to pressure drop across the cake. However most materials have the property of becoming less permeable per unit mass of solids as pressure drop increases due to compression or increase in particle packing in the cake. Almost all materials exhibit compressible effects to some extent and increased pressures do not increase flow rates in proportion. Highly compressible materials may show very little increase in filtration rates with large increases in pressure in filtrations carried out at a constant pressure differential. Examination of cake permeability provides a basis for deciding whether optimum economic operation is obtained by high or low pressure filtration equipment.

The selection of filter media requires skillful judgement because of mechanical and operational design factors of high sensitivity.[56] The mechanism of filter media operation has been closely studied in order to develop fundamental criteria to be used in selecting the most applicable medium material for a given filtration problem.[19,26,27] Studies of dilute slurry filtration indicate that particles are trapped in pores or interstices throughout the interior of the medium during initial stages of filtration.[26,30] Fines sometimes pass through a new or porous medium during the first few moments of use resulting in cloudy filtrates. Eventually pore entries at the surface of the medium are bridged by particles piling up; filtration then takes place at the surface of the medium with the beginning of cake formation.

A medium exposed frequently to operation during which fines are allowed to reach its interior will become plugged (blinded). Greatly increased flow resistance is an indication of medium blinding and is the principal factor necessitating replacement of media.

A filter medium is chosen on a basis of such factors as retentiveness for the finest particles present in a given slurry, resistance to deterioration, tenacity with which cake is held, cost, tendency to plug, and strength. Media are often obtained from textile stocks developed originally for other uses; but woven wire, matted felt, plastic felt, monofilament plastic based textiles, and porous stainless steel are examples of materials developed specifically for filtration.[56] Special fabrics woven from polyethylene, polyvinylidene chloride, fluoroethylene plastic fibers, etc., have been employed to advantage in corrosive systems. In considering woven textiles for use as media, size of filaments or fibers, number of strands in a yarn (or denier), tightness of weave, and nature of twist in the weave are important variables influencing the rate of filtrate flow and retention properties. Studies indicate that in media based on textile stocks, a major proportion of filtrate is forced through the yarn itself during the course of filtration.[26] This factor tends to limit the tightness to which yarns in textile media can be twisted to yield desirable filtration rates.

Logical choice from available equipment designs and filter media styles can be made from examination of the process problem and general slurry characteristics. The principle engineering problem associated with filter specification is concerned with determining filter area requirements by referring to calculated or experimental rate data. Data on filtration rates are often difficult to obtain reproducibly and accurately in laboratory tests and pilot plant runs. Filter cake permeability, the rate determining factor, is dependent on physical properties such as effect of electrolytes on particle surfaces and other characteristics which have not been fully explained theoretically. These phenomena affect slurry properties in such a way as to cause wide variation in observed data on filtration rates in many applications.

Three main sources of filtration rate data are available: data from full-scale equipment tests, from scaled-down pilot plant or laboratory equipment, and from studies made on fundamental properties of the suspensions and solids. The objective of filtration theory is to ultimately develop methods for analysis of data to make it possible to proceed in filtration design from fundamental quantities. Progress made in theoretical analysis of filtration indicate areas of mathematical and technical inquiry which will lead to greater fundamental understanding.

II. ANALYSIS OF FILTRATION PROCESSES

Examination of the basic manner in which filtration is effected is necessary as a prelude to mathematical analysis. Classification of filtration processes can be made according to the method of supplying slurry to the filter. Essentially there are three distinct methods for providing feed: (1) operation under conditions of constant pressure, (2) constant rate of feed, and (3) slurry feed rate and filtration pressure both varying. All filtration methods, both batch and continuous, can be shown to operate by one of these processes.

Batch operation with slurry supplied from a tank under constant pressure to a filter press is an example of constant pressure filtration. Constant pressure conditions are approximated in continuous rotary drum and rotary disc operations when the change in static head of slurry on the filter surface is neglected.

Constant rate filtrations result most often when feed arrangements are utilized having slurry supplied with reciprocating and diaphram type pumps. This type of filtration is always batchwise in nature. Back pressure against the pump increases steadily as resistance to flow builds up during deposition of cake. The filtration cycle is completed when pressure drop across the cake and septum reaches some limiting value.

Rotary vacuum filtration is a constant rate operation from throughput standpoint as slurry feed rate is constant at steady state with constant withdrawal of filtrate and discharge of cake. Calculation treatment is based on individual segments of the rotary element with pressure an independent variable in deriving the rate equations. Continuous filters operate in repeating cycles by means of regular travel of filter elements through mechanical movements. A series of operations may be performed in addition to the solids-liquid separation step. Provision for cake washing, drying, and reslurrying may be made in the cycle for processes requiring these operations.

The most common method for supplying slurry to batch filtrations is by means of centrifugal pumps. The centrifugal pump is characterized by high output rates at low back pressures and a decreasing rate as head increases. Consequently filtration with centrifugal pump feed results in operation under variable rate and pressure conditions, the slurry rate depending upon the pressure buildup across the filter and the characteristic performance curve of the pump. Constant rate conditions may be approximated if the pump output curve is flat over a considerable pressure range or output does not vary much over a wide range of pressure. The impeller housing design of the pump controls the performance characteristics. A pump should not have large excess capacity for the size of filter in a particular application because slurries often become more difficult to filter after being subjected to violent agitation in the impeller housing due to flocculant breakdown and particle dispersion.

Figure (1) illustrates three continuous filter designs, rotary disc, rotary drum, and rotary pan filters. Another type is an endless belt filter similar in operation to the drum. Pressure differential acting as a driving force for filtrate flow is usually obtained by maintaining a vacuum in the filtrate reservoir. This vacuum is usually held constant, but the static head of slurry at different points in the cycle is variable causing the filtration pressure for a given segment of filter surface to vary as it moves through the cycle. Although computational methods can be used to account for variation in total filtration pressure for these types of filters, the effect of which can be significant when operating under low pressure differentials with large size equipment, most calculations for rotary continuous filtrations have been simplified by assuming an average constant pressure. The few authors treating rotary filtration in the literature have neglected the effect of variable head.[43,52,55]

Precoat rotary filtration is a technique for clarification of dilute suspensions in which a layer of porous material on a drum filter is the filtering medium. Rotary precoat filtration is continuous except for intermittent periods to replace the precoat. Flow in precoat filter operation may gradually change in rate with time because of reduction in precoat thickness as the surface is renewed changes the total resistance of the cake. Flow of filtrate per cycle is usually minimum at the moment a new precoat is put into use and maximum when the coat is cut away to its thinnest point. This applies if the knife cut is deep enough to completely shave off the section of precoat containing penetrated solids.[2] Precoat operations most generally employ vacuum although precoat rotary drum filtration using positive pressure in a flanged enclosure has been described.[21]

Line filters taking a small slip stream from a continuous process stream such as an oil filter may operate essentially at constant pressure if the flow through the line filter is small compared to the flow volume in the total process. Line filters are often used in clarifying or polishing service. The solids being removed in the filter are usually in low concentration in the stream and the operation of the filter often encompasses a mixture of cake filtration and medium filtration.

Filtration performance is analyzed by examination of phenomena taking place during deposit of solids to form a cake and subsequent flow of filtrate through the porous solids. Filtration is initiated with separated solids being retained on the medium following bulk flow of filtrate through the filter. Continued flow of filtrate results in the filter cake surface becoming the retaining medium with the additional solids accumulation building up the cake thickness with filtrate passing through tortuous passages between the deposited particles in the cake. For given pressure drop across the cake and medium, the rate of filtrate flow out of the cake will be dependent upon the difficulty attendant to flow through the cake and resistance to flow through the cake pores.

The factors responsible for flow resistance of the cake, according to hydrodynamic principles, are size and tortuosity of passages between particles and the amount of solid surface exposed to shear stress generation by flowing fluid. Therefore pressure drop is a function of liquid shear stress and geometry of the solid structure. Filter cakes deposited from slurries containing particles of widely distributed sizes and shapes have complex internal geometrical arrangements, and cake structure is not well understood. An appraisal of cake structure can be made by measurement of porosity, volume voids per volume of cake, and particle size distribution. Filter cake porosities vary over a considerable range, values having been reported as high as 0.98 by Grace for silica fines and as low as the range of 0.3 for mixtures of fine and coarse sands.[11,24]

In many practical filtrations of fine solids, the space between solid particles will be ordinarily quite small, on the order of microns (one micron = one-millionth of a centimeter). Flow through the cake is restricted because of friction in the liquid contacting the solids. The physical theory describing flow of viscous fluids attests to the existence of two systems of flow, laminar and turbulent. Laminar flow occurs when the flow pattern is regular and energy is not dissipated because of rapid changes in direction of superimposed flow patterns, or eddies, this latter regime of flow being turbulent. It has been determined from experimental data taken in pipeline flow that pressure drop is directly proportional to viscosity to the first power when laminar flow is taking place whereas during turbulent flow pressure drop is proportional to viscosity to a power less than one. Dimensional analysis has been used to develop a means of correlating friction loss in hydraulic flow by means of the Reynolds number-friction factor relationship. A sharp break occurs in a plot of friction factor vs. Reynolds number in data taken during pipeline flow in the region of Reynolds number magnitudes at which flow is observed to become turbulent. Flow through a filter cake can be examined from the Reynolds number standpoint. Consider flow of water at a rate of one gallon per minute per square foot at 70°F. through a cake of 0.50 porosity. Calculation of Reynolds number for flow in the cake cross section can be performed by considering all interstices having circular cross-section as an approximation. Velocity through the cake, taken as equal in each pore is

$$q = \left(\frac{\text{one gallon per minute}}{\text{one square foot}}\right)\left(\frac{\text{60 min. per hr.}}{\text{7.48 gal. per sq. ft.}}\right)\left(\frac{\text{1 vol.}}{\text{0.50 voids}}\right)$$

$$= 16.1 \text{ ft./hr.}$$

For particles of one micron in diameter and a packing in which the area for flow is equal to that for cubic arrangement (see page 30)

$$A = \frac{\pi}{4}D^2 = 1 - \frac{\pi}{4}$$

From this an equivalent diameter of 1.8 (10^{-8}) feet is calculated. Substituting into the Reynolds number equation in consistent units yields

$$Re = \frac{D\ U\ \rho}{\mu} = \frac{(1.8)\ (10^{-8})\ (16.1)\ (62.4)}{(2.42)} = 7.45\ (10^{-6})$$

This simplified analysis indicates the extremely low magnitude of Reynolds number that is calculated by assuming flow passages to be equal sized circular capillaries. On this basis it would not be surprising if flow through a filter cake composed of fine solids were always laminar.

Precise definition of the flow patterns taking place in filter cakes is difficult because of the irregular nature of the small passages in the cake with constant contractions, expansions, and reversals. Experimental evidence indicates Newton's law for viscous shear stress is obeyed in flow through beds of fine particles because pressure drop becomes directly proportional to viscosity to the first power. Shear stress over the surface area in the cake is a linear function of the velocity gradient of filtrate flowing through the cake pores following

Newton's law. Viscosity, the proportionality constant in the mathematical definition of ideal viscous flow

$$\text{shear stress} = \mu \frac{du}{dy}$$

$$\text{velocity gradient} = \frac{du}{dy}$$

will be assumed constant in all flow patterns throughout the cake based on the previous discussion of experimental work. Pressure drop through a filter cake resulting from frictional losses will therefore be proportional to viscosity of the filtrate and length of the flow path.

It has been observed that many filter cakes tend to compress or increase in apparent density under the effect of changing pressure, especially when particles in the cake are very fine. In view of this, it has become the practice to express resistance of the cake in terms of the mass of solids per unit area in the cake. The term for cake resistance per unit mass per unit area is specific resistance. Compression of the filter cake reduces its void volume or porosity and this increases resistance to flow through the cake since less pore volume is available for flow. The criterion for compressibility is observed increase in specific resistance with pressure by analysis of experimental filtration data. When resistance to flow expressed in terms of cake mass is constant, the cake is regarded as incompressible. More detailed analysis of these phenomena is brought out in development of the theory of resistance to flow in porous structures.

In Figure (2) a typical filter cake is represented. The pressure drop across the filter consists of the sum of pressure drop across the

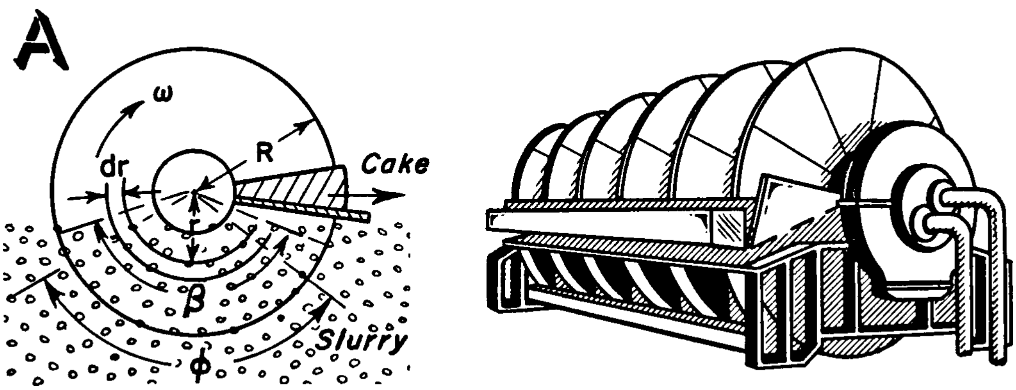

ROTARY DISC FILTER

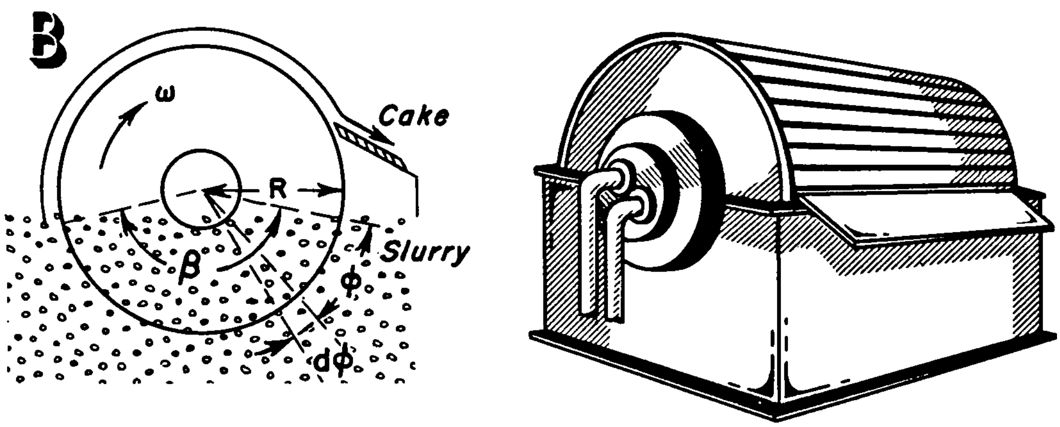

ROTARY DRUM FILTER

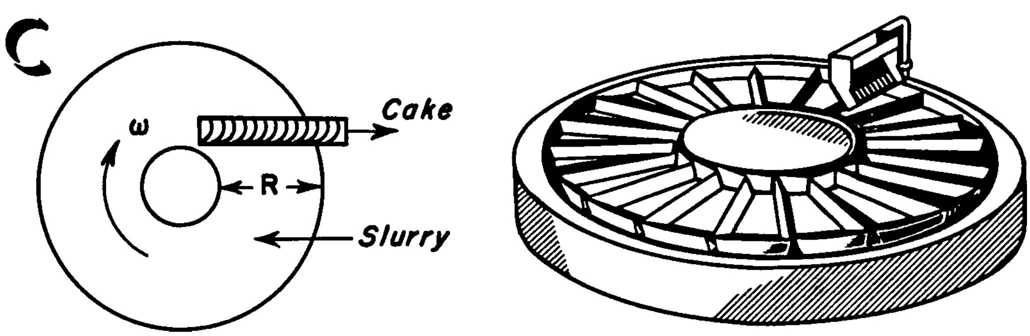

ROTARY PAN FILTER

FIGURE 1
CONTINUOUS ROTARY FILTERS

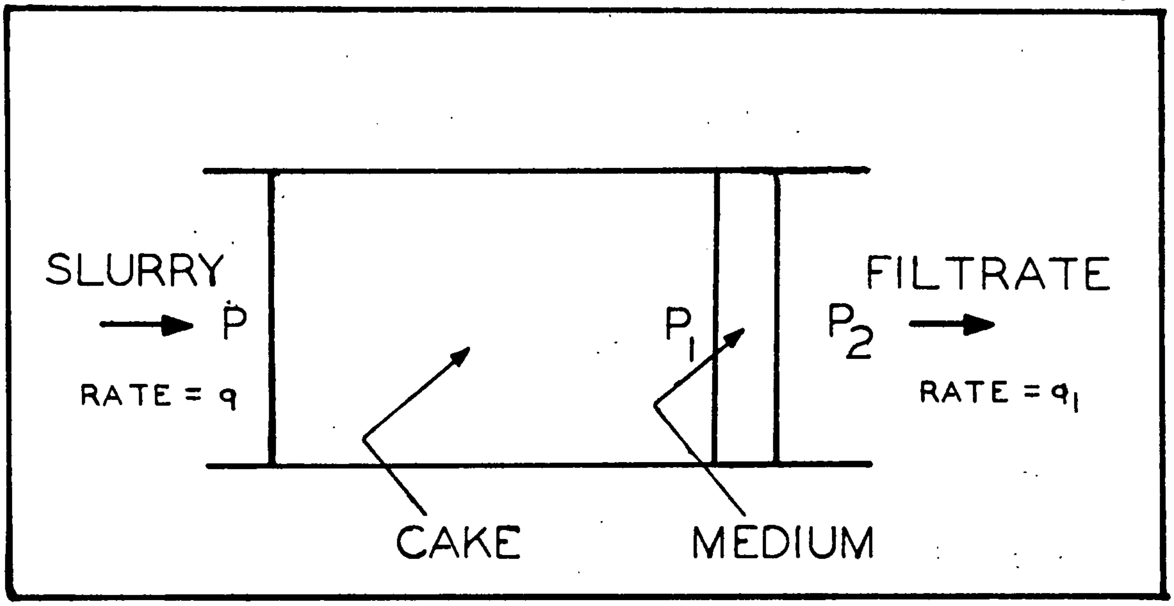

FIGURE 2.

FILTER CAKE

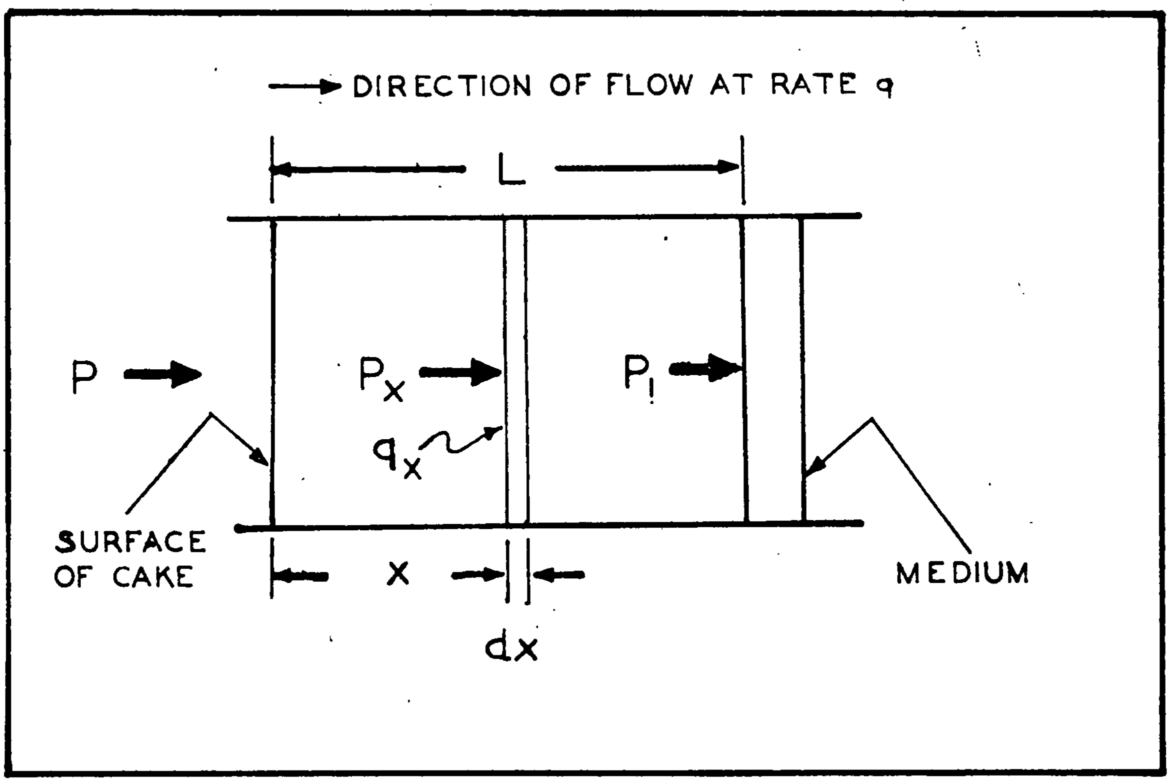

FIGURE 3.

FILTER CAKE REPRESENTED AS CONTINUOUS MEDIUM cake, $(p - p_1)$, and pressure drop across the filter medium, $(p_1 - p_2)$. Since uniform laminar flow is assumed, pressure drop through the cake is proportional to fluid viscosity and velocity of flow in a cake of given mass

$$- \Delta p = p - p_1 \propto \alpha\, q\, \mu \qquad (1)$$

The proportionality of Equation (1) becomes an equality with the insertion of a constant of proportionality per unit mass, α, and cake, w

$$- g_c \Delta p = \alpha\, q\, \mu\, w \qquad (2)$$

In English units, the constant of proportionality, α, has the dimensions (pressure drop, lbf.)/(unit mass of cake, lbm.)(unit viscosity)(unit flow rate, ft./sec.) reducing to ft./lbm. Since cake masses are usually given in pounds (engineering units), to obtain pressure drop in consistent force units it is necessary to multiply by the force proportionality constant, g_c, as indicated in Equation (2). Note that the negative sign indicates flow in direction of decrease in pressure.

The simplified expression given in Equation (2) is valid only when cakes are incompressible, or porosity does not change with pressure to a measurable extent. The more general case is represented by the differential equation given in Equation (3). Referring to Figure (3), in a differential thickness dx the cake, of over-all length L from surface to medium, filtrate hydraulic pressure is reduced by the differential amount dp_x for filtrate flow rate q. By analogy to Equation (2), the pressure drop dp_x is given by

$$-g_c \frac{dp_x}{dw_x} = \mu\, \alpha_x\, q \qquad (3)$$

with α_x corresponding to the resistance per unit mass of mass dw in the thickness dx. The constant α is called specific or filtration resistance. Equation (3) is basic to all filtration theory and has come to be known as the fundamental equation of filtration. At present values of α are only known empirically.

The quantity dp_x in Equation (3) referred to pressure drop in the thickness of cake dx in which cake dimensions and mass are related by

$$dw_x = \rho_s(1 - \theta_x)dx \qquad (4)$$

where ρ_s is true solid density and θ_x represents porosity of the cake in the thickness dx. The fundamental equation in terms of cake differential thickness is then

$$-g_c \frac{dp_x}{dx} = \mu\, \alpha_x(1 - \theta_x)\rho_s\, q \qquad (5)$$

Integration of this expression can be carried out by integrating dp_x between the limits of operating pressure at the cake surface and the pressure p_1 between the cake and medium, the cake length corresponding to these limits being L shown by Figure (3). Similarly in Equation (3), cake mass is integrated between zero and w, the total cake mass. When compressible materials are being filtered and specific resistance and porosity are variable with pressure, analytical integration is not usually possible.

To analyze behavior of filter cakes under the effect of pressure stress, examination is made of hydraulic pressure drop resulting from frictional drag. Curve A in Figure (4) indicates variation of hydraulic pressure in a filter cake. Pressure drop is dp_x in the differential thickness dx following the derivation of the fundamental equation. As this pressure drop represents a change in a force, a counterforce must also exist in this differential thickness, because if a force unbalance occurs Newton's second law of mechanics requires that an acceleration of mass take place. The counterforce per unit area distributed over a surface in which a hydraulic pressure is acting is defined as solids pressure. By definition solids pressure is opposite in vectorial sign to hydraulic pressure, and a differential decrease in hydraulic pressure is equal in magnitude to a differential increase in solids pressure in absence of cake acceleration and for constant superficial filtrate velocity q through the cake. It can be shown that filtrate flow rate variation dq/dx occurs in a cake cross section for compressible materials but the acceleration effect due to changing flow is negligible.

Solids pressure results from accumulation of forces resulting from shear stress over particle surface in contact with flowing fluid. Force is transmitted through the cake through contact between solids particles. Reaction force is zero at the cake surface and increases to a maximum at the filter medium. The physical implication of this force system is illustrated in Figure (5) based on a model devised to describe solids pressure. In Figure (5) p_{x1} represents hydraulic pressure upstream and p_{x2} hydraulic pressure downstream. F_1 denotes reaction force upstream and F_2 reaction force downstream. A balance of forces acting on the particles based on these definitions is

$$F_2 + p_{x2}aA = F_1 + p_{x1}aA \qquad (6)$$

where A is the projected area of the cake cross section associated with the particle as shown in Figure (5) and a is the fraction of the projected area over which solids are in mass contact, liquid not penetrating the area aA. By the definition of a its value for point contact is unity. Reducing Equation (6) to differential form by assuming a system in which particles are infinitely small

$$dF + aA\,dp_x = 0 \tag{7}$$

For point contact between particles, Equation (7) reduces to

$$dF + A dp_x = 0$$

It is not possible to assign a functional relationship to a to obtain values of true solids pressure which would be given by

$$dp_s = \frac{dF}{aA} \tag{8}$$

The magnitude of a probably decreases from close at unity at the cake surface to a msaller value at the medium. If a were unity, the area of solid contact would approach zero and the stress at contact would be a large value. Instead solids pressure is substituted by the expression

$$\frac{dF}{A} = dp_s \tag{8a}$$

or solids pressure is taken as the distributed reaction force over an entire area. By this expression a piston acting on a mass of filter cake in a porous cylindrical cup would be opposed by solids pressure of magnitude

$$p_s = \frac{F}{A}$$

where F is the force exerted by the piston and A is cross sectional area of the cylinder.

The relationship of solids pressure and hydraulic pressure is

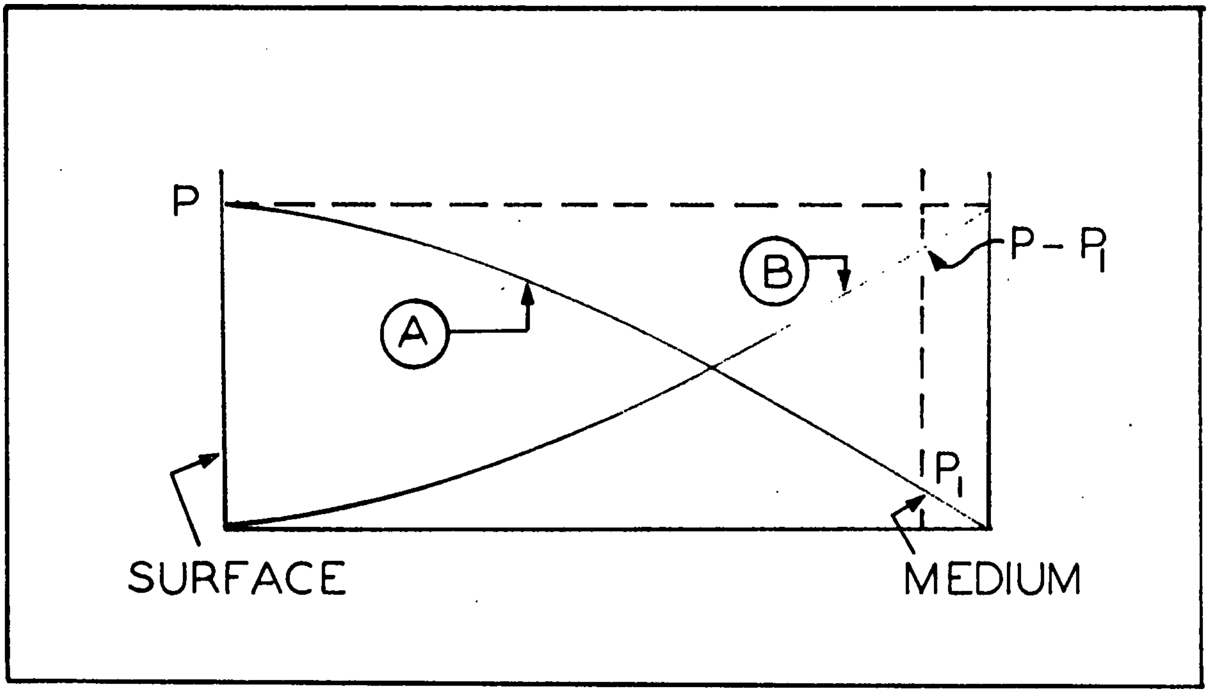

FIGURE 4.

SCHEMATIC DISTRIBUTION OF PRESSURE IN FILTER CAKE

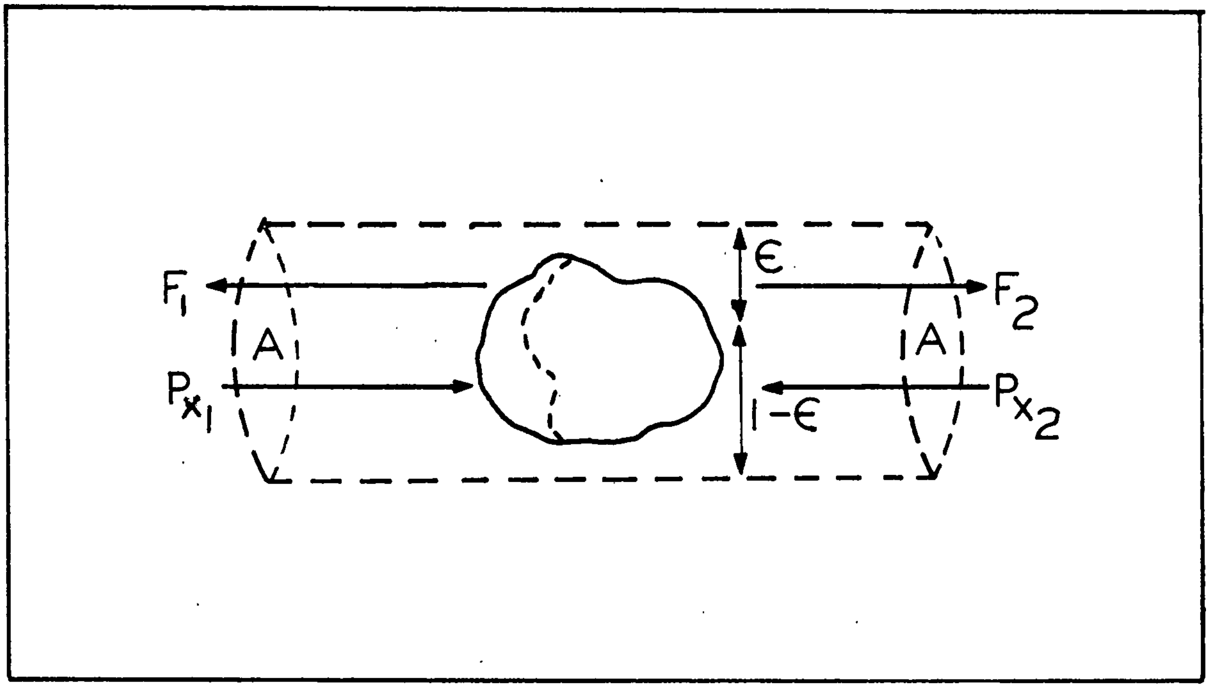

FIGURE 5.

FORCE BALANCE ON ISOLATED PARTICLE UNDERGOING SHEAR then given by

$$dp_s + dp_x = 0 \tag{9}$$

Hydraulic pressure decreases from an upper limit of p to a lower limit of p_x. At the cake surface, solids pressure is zero. Integrating Equation (9) according to these limits

$$\int_{p_x}^{p} dp_x + \int_{0}^{p_s} dp_s = 0$$

$$p = p_x + p_s \tag{10a}$$

Equation (10a) defines p_s which may be written as

$$p_s = p - p_x \tag{10b}$$

This result is shown in Figure (4), curve B illustrating the increase in solids pressure from zero to a maximum of $(p - p_1)$ at the medium. The sum of solids pressure and hydraulic pressure at all points in the cake is equal to total pressure p.

Previously the statement was made that filter cakes compressed due to increased pressure. It is now clear that this statement is only partly correct and that filter cakes compress void volume decreases when solids pressure $(p - p_x)$ increases. This distinction is amplified by considering operation of a filter under a pressure drop from 100 p.s.i. to 75 p.s.i., an example being a line filter. The maximum solids pressure in the filter cake is 25 p.s.i. If the filter were operating between 15 p.s.i.g. and a vacuum filtrate receiver in which the pressure is -10 p.s.i., a maximum solids pressure would be obtained at the cake-medium interface of 25 p.s.i. also.

III. FILTRATION RESISTANCE

The objective of filtration engineering development is to find a means to predict resistance from theoretical considerations. Experimental measurements of filtration resistance are interpreted by criteria provided by theoretical analysis, but the empirical approach to evaluation of resistance is still necessary.

The complexity of interal gometry in a filter cake is the chief obstacle to development of a practical theory of filtration resistance. Statistical analysis by means of models is an approach now being investigated as a means of expression for flow through randomly oriented beds of packed particles to permit prediction of shear stresses over surface areas in filter cakes under practical conditions. Simple models have been devised depicting the filter cake as a series of parallel fine capillaries and reasonable success has been achieved by this method in analysis of filtration problems.

Analysis of factors which result in filtrations resistance in flow through cakes initiates with examination of the processes in formation of the cake. In the previous section the filter cake was represented as continuous substance for development of the fundamental equation based on differential analysis when actually the microstructure of the cake is not continuous, being an agglomeration of individual particles deposited in random orientation. Therefore an approach from differential analysis is useful only from an empirical point of view with respect to factors influencing resistance to flow.

Studies of arrangements of various simple shapes show that different ordering of uniform particles can result in a wide range of porosities. The most readily handled case, homogeneous spheres, have been extensively treated from a mathematical viewpoint, examples of this work being that of Graton and Fraser and also of Carman.[11,27] For the situation of particles all being homogeneous spheres touching one another, a filter cake can have a maximum porosity of 0.875 (each sphere touching three others) and a minimum porosity of 0.259 (each sphere touching six others in rhombohedral arrangement).[27,34] Packing of uniform spheres in cubic arrangement can be demonstrated to result in porosity of 0.476.

$$e = \frac{\text{Cube volume} - \text{sphere volume}}{\text{cube volume}} = \frac{D^3 - \pi D^3/6}{D^3} = 0.476$$

When a variety of sizes of a given shaped particle is present or if geometries of particles are dissimilar, an indenumerable number of possible porosities can result. Figure (6) illustrates a possible rearrangement of particles in a cake formed from a slurry containing small and large size spheres.

Formation of filter cakes is indicated schematically in Figure (7) from an idealized standpoint. The driving potential for flow across the cake is the pressure difference $(p - p_1)$. At the surface of the cake, or interface of slurry and cake, the solids are in general loosely packed. More dense packing becomes evident in compressible cakes as reaction to the stresses developed by fluid flow builds up. The most densely packed solids are found at the medium. Density of packing, expressed as porosity, changes because of compression of particles from loosely packed structures to more stable arrangements.

It will be brought out later that experimental evidence indicates actual deformation of filter cake particles is less common than re-arrangement of particles in relation to one another. Demonstration of behavior during compression of cakes composed of fine particles is given in examining the processes taking place in a consolidometer, the results being shown in Figure (8) following Tiller.[61] A consolidometer consists of a porous cylindrical cup filled with a liquid saturated sample of fine solids, usually clay or earth. A weighted piston fitted into the cup resting on top of the solids will settle into the cup until the solids have arranged themselves in a configuration that supports the pressure of the piston. In Figure (8b) a greater weight on the piston causes the solids to compress, excess liquid being squeezed out through the porous walls. When force on the solids is increased by an additional weight placed on the piston, the reaction force in the sample is instantaneously the sum of the equilibrium solids pressure F_1A and that due to hydraulic pressure, a neutral stress N. The neutral stress drops to zero as liquid passes through the porous walls at which point the solid structure has attained an arrangement capable of counteracting the force of the piston, shown as F_2 by Figure (8c). The consolidometer has been applied by Tiller for evaluating porosity variations of filter cakes under various mechanical loadings.[61]

The soil consolidometer as described is a device which causes solids to assume a stable configuration under the effect of mechanical stress. Mechanical pressure exerted on the top of the solid mass and transmitted throughout the sample decreases its porosity. When flow

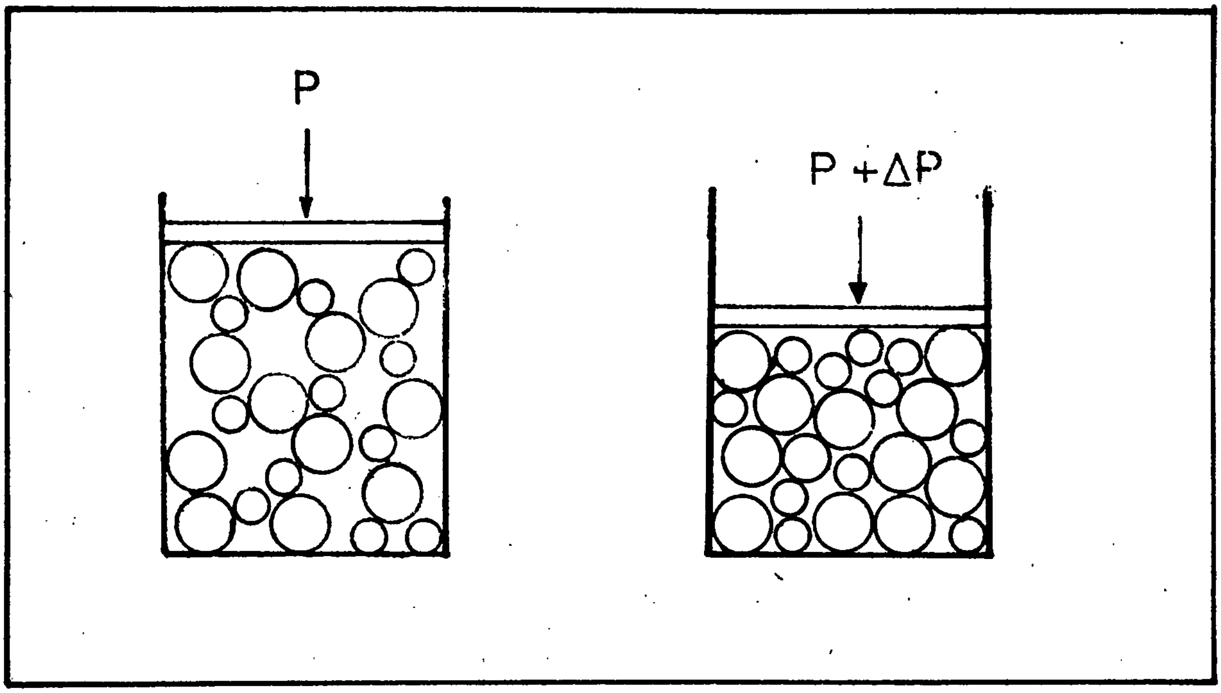

FIGURE 6.

CONSOLIDATION IN BED OF NONUNIFORM SPHERES

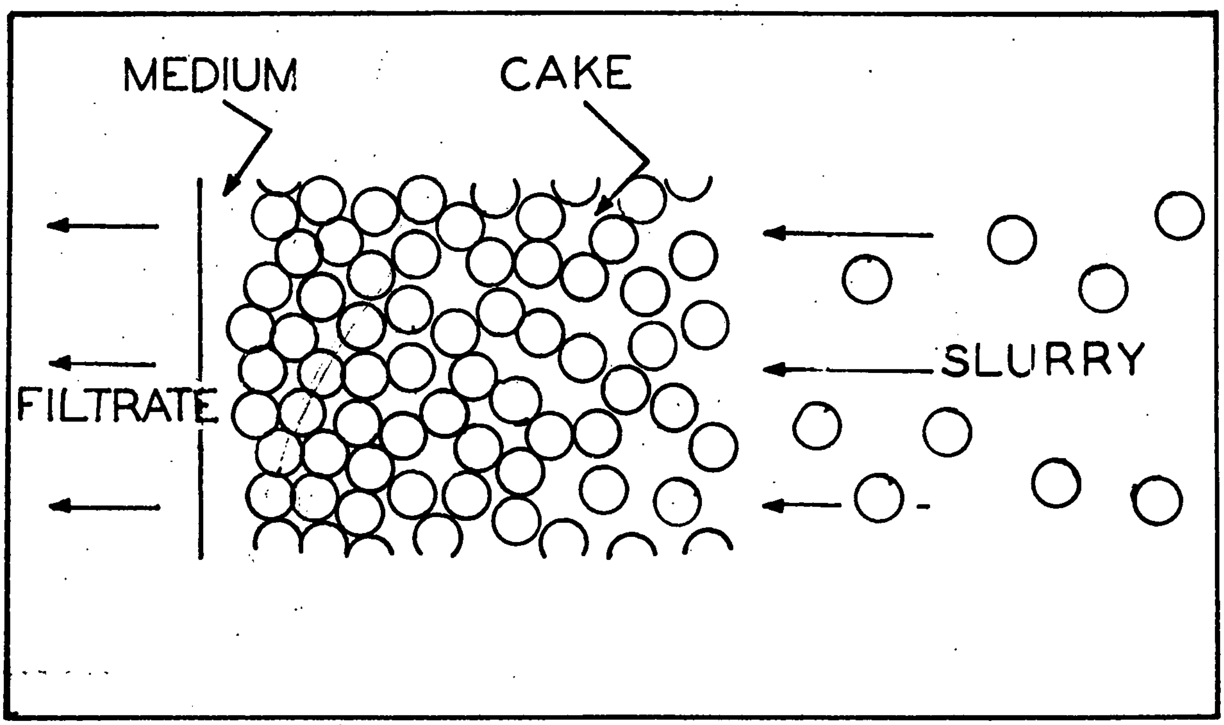

FIGURE 7.

PARTICLE PACKING DENSITY FROM SURFACE TO MEDIUM IN FILTER CAKE from the consolidometer ceases, mechanical solids pressure and porosity are uniform throughout the sample. A filter cake can be contrasted with a mass in a consolidometer in that the solids pressure and porosity vary throughout the material. Flow through a filter cake results in accumulation of solids pressure due to shear stresses generated by the flowing fluid as shown previously. The net result of this as depicted in Figure (9) is the building up of compressive mechanical stress which is assumed equivalent in effect to the mechanical force of the piston acting on the surface of the cake in the soil consolidometer. In Figure (9) particles are shown contacting each other at a point. Accumulation of solids pressure can result in instability in the structural arrangement of the particles to bring about reorientation of the structure until equilibrium is attained. This hypothesis explains variation of porosity from the surface to the medium in a filter cake. Existence of porosity gradients has been confirmed experimentally by several investigators.[24,35,68] A porosity variation with pressure is detectable by decreased thickness of cake.

The assumption of equivalence of mechanical stress and accumulated shear stress is utilized in an instrument called a compression-permeability cell invented by Ruth.[50] This device is becoming useful in obtaining technical data for filtration.[24,35,37] Figure (10) shows a schematic diagram of the features of a compression-permeability cell according to Grace.[24] A pressure cylinder (A) is fitted with a hollow piston with porous end (B) and a porous drainage base (C). A saturated cake (D) is uniformly deposited under zero pressure stress in the

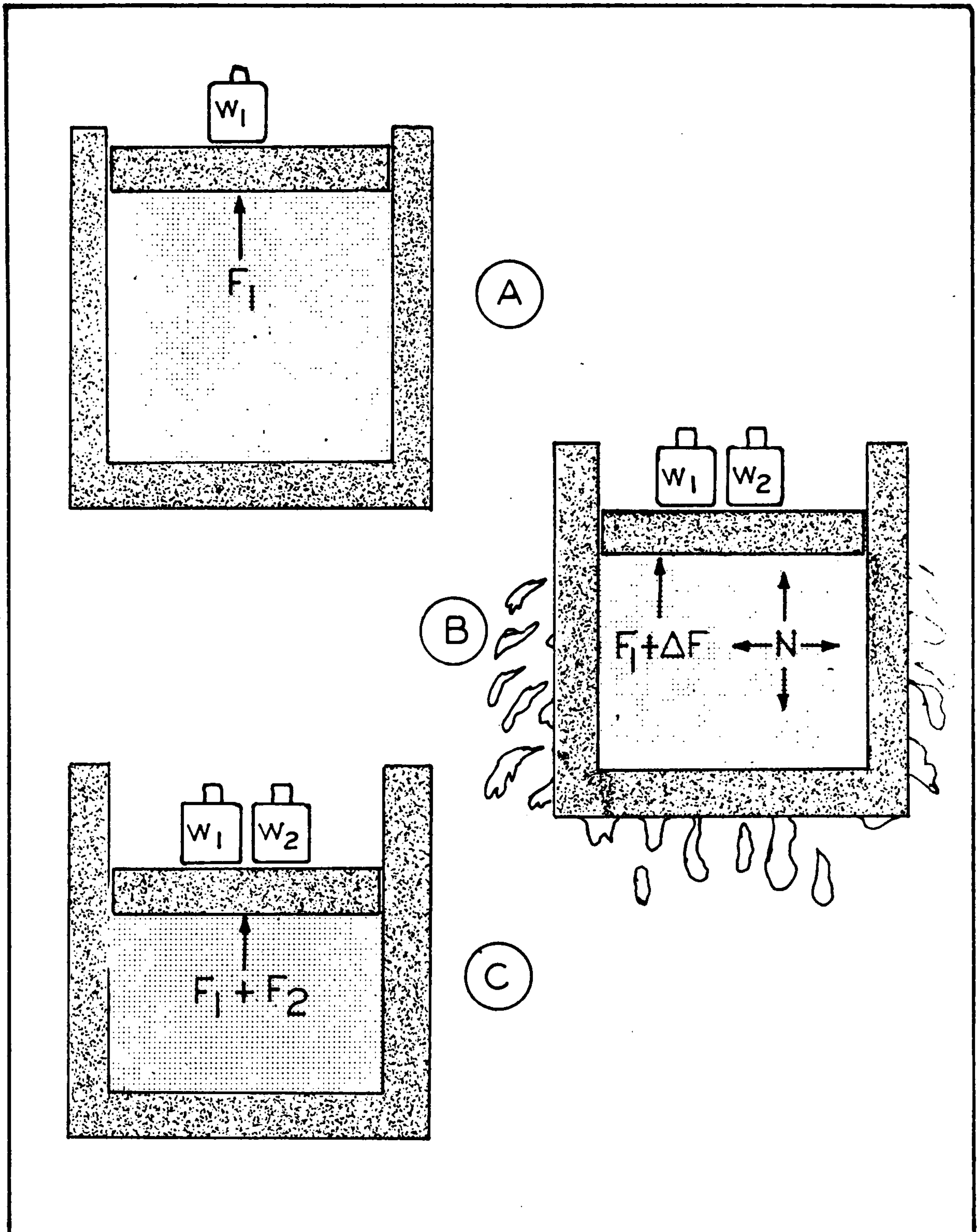

FIGURE 8.

OPERATION OF SOIL CONSOLIDOMETER

cylinder cavity. A very small flow of filtrate maintained under constant head (E) is allowed to flow through the cake which is compressed under known mechanical stress by means of weights placed on the piston. The flow rate is held constant and measured with a burette or graduate placed under the drainage base (F). In using a low filtrate head, the frictional pressure drop is small in comparison to the mechanical stress developed through the piston. Variation in porosity through the cake will be negligible because of this dependence on mechanical stress alone and filtration occurs in a constant porosity cake. Following this, it is assumed that specific resistance of the cake is constant throughout the cake at constant solids pressure. Specific resistance can be calculated from Equation (5) in integrated form, since integration can be performed directly with all the factors in the expression constant with pressure and thickness. Equation (5) becomes

$$\alpha = \frac{\Delta p}{\frac{\mu}{g_c}\, q\, \rho_s\, (1 - \epsilon)\, L} \tag{10}$$

The thickness of cake is measured with micrometers or calipers and porosity calculated using the known mass of solids in the cake. By increasing the mechanical pressure in stages by adding weight to the piston, a series of values can be obtained which indicate the change in specific resistance and porosity with pressure for compressible materials. Examples are given in a later section for technical calculations using compression-permeability cell data.

From its definition in Equation (2) specific resistance has units of pressure drop per pound mass of dry solids per unit viscosity per unit over-all velocity in English engineering units, these units reducing to (ft./lb/mass). As a result of using the English engineering units as defined specific resistance will have values on the order of magnitude of 10^{10} to 10^{12}. This can be illustrated by an example. Consider a filter operating at one hundred p.s.i. through which one gallon per minute filtrate is flowing per square foot of filter. Cake thickness is one inch and cake porosity is 0.60. Solids density is two hundred pounds per cubic foot and filtrate viscosity is one centipoise. Converting inches to feet and centipoise to feet per pound mass per second, these values are substituted into Equation (10) with the result

$$\alpha = \frac{(32.2)\ (1388)\ (100)\ (144)\qquad (12)}{(1)\ (0.00027)\ (200)\ (1 - 0.60)\ (1)} = 2.48\ (10^{11})\ \text{ft./lbm.}$$

where gallons per minute per square foot is converted to cubic feet per square foot per second. One g.p.m. per square foot is equivalent to 0.00027 (cu.ft.)/(sq.ft.) (sec.).

Specific resistance and porosity data obtained using compression-permeability cells have been published by several investigators.[24,37,50] It is interesting to note that data relating α and ϵ to p_s often is linear when plotted on log-log coordinates. Figures (11) and (12) demonstrate this for several materials investigated by Grace.[24] The linear log-log relationship is utilized for approximate technical calculations, the development of which will be presented later.

Grace has extensively studied the characteristics and physical properties of compressible and non-compressible filter slurries, the specific resistance and porosity data for several of these materials being plotted in Figures (11) and (12). Microscopic examination of slurry particles to study their size and shape resulted in better qualitative understanding of behavior in cake formation during filtration. Figure (13) reproduces photo micrographs of particles in typical slurries for which data are given in Figures (11) and (12). Solka-Floc is seen to be composed of pulpy physically deformable particles. Data for Solka-Floc indicate rapid change in specific resistance with pressure over the pressure range shown while change in porosity over the same pressure interval is not very great. The conclusion can be drawn that Solka-Floc particles tend to change shape in the cake under increased solids pressure, resistance to flow being greatly increased but not resulting in closer orientation of particles physically to cause appreciable porosity changes. Another material, talc C, forms cakes having a higher degree of compressibility in which specific resistance changes rapidly with pressure increase. As seen in Figure (13) talc C particles are angular crystalline forms which are resistant to elastic deformation. The data for carbonyl E indicate cakes from this material are relatively incompressible above a few pounds per square inch solids pressure, this finding being suggested by the photomicrograph in Figure (13) which indicates iron carbonyl E consists of spherical particles appearing to be nondeformable. Equilibrium porosities in carbonyl E filter cakes would be reached upon attaining low solid pressure stresses. Grace's investigation covered seventeen different slurries over a wide range of properties and size distributions. Analysis of the aggregate of Grace's findings produced the interesting information that for a rule of thumb, slurries containing particle sizes of 3-5 microns and smaller form compressible cakes while larger particle sizes tend to be

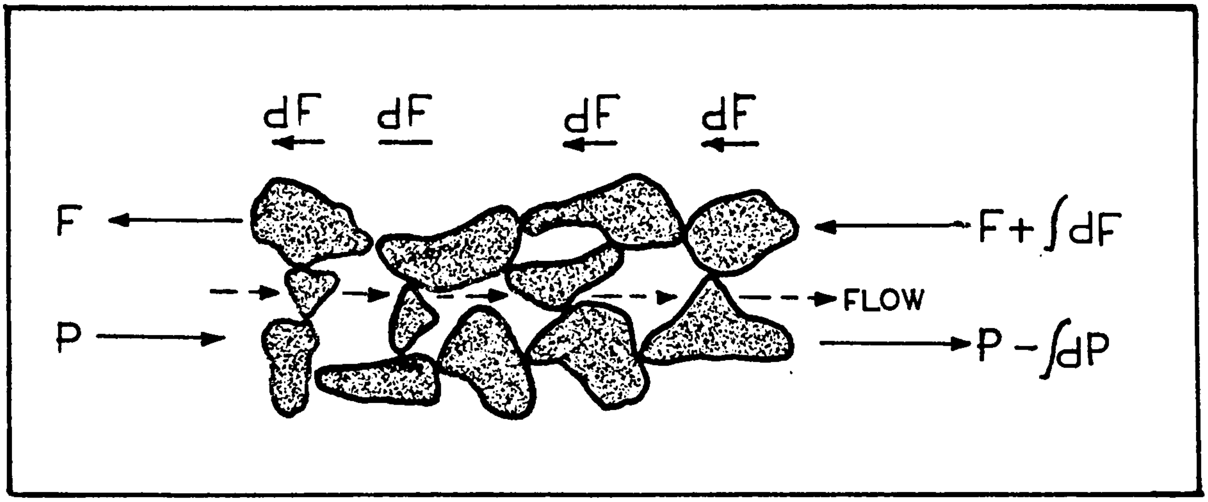

FIGURE 9.

PRESSURE TRANSMISSION BY POINT CONTACT IN BED OF PARTICLES

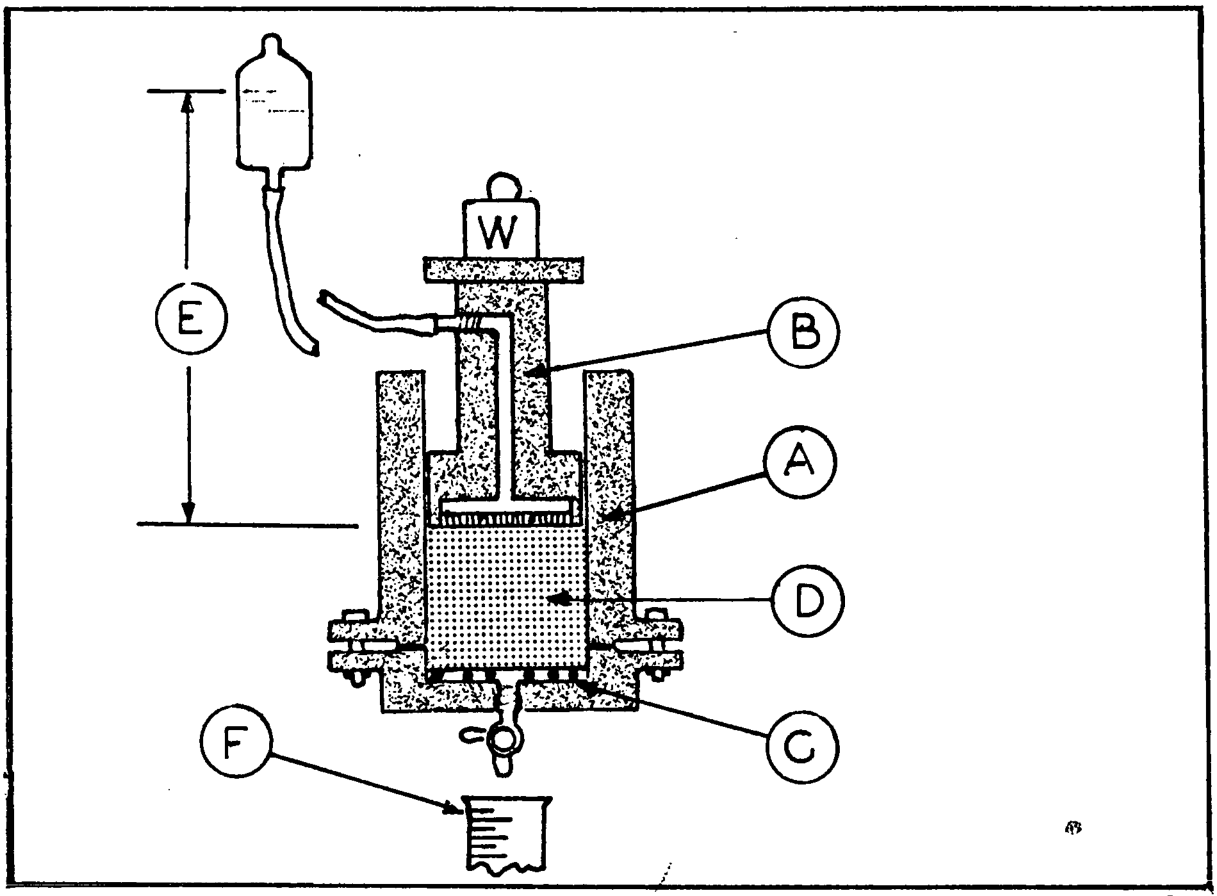

FIGURE 10.

COMPRESSION-PERMEABILITY CELL

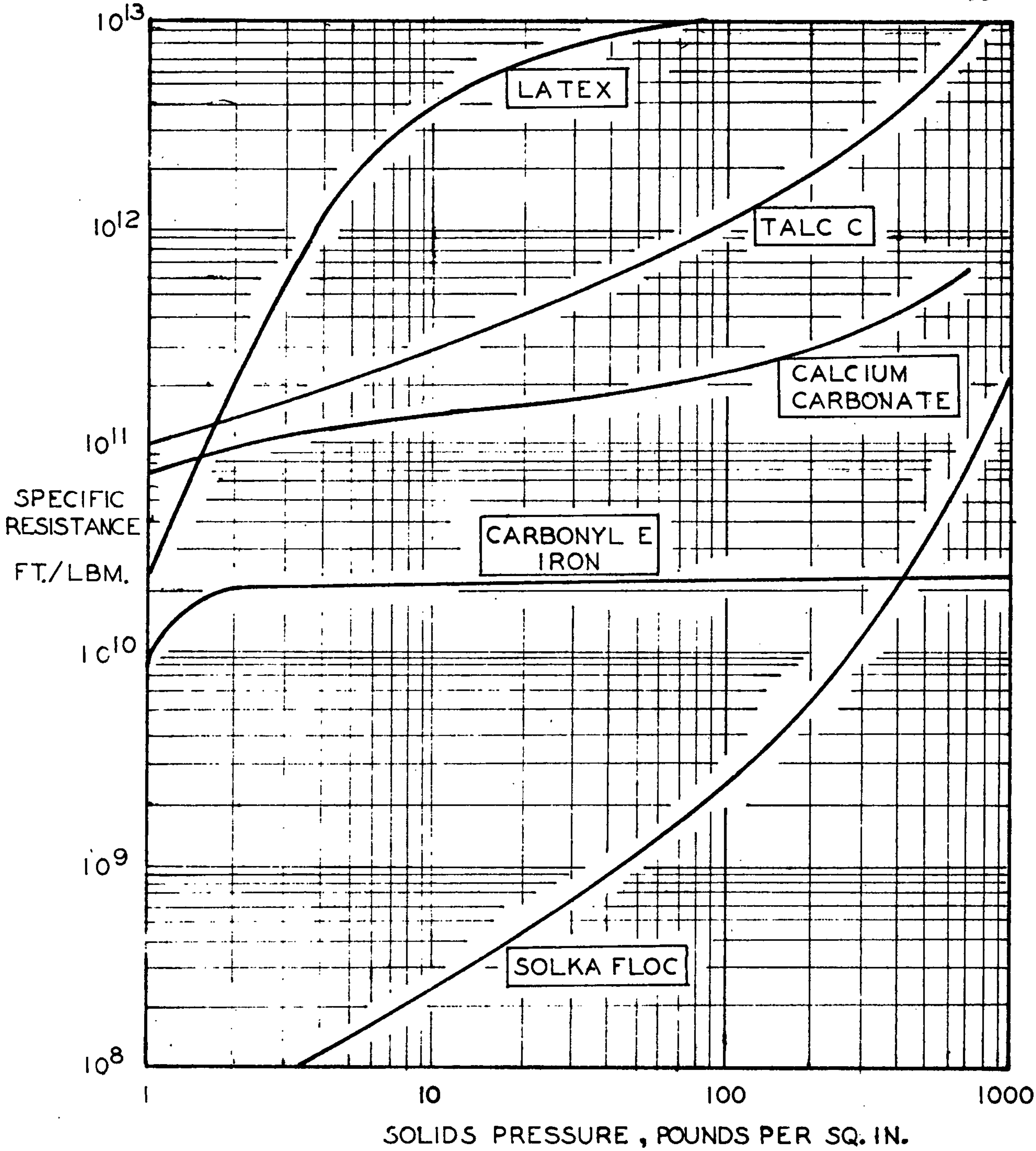

FIGURE 11.

SPECIFIC RESISTANCE OF SOLIDS VS. SOLIDS PRESSURE

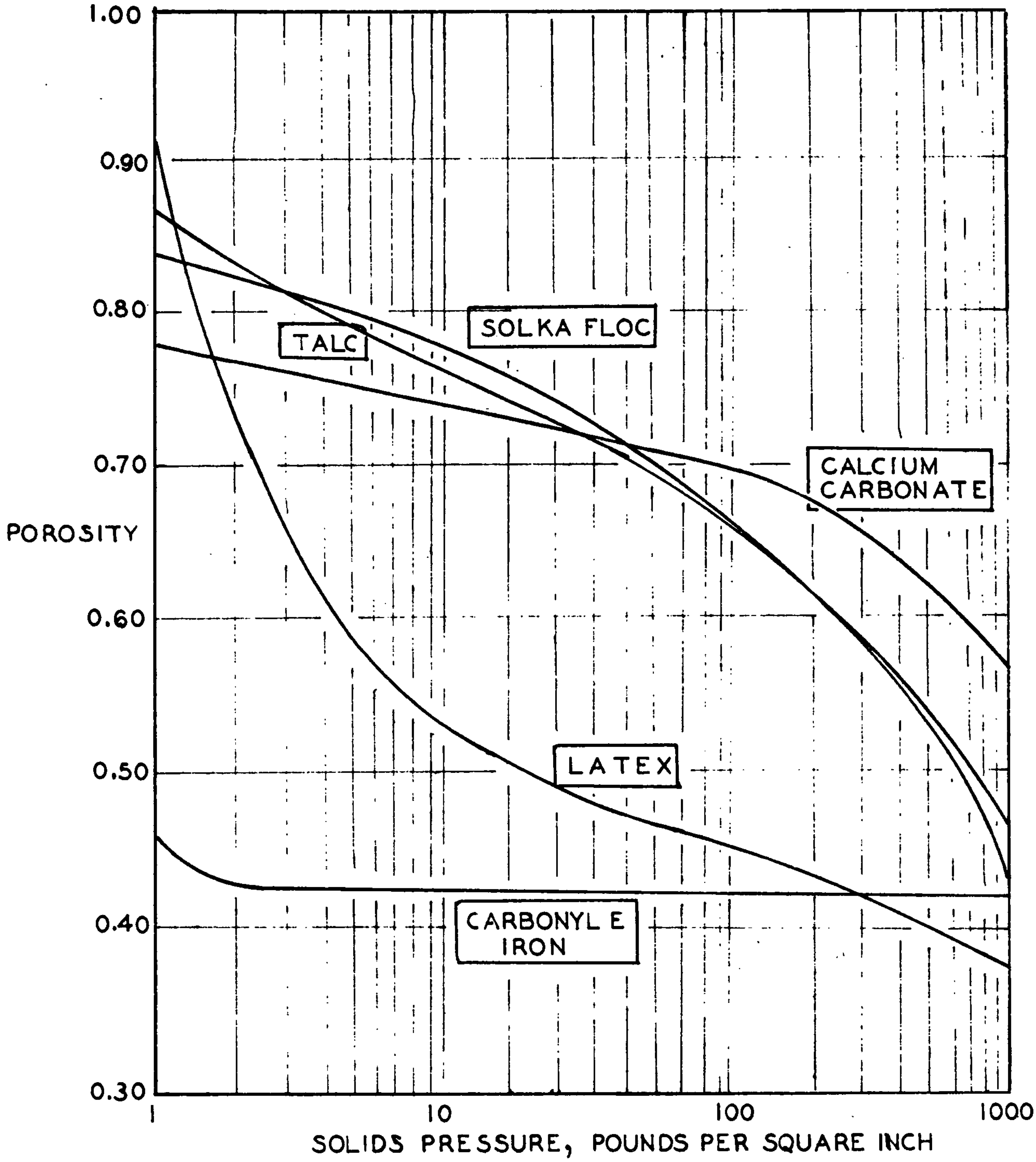

FIGURE 12.

POROSITY OF SOLIDS VS. SOLIDS PRESSURE

non-compressible in the normal range of filtration pressures (less than 150 p.s.i.).

An aspect of filter cake compressibility worthy of consideration is the degree of reversibility of the compressed cake after removal of pressure stress. Tiller studied several compressible samples under mechanical stress in a soil consolidometer and found only slight recovery (or expansion) of the compressed cake after removal of the piston.[61] The samples were crushed limestone, kaolin, and asbestos, these being crystalline materials in which compression would be assigned to rearrangement rather than deformation. Hutto measured expansion of compression-permeability cell cakes and found one to two per cent volume increase after removing the mechanical pressure.[35] Waterman has reported data taken with filter cakes composed of certain types of adsorbent carbon used as filter aids in which significant elastic recovery was obtained.[66] The carbon samples were chiefly typical amorphous skeletal forms obtained by destructive distillation of organic material. Extending this discussion to a parallel topic, the time required for a sample placed under mechanical stress to come to equilibrium compression is of technical interest. In compression-permeability cell measurement Grace found that the time interval between equilibrium compression for slightly or moderately compressible cakes was two to five minutes whereas ten to fifteen minutes were required for attaining equilibrium with highly compressible materials.[24] Tiller investigated the time rate of change of porosity of crushed limestone (calcium carbonate) in consolidometer tests at various pressures.[61] Exponentially decreasing porosity vs. time data were obtained with equilibrium being essentially attained in one minute at 7.25 p.s.i. and in five minutes at 70.3 p.s.i. although the final equilibrium porosities obtained at various pressures indicated that the material was only slightly compressible. Consolidometer tests on soils, especially clay, have demonstrated that up to twenty-four hours are needed to attain equilibrium consolidation. Secondary effects appearing to extend indefinitely in soil tests have been noted in addition to primary bulk consolidation.[61]

The filter cake is a special case in the general problem of flow through porous media, the analysis of which is hampered by difficulties identified with geometries of porous structures with the added complication that compression of the media take place during the process of flow. Partially successful developments based on fundamental principles have been achieved through the use of models created to approximate the nature of flow through the filter cake in spite of the difficult problem of mathamatical representation.

Kozeny, in analyzing flow of ground water through sand and soils, idealized the geometry of a porous structure by considering flow to take place in a series of straight capillaries through the cake as illustrated in Figure (14).[38] Pressure drop for viscous flow of Newtonian fluids through straight circular passages is described by the Poisueille equation derived from hydrodynamic principles

$$\frac{dp}{dx} = -32 \frac{\mu}{g_c} \frac{u}{D^2} \tag{11}$$

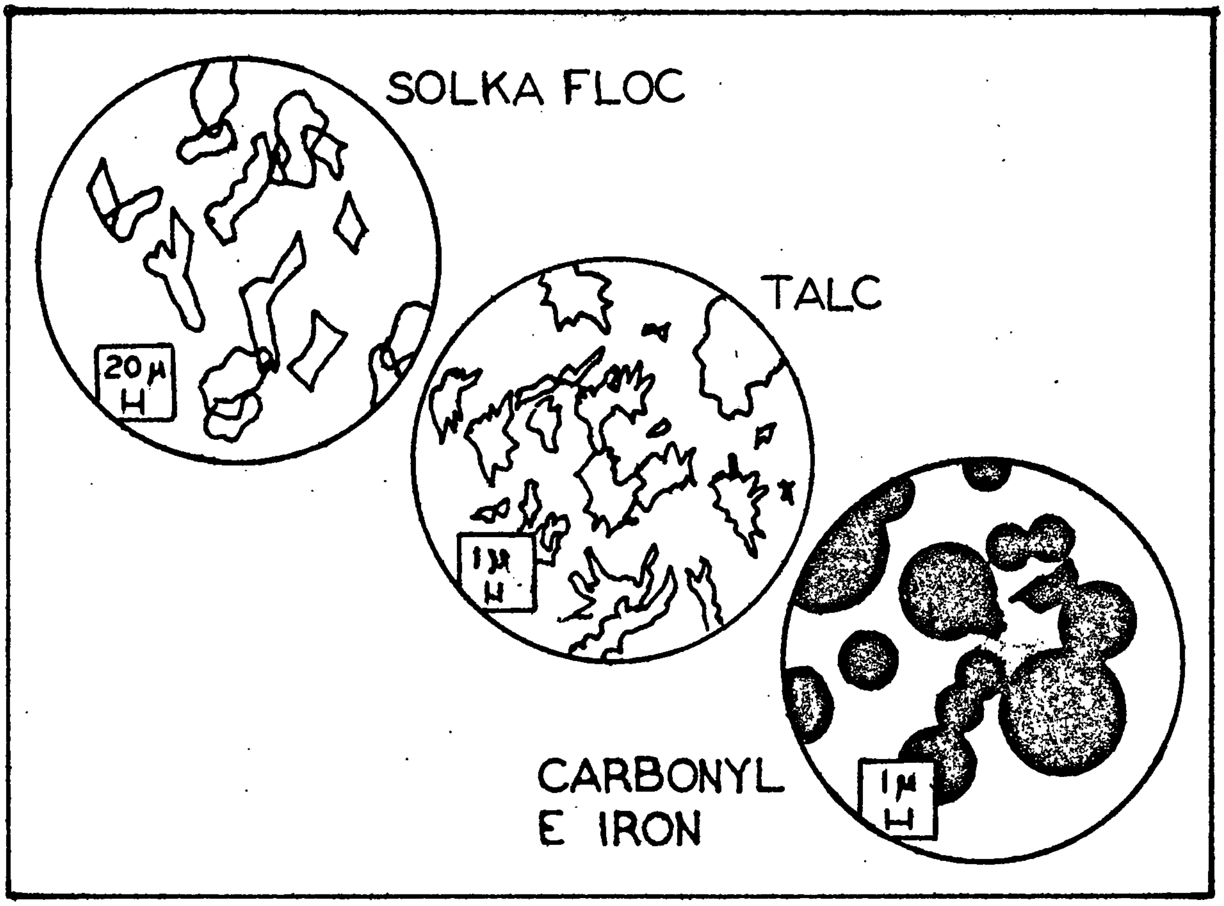

FIGURE 13.

MICROPHOTOGRAPHS OF SLURRY PARTICLES

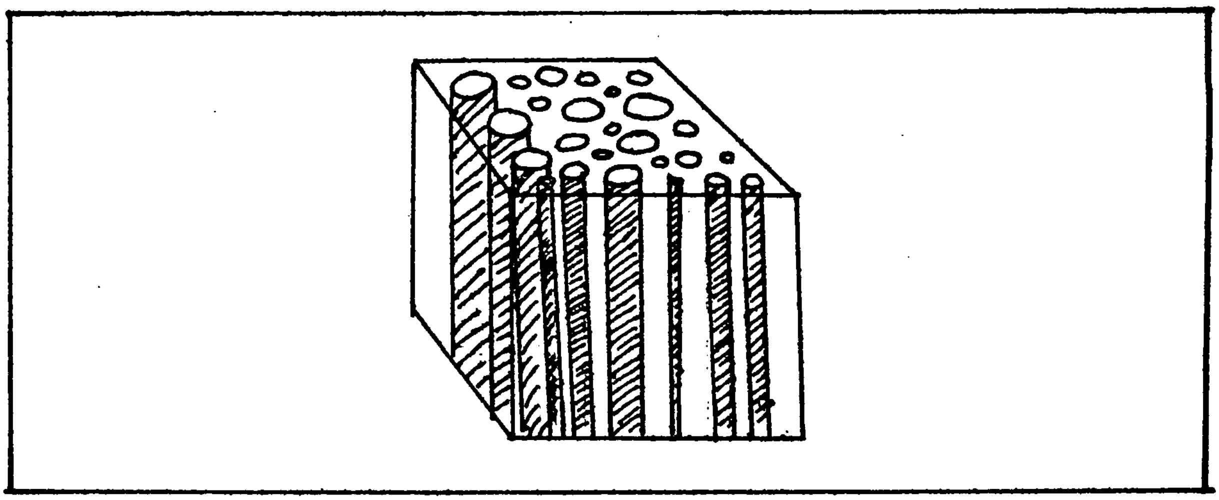

FIGURE 14.

STRAIGHT CAPILLARY MODEL OF FILTER CAKE

where u is the average velocity in the passages and D is capillary diameter.[39] In the general case considering noncircular straight passages, the hydraulic radius, R_H, is substituted for diameter where

$$R_H = \frac{\text{flow area}}{\text{wetted perimeter}}$$

The multiplier 32 occurs in the Poisueille equation in consequence of its derivation for circular passages; in the general case a multiplier k is employed such that

$$\frac{dp}{dx} = -k \frac{\mu}{g_c} \frac{u}{D^2} \tag{12}$$

Referring to Figure (14) an expression for R_H for a filter cake over unit cross section for cake thickness L for the Kozeny model is given by

$$R_H = \frac{(\text{flow area})(\text{length of path})}{(\text{wetted perimeter})(\text{length of path})} = \frac{\text{void volume}}{\text{surface of solids}}$$

Void volume is given in the filter cake by

$$\text{void volume} = \frac{\epsilon}{1 - \epsilon} \text{(volume of solids)}$$

Defining S_o as surface area of solids per unit volume of solids, R_H is defined by

$$R_H = \frac{\epsilon}{1 - \epsilon} \frac{1}{S_o} \tag{13}$$

The average velocity in a passage is given by the superficial flow rate through the cross section, q, divided by the fraction voids in the cross section, ϵ

$$u = \frac{q}{\epsilon} \tag{14}$$

Substituting Equations (13) and (14) in Equation (12) results in

$$-\frac{dp_x}{dx} = k \frac{\mu}{g_c} \frac{(1 - \epsilon)^2}{\epsilon^3} S_o^2 q \tag{15}$$

where $-dp_x = dp_s$ according to Equation (9).

Comparing Equations (5) and (15) a theoretical expression for specific resistance in terms of the Kozeny model is

$$\alpha = k \frac{(1 - \epsilon) S_o^2}{\epsilon^3 \rho_s} \tag{16}$$

which indicates that specific resistance is a function of porosity alone if specific area, k, and solids density are constants. This development was first applied to filtration by Carman.[8]

The dimensionless constant k introduced into the modified Poisueille equation has been observed to be relatively constant for single phase flow through packed beds of randomly arranged particles of size above the compressible threshhold. This was reported by Carman who determined values of $k = 5.0 \pm 0.10$ from data taken during liquid flow in packed beds of fine particles.[9] Coulson later made more extensive investigations using solids of measured size and known shapes, calculating values for k mainly between 4.0 and 6.0, k for an individual shape varying somewhat with the packing density.[17] For particle sizes large enough to be incompressible, Kozeny's law using $k = 5.0$ has been extensively used for estimating surface area of particles from pressure drop measurement in gas flow at known rates.[1,14,31,40]

The assumptions used in deriving Kozeny's equation are of little generality with the result that the theoretical formula for α breaks down in comparison to experimental values obtained in examination of cakes composed of very fine, flocculating particles. Flocculation is the aggregation of groups of particles in the slurry into loose structures or flocs. Strength of the flocs or resistance to degredation depends upon fineness of the particles (surface to volume ratio), the extent of surface contact between particles in the slurry, the amount of interlocking that can take place upon solid to solid contact, and the strength of surface forces causing particle adhesion.[18] Flocculation is found to be related to chemical conditions in slurries of fine and irregular shaped particles being mainly a surface effect judging from evidence presently available. Cakes formed from slurries subject to flocculation will tend to break down under pressure stress because of changes in floc structure, flocs ordinarily not being capable of withstanding more than small stresses. In practical filtration of fine particles, rates are found to be sensitive to impurities in trace amounts, to handling of the slurry or aging, and other variables that are difficult to control which are thought to have some effect on the degree and nature of flocculation. Grace investigated the change in specific resistance of a slurry of R-110 titanium dioxide, the particles having an average size of 0.18 micron and being of very irregular shape.[25] Figure (15) illustrates the results obtained as electrolyte concentration and pH were increased in the slurry, the graph showing average specific resistance taken from filtration data as a function of the light extinction coefficient, a quantity dependent upon the degree of particle flocculation.

The Kozeny relationship appears to be capable of predicting the point change in cake resistance in terms of porosity within reasonable error until particle size in a slurry becomes so small that flocculation becomes evident, the size being below 3-5 microns. Carman and

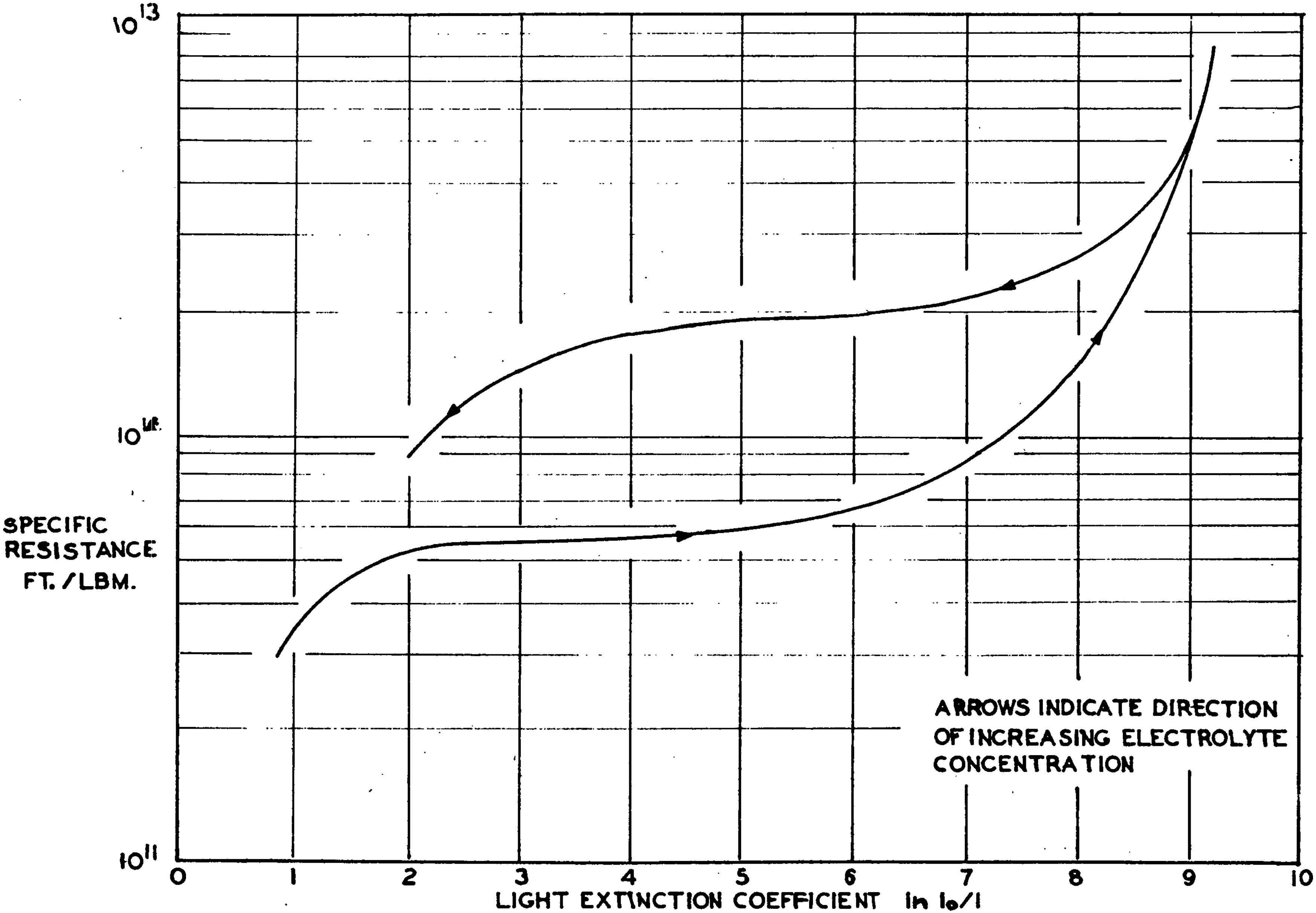

FIGURE 15.

VARIATION OF AVERAGE SPECIFIC RESISTANCE OF TITANIUM DIOXIDE FILTER CAKE WITH CONCENTRATION OF ELECTROLYTE

Malherbe limit the application of the Kozeny equation to cakes in the porosity range 0.4 to 0.5.[14] Grace's data indicate that the Kozeny expression holds for cakes in this porosity range.[24] Grace calculated specific surface from the Kozeny equation using k = 5.0 using observed specific resistance and porosity data obtained in compression-permeability cell measurement. The criterion used by Grace was a plot of the effective specific surface vs. porosity, this relationship indicating validity of the Kozeny equation when S_o becomes constant with porosity measured over a range of pressures. Figure (16) shows this data for several materials, indicating that the Kozeny relationship can be applied to materials which are relatively incompressible. Figures (11) and (12) contain observed specific resistance and porosity data for these materials.

Other factors related to the geometrical structure in beds of fine particles may also be responsible for the failure of the Kozeny model for compressible materials. The constant k in the Kozeny relationship has been shown to be variable for flow through beds of irregular shaped particles by the work of Coulson.[17] Coulson's study was conducted using large size particles; the effect of particle size variation on magnitude of k observed experimentally has never been reported in detail. Kozeny's model, based on flow in parallel capillaries of noncircular cross section, permits analytical solutions for numerical k values for a given cross section. A circular cross section leads to a theoretical value for k of 0.2 and other cross sectional geometries lend themselves to evaluation similarly.[54] Thus

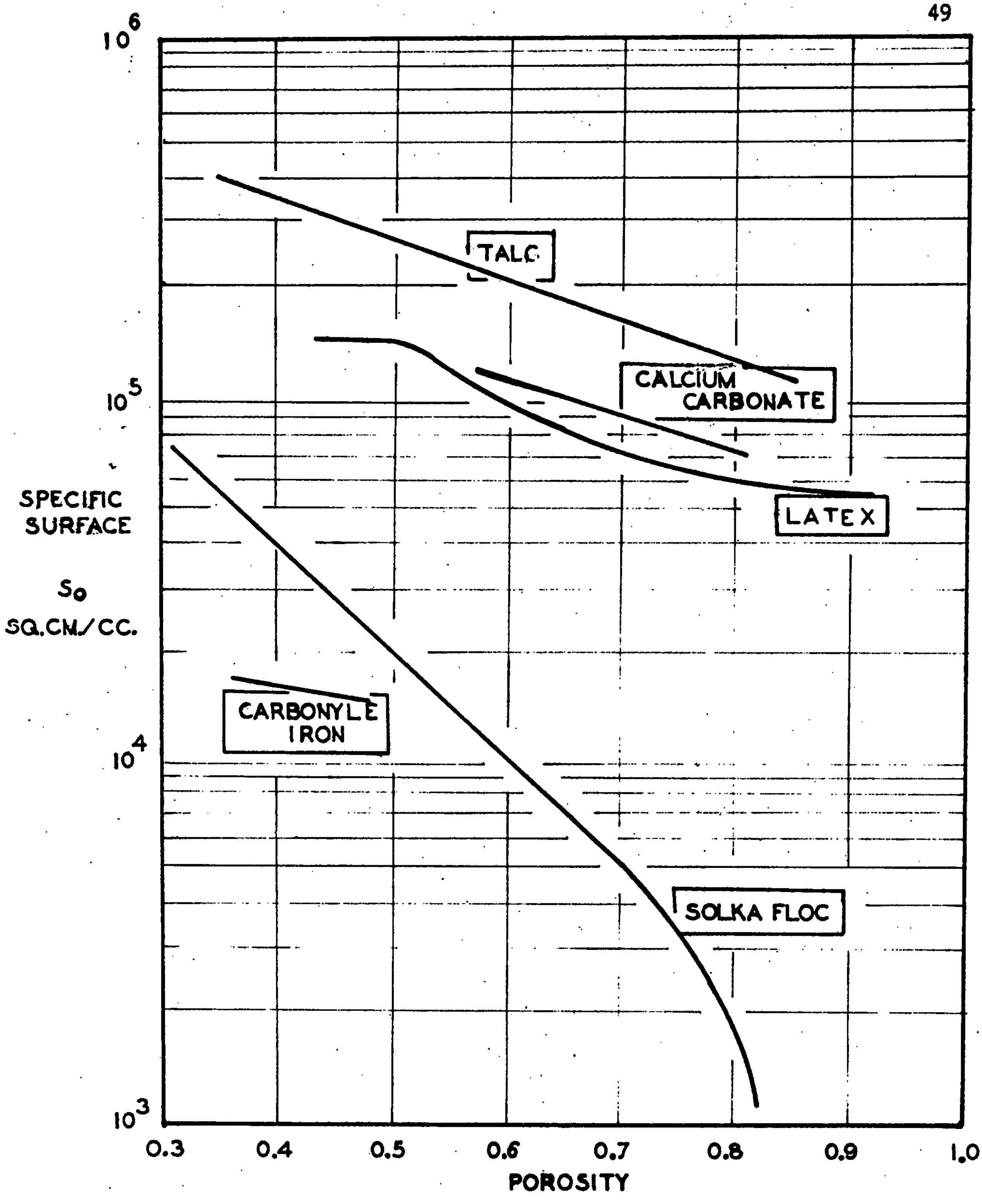

FIGURE 16.

EFFECTIVE SPECIFIC SURFACE VS. POROSITY OF COMPRESSIBLE SOLIDS the values of k reported by Carman and Coulson contain an experimentally derived correction factor to empirically establish agreement between the model and observed data. The most serious limitation of the Kozeny derivation can be assigned to the assumption of flow in straight lines through the media. In discussing the applicability of Kozeny's derivation Scheiddeger shows that the Kozeny model using an empirical k holds adequately when particles are of large enough size for flow to take place through the cake with reversals being a less significant factor than friction as a cause of pressure gradient.[53,54] In cakes composed of subsieve particles (less than 360 wire mesh), interstices for flow between particles are greatly reduced in size and increased tortuosity of passages becomes a significant factor in appraising the regime of flow.

A model avoiding the concept of idealized capillary flow through the filter cake was introduced by Scheiddeger, this model being based on development of a statistical probability equation encompassing the random path of flúid flow through a porous structure.[53] A third descriptive variable, dispersivity, arises to characterize the tortuous nature of flow through the media. Dispersivity appears as a term analogous to standard deviation in the Gaussian error integral in Scheiddeger's development and is based proportionately on the structural complexity causing pressure gradients due to flow reversals. These effects are absorbed heuristically by the constant k in Kozeny's model. Analysis by means of Scheiddeger's model has not progressed sufficiently to adequately compare the hypothesis of this development to experimental data. It will be interesting to develop applications of this theory as it is hoped that application of fundamental factors can be extended beyond the point at which Kozeny's model breaks down as a descriptive tool.

A qualitative verification of the principle tenet in the statistical model can be drawn from consideration of pressure drop data taken in flow through porous structures. The data of Carman for flow through granular beds in which a modified Reynold's number based on porosity is plotted vs. a pressure drop function based on Kozeny's equation shows a correlation in a single curve.[9] As shown in Figure (17), this curve on log-log coordinates gradually changes from a constant slope in the low range to another constant slope in high Reynold's number range. By analogy to flow in pipes, the low range can be considered to be in nominal viscous flow and the high range in dispersed or turbulent flow. The intermediate range, given by Reynold's number values in the smooth curve connecting viscous and dispersed flow, can be deduced to consist of mixed turbulent and viscous flow as a result of the nonuniformity of flow areas in a bed cross section. Thus filter cakes in which flow passages are large enough to permit principally viscous flow are plausibly amenable to analysis by the simplified Kozeny model. Decrease in size of flow passages to the magnitude of those contained in cakes of fine particles may require that adequate description is possible only by basing treatment on a dispersed flow regime. A statistical treatment of flow through packed beds has been reported utilizing Monte Carlo sampling to find parameters through known boundary conditions.[45] The reference cited is concerned with flow through ion exchange beds.

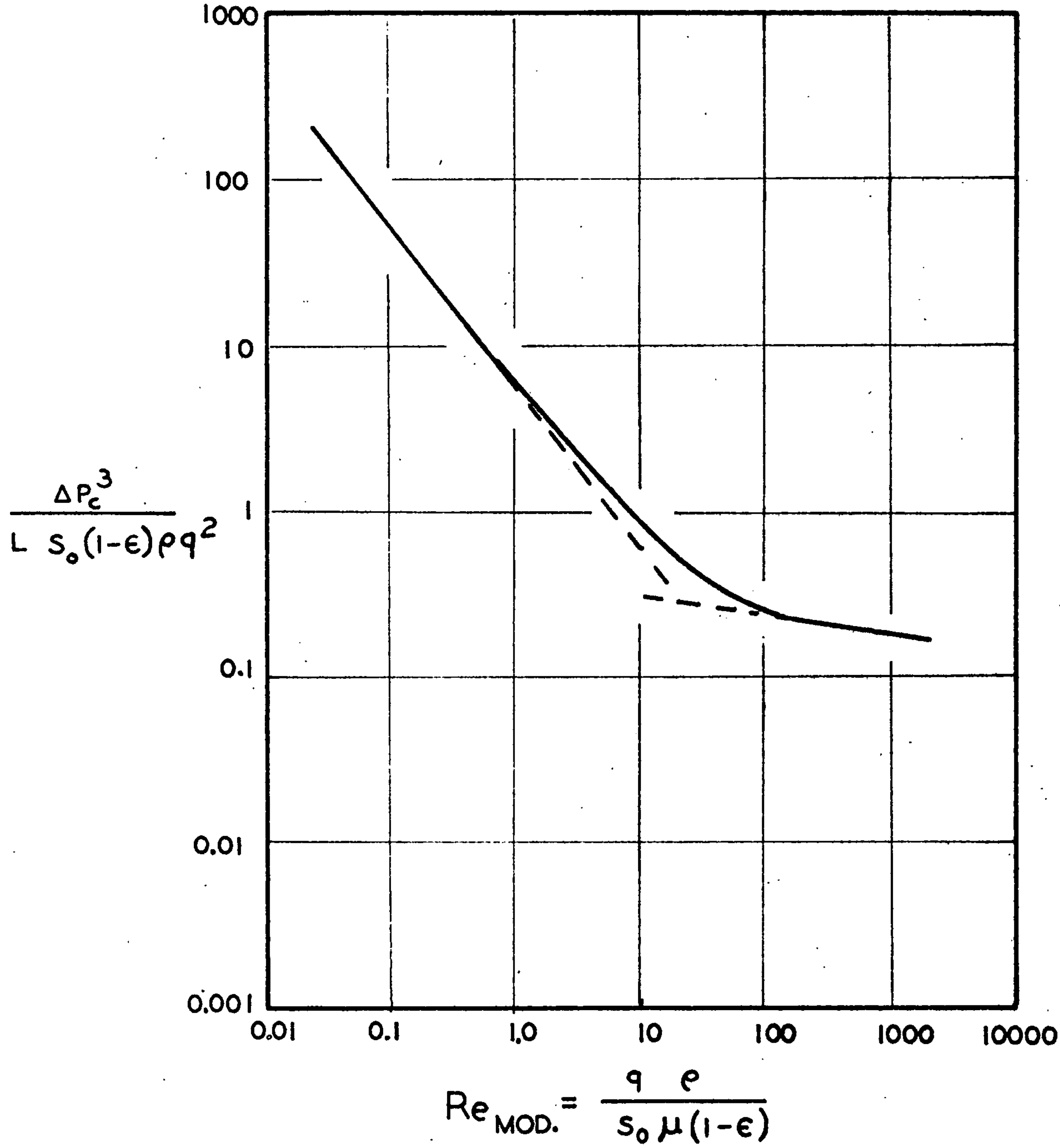

FIGURE 17.

MODIFIED REYNOLDS NUMBER
CORRELATION FOR PRESSURE DROP
IN FLOW THROUGH PACKED BEDS

IV. FILTRATION RATES

Filtration rates depend on the magnitude of available pressure drop, how much resistance is contained in the cake structure, and viscosity of the filtrate. The object in calculating rates for a particular operation is to develop means of determining volume of filtrate as a function of time when the rate of flow can be calculated from particular pressure drop, resistance, and viscosity data. Expressions for calculating rates are developed by means of the fundamental equation of filtration, Equation (3), in the general differential form

$$- g_c \frac{dp_x}{dw_x} = g_c \frac{dp_s}{dw_x} = \mu\, q\, \alpha_x \tag{3}$$

The variables in Equation (3) are separable if assumptions are made: (1) α is a function of solids pressure alone, (2) q is constant through the thickness of cake at any instant (or $q \neq f(x)$, $0 \leq x \leq L$), (3) flow is laminar and follows Newtonian behavior.

Integration of Equation (3) results in

$$\int_0^{p-p_1} \frac{dp_s}{\alpha} = \frac{\mu}{g_c}\, q\, w \tag{17}$$

It is indicated in Equation (17) that pressure is integrated from zero to a maximum of $(p - p_1)$; and mass of cake, w, is integrated from zero to w with the constant of integration disappearing since at $w = 0$, $(p - p_1) = 0$.

The hydraulic pressure at the cake-medium interface is p_1 and the total pressure driving force across the cake and medium is p as shown graphically by Figure (5). By the definition of solids and hydraulic pressures expressed by Equation (10), the maximum solids pressure is $(p - p_1)$. Hydraulic pressure at the medium-cake interface, p_1, is calculated from the medium resistance. Following the empirical expression known as D'Arcy's law, p_1 is assumed proportional to the resistance of the medium, R_m, and inversely proportional to the flow rate[22]

$$g_c \; p_1 \; q = \mu \; R_m \tag{18}$$

R_m takes on dimensions (1/ft.) in English units by Equation (18). It is usually unrealistic to determine accurate values of medium resistance during a filtration because R_m is generally variable with time and rate of filtrate flow due to penetration of small solid particles through the medium surface and alteration of the internal medium structure. Very often medium resistance during filtration is negligible compared to the resistance of deposited cake solids and is either neglected or assumed constant. It is to be recognized that initial flow rates of filtrate are determined by the magnitude of initial medium resistance. One method for estimating medium resistance is based on extrapolation of filtrate flow rates in constant pressure filtration against time to zero time.

Using the instantaneous pressure-filtrate rate expression, Equation (17), the volume of flow is obtained as a function of time by a second integration based on assumption that filtrate rate, q, is constant through the cake and equivalent to the time rate of change of filtrate volume, v

$$q = \frac{dv}{d\theta} \tag{19}$$

where θ represents time. The volume of filtrate, v, is related to the mass of cake solids, w, by material balance

mass of slurry filtered = mass of cake + mass of filtrate

The mass of cake can be related to mass of solids by a proportionality constant, m, equal to the ratio of mass of wet cake to mass of dry solids. The material balance is then written

$$\frac{w}{s} = m\,w + v\,\rho$$

where s is weight fraction solids in the slurry and ρ is filtrate density. The material balance can be arranged to

$$w = \frac{s\rho}{1 - ms}\,v \tag{20}$$

expressing mass of cake solids in terms of volume of filtrate. Substitution of Equations (19) and (20) into Equation (17) yields a basic relationship from which filtration rates are evaluated

$$\frac{p - p_1}{\alpha_{av}} = \int_0^{p-p_1} \frac{dp_s}{\alpha} = \frac{\mu}{g_c}\;\frac{sp}{1 - ms}\,v\,\frac{dv}{d\theta} \tag{21}$$

A modification introduced into Equation (21) is employment of the term average specific resistance, α_{av}, defined by[24]

$$\alpha_{av} = \frac{p - p_1}{\int \frac{dp_s}{\alpha}} \tag{22}$$

the limits of the integral being taken between 0 and $(p - p_1)$. The average specific resistance term is considered to be a function of Δp. For calculations involving compressible cakes when medium resistance is not negligible, it is often convenient to express the total resistance of filtration in one term, $(\alpha_{av}w + R_m)$, this term being evaluated from experimental data.

The factor m in Equation (20) cannot be taken as constant if the filter cake compresses during the filtration as m is a function of the average porosity of deposited solids,

$$m = \frac{\text{mass wet cake}}{\text{mass dry cake}} = \frac{w + \epsilon_{av}\rho L}{w} = 1 + \frac{\epsilon_{av}\rho}{(1 - \epsilon_{av})\rho_s} \tag{23}$$

In Equation (22), ϵ_{av} represents the over-all, or average, porosity of the cake. Equation (4) relating w to ϵ and L was employed to obtain Equation (23). To illustrate a typical variation in m during filtration of a compressible material, the change in m for average cake porosity changing from 0.85 to 0.75 is given by: $\epsilon_{av} = 0.85$, $m = 2.77$; $\epsilon_{av} = 0.75$, $m = 1.93$ ($\rho = 62.4$ lb. per cu. ft. and $\rho_s = 200$ lb. per cu. ft.).

If the slurry being filtered is dilute, for example less than five per cent solids by weight for cake porosities on the order of 0.75, a variation in m of the magnitude given above will have negligible effect on calculations of volume of filtrate vs. time. Calculations are simplified for these cases by assuming m to have some average value during the entire filtration.

In the development of an expression for calculating the volume of filtrate vs. time leading to Equation (21), a number of simplifying assumptions were introduced. These assumptions are reviewed in the following outline:

(1) Equilibrium porosities are obtained instantaneously during the course of filtration. This assumption is probably valid in a practical sense for filtrations carried out slowly and for moderately compressible materials.

(2) Solid particles in the cake are in point contact. Derivation of Equation (9) defining solids pressure in terms of hydraulic pressure depends on contact at a point rather than over a surface.

(3) Filtrate flow through the cake is constant and equivalent to the flow rate through the medium. In filtration of dilute slurries little error results from this assumption because the volume of flow through the cake is large compared to filtrate produced as a result of decreasing cake porosity with increased pressure.

(4) Resistance of the medium is constant. Medium resistance may vary during filtration because penetration of solid particle causes blocking of flow passages and decreased permeability. Constant pressure filtration data has indicated medium resistance is in the range 0.01 to 0.1 of final cake resistance when the correct medium is employed.[25]

(5) Flow resistance in the cake at any point is a function only of solids pressure at that point.

(6) Data from compression-permeability cell measurement, in which mechanical solids pressure is imposed on the cake, are equivalent to data obtained during actual filtration conditions in which solids pressure is developed by accumulated reaction to hydraulic shear stresses.

(7) Flow through the cake follows hydraulic laws for viscous flow of Newtonian fluids (constant viscosity).

(8) Changes in average cake porosity can be ignored in calculating time rate of change of volume of filtrate.

Equations for calculating filtrate for the three categories of filtration methods (constant pressure, constant rate, and variable pressure-rate using centrifugal pumps) are separately developed according to the conditions imposed by the method. Illustrations are provided to demonstrate application of these equations.

Values of cake resistance to be used in the calculations are established experimentally. The possible experimental approaches that can be employed depend to some extent on properties of the solids in the slurry. Three classifications for solids properties are: (1) specific resistance constant and the material considered incompressible; (2) filtration resistance variable, following Kozeny's relationship; (3) filtration resistance variable and evaluated by experimental data. When case (1) holds, a single test filtration yields a value of specific resistance which then can be applied to calculations at any pressure in the normal filtration range. Case (2) requires a single filtration and measurement of porosity to obtain the Kozeny term, kS_o^2. Further porosity measurements at a range of pressures are required to determine the manner in which porosity varies with pressure. Since Kozeny's relationship has been shown previously to have serious limitations in its applicability, it is preferable to follow the procedure of case (3) when there is reason to believe cake compressibility is significant. The case (3) situation is most general, requiring test work bracketing the proposed range of operating pressure to establish the resistance-pressure relationship. Average specific resistance may be calculated by numerical integration from compression-permeability cell data or may be obtained in filtrations performed under set conditions. The technique of performing these calculations will be demonstrated by examples. The next section, "Experimental Methods", describes procedures used to establish resistance data.

Constant Pressure Filtration

When calculations are to be made for a compressible cake and medium resistance having a finite value, results are obtained by numerical integration of Equation (21). Analytical treatment is not possible in general because α_{av} is a function of $(p - p_1)$ determined by experimental data. The calculation procedure follows three steps. First, a relationship of α_{av} vs. $(p - p_1)$ is established by taking data from a series of constant pressure filtrations or from compression-permeability cell data as described in the next section. In the second step, values of filtrate volume v are calculated corresponding to filtrate rates q by Equation (24)

$$q = \frac{1 - ms}{s\rho} \frac{g_c}{\mu} \frac{1}{v} \frac{p - p_1}{\alpha_{av}} \tag{24}$$

Equation (24) is combined from Equations (17), (20), and (21). At constant pressure and constant medium resistance $(p - p_1)$ is determined by q through Equation (18). Values of α_{av} corresponding to $(p - p_1)$ are substituted into Equation (24) for each calculation. In the third step, a tabulation of time vs. filtrate volume is obtained by stepwise numerical integration of Equation (25) integrated from Equation (19)

$$\theta = \int_{\theta}^{v} \frac{dv}{q} \tag{25}$$

This calculation procedure is illustrated by Example 1. for constant pressure filtration of talc.

Example 1. Constant Pressure Filtration of Talc for Resistance of Filter Medium Having Constant Finite Value R_m

A five per cent (s = 0.05) slurry of talc is to be filtered at fifteen pounds per square inch pressure differential. Medium resistance is constant at 10^{10} ft. $^{-1}$. Viscosity of filtrate is taken as 0.001 (lbm.)/(ft.)(sec.) (μ = 1.49 centipoise), solids density as 167.0 (lbm.)/(cu.ft.), and filtrate density as 62.4 (lbm.)/(cu.ft.). Average specific cake resistance is plotted vs. pressure in Figure (18), the data being considered to adequately characterize the specific slurry being filtered. As may be noted from the curvature in the plotted values of α_{av} vs. Δp, the talc slurry forms a compressible cake. In Table I the first column contains values of filtrate flow rate q selected to provide a suitable array of terms to plot for subsequent numerical integration. The second column contains corresponding values of medium interface pressure p_1 calculated from R_m and q by Equation (18) in the form

$$p_1 = \frac{\mu}{g_c} R_m \, q = \frac{(0.001)(10^{10})}{(32.2)} \, q$$

in which q is given in units (cu.ft.)/(sq.ft.)(sec.) and p_1 has units of pounds force per square foot. The terms in the column under medium pressure are converted to pounds force per square inch. Values of average specific resistance taken from Figure (18) corresponding to (15 - p_1) are tabulated next. Using Equation (24) filtrate volume v is calculated for each q using m = 2.65

$$v = \frac{1 - (2.65)(0.05)}{(0.05)(62.4)} \frac{32.2}{0.001} \frac{1}{q} \frac{p - p_1}{\alpha_{av}}$$

These values of v are plotted vs. reciprocal filtrate rate 1/q in Figure (19). Using Simpson's rule for numerical integration, Equation (25) is integrated for time in increments of v. The first integration, corresponding to an increase in filtrate volume from zero to 0.004 (cu.ft.)/(sq.ft.), is illustrated

v	n	1/q
0	1	143
0.001	4	144
0.002	2	147
0.003	4	150
0.004	1	153

$$\theta = \frac{\Delta v}{3} \Sigma\, n(1/q)$$

$$\theta = \frac{0.001}{3} (1766) = 0.59 \text{ sec.}$$

The calculation procedure just outlined can be greatly simplified if hydraulic pressure at the medium p_1 is considered constant during filtration. Integration of Equation (21) can be carried out since α_{av} and m become constants determined by $(p - p_1)$. Substituting Equation (18) into Equation (21) and solving for $\frac{dv}{d\theta}$

$$\frac{dv}{d\theta} = \frac{g_c\ p}{\mu \left(\frac{s\rho}{1 - ms} \alpha_{av}\ v + R_m\right)} \tag{24a}$$

with integration resulting in

$$\mu \left(\frac{s\rho}{1 - ms}\right) \alpha_{av} \frac{v^2}{2} + \mu\, R_m\, v = g_c\ p\ \theta + C \tag{26}$$

The constant of integration drops out since initially time and volume of filtrate are both zero. Equation (26) is demonstrated in Example 2. for filtration of talc under the same conditions as used in the calculations of Example 1.

Example 2. Constant Pressure Filtration of Talc for Hydraulic Pressure at Medium Neglected

Using the same data for calculations as utilized in Example 1., the time θ to collect volumes of filtrate of 0.020, 0.100, and 0.180 (cu.ft.)/(sq.ft.) will be calculated using Equation (26). Average specific resistance at fifteen pounds per square inch is taken from Figure (18) as 1.81 (10^{11})(ft.)/(lbm.).

$$\theta = \frac{1}{2} \frac{(0.001)}{(32.2)} \frac{(0.05)(62.4)}{1 - (2.65)(0.05)} \frac{(1.81)(10^{11})}{(15)(144)} v^2 + \frac{(.001)(10^{10})}{(32.2)(15)(144)} v$$

TABLE I

CONSTANT PRESSURE FILTRATION OF TALC

q	p_1	α_{av}	v	θ
cu.ft./(sq.ft.)(sec.)	lbf./sq.in.	ft./lbm	cu.ft./sq.ft.	seconds
6.96 (10^{-3})	15.0	0.32 (10^{11})		
			0.004	0.59
6.00	12.9	0.71	0.0063	
			0.008	1.24
5.00	10.8	1.01	0.0107	
			0.012	2.02
4.00	8.63	1.29	0.0159	
			0.016	2.94
			0.020	4.00
3.00	6.47	1.40	0.0262	
2.00	4.31	1.54	0.0448	
			0.060	22.48
1.50	3.24	1.63	0.0622	
1.00	2.16	1.69	0.0976	
			0.100	55.74
0.75	1.62	1.72	0.1339	
			0.140	105.90
			0.180	171.18
0.50	1.08	1.75	0.2048	

Calculations using this expression result in

v (cu.ft.)/(sq.ft.)	θ (sec.)
0.020	4.75
0.100	61.2
0.180	178

Comparison of the results calculated in Examples 1. and 2. indicates that an error of small magnitude arises from assumption of negligible change in medium pressure drop. In Figure (19) calculated values of 1/q and v are plotted for the purpose of carrying out the numerical integration indicated by Equation (25). The plot of 1/q vs. v is linear except for the initial portion corresponding to small values of time. When the terms of Equation (26) are divided by the product $(p)(v)(g_c)$ the linear equation is obtained

$$\frac{\theta}{v} = \frac{1}{2}\frac{\mu}{g_c}\frac{s\rho}{1 - ms}\frac{\alpha_{av}}{p}\,v + \frac{\mu}{g_c}\frac{R_m}{p} \tag{27}$$

The slope of the plotted points of the linear portion of $\frac{d\theta}{dv}$ vs. v in Figure (19) calculated in Example 1. corresponds to the term $\frac{1}{2}\frac{\mu}{g_c}\frac{s\rho}{1 - ms}\frac{\alpha_{av}}{p}$ from Equation (27). The agreement between results calculated by the procedure outlined for Example 1. and the simplified method of Example 2. becomes good when data indicate less compressible systems and filtration pressures become higher. It is safe to use the simplified approach with good accuracy in calculations for filtrations above fifteen pounds per square inch pressure. Below this pressure, especially in vacuum filtration calculations in which low pressures are encountered, greater errors may result if the solids being filtered are compressible.

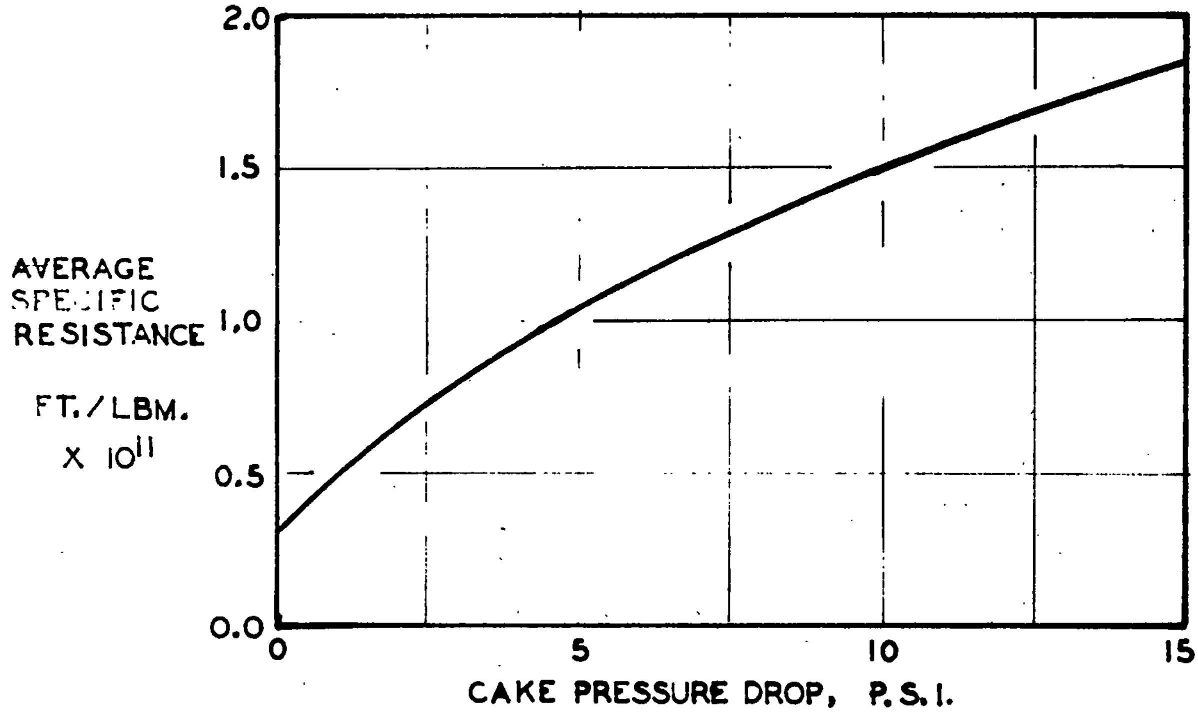

FIGURE 18.

AVG. SPEC. RES. VS. SOLIDS PRESSURE TO 15 P.S.I. FOR TALC C

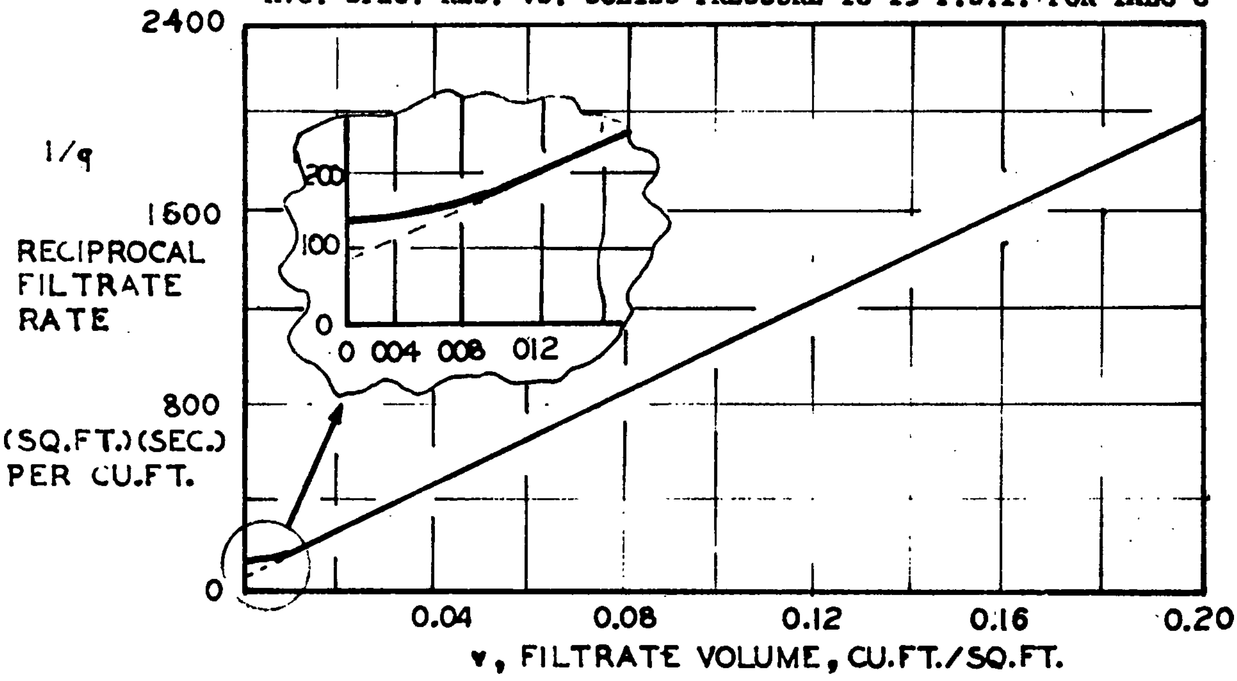

FIGURE 19.

CONSTANT PRESSURE FILTRATION OF TALC -- INTEGRATION FOR TIME

Examination of medium resistance during constant pressure filtration is frequently accomplished by plotting observed time-filtrate volume data according to Equation (27). When the straight line obtained by plotting the data is extrapolated to zero on the abscissa, the value of the intercept is used to calculate a value for R_m. Inherent error will result in this method if the solids are compressed during the filtration since a linear extrapolation is generally incorrect as shown in Figure (19). However, medium resistance values obtained in this manner generally cannot be relied upon as accurately representing true conditions because the resistance of the filter medium can be a function of several variable factors dependent upon transient conditions existing during the course of filtration. Initial medium resistance depends on the characteristics of solids imbedded in the medium surface, these characteristics being determined by initial velocity of flow into the medium, partial classification of particle sizes during the early stages of filtration, and the rapidity with which full filtration pressure is attained. Equations previously developed describing the filtration process are based on the assumption that cake filtration begins instantaneously whereas a finite interval of time is needed to intercept particles to form the initial layer of cake. It has been shown experimentally that filtration taking place in the interior pores of the medium is more accurately described by expressions other than the Poisueille law.[30] In discussing medium resistance it is often overlooked that permeability of a new medium will increase from very low values at the first instant of filtration to higher values immediately after solid particles embed in surface pores. Consequently the instantaneous initial flow rate of filtrate is not necessarily related to a value of medium resistance found after the filtration is completed. It has been reported that a solids layer at the interface of cake and medium is a chief source of flow resistance, particularly in precoat systems in which the precoat solids are usually free filtering.[29] This observation is explained by the likelihood of particle size classification during initial flow causing pores of the medium to be blocked by fine particles producing high localized flow resistance. Analysis of medium resistance characteristics leads to the conclusion that evaluation of medium resistance magnitude from usual filtration data has no fundamental significance. Data obtained by this means to be utilized in technical calculations must be discounted due to the possibility of unrealistic results being obtained.

Rotary vacuum filtration is a commonly encountered method for carrying out large scale industrial filtrations in continuous processes. It has been previously pointed out that rotary filtrations are frequently performed under variable pressure conditions but are treated analytically as taking place at constant pressure if a pressure correction for the changing static head of filtrate above the filter surface is added to the constant operating pressure differential. Pressure corrections for disc and drum types of filters are necessary because the static pressure on the submerged filter surface may be a significant portion of the pressure differential supplied by the pump.

Rotary pan filter pressure differentials are not readily corrected for static head because the depth of slurry is small and is continuously added during filtration to a maximum depth of only a few inches on the pan.

In rotary disc filtration, the static pressure at the centroid of the submerged section of the disc is added to the operating pressure differential. The static head correction, p_s, is calculated from Equation (28) obtained by integration for the position of the centroid

$$p_s = \rho_f \, h_{cent} = \frac{2}{3} \rho_f \, R \, \frac{\cos^2(\beta/2) - 1}{\sin^2(\beta/2)} \tag{28}$$

where ρ_f is slurry density, R is disc diameter, and β is angle of submergence of the disc taken from its axis of rotation as shown in Figure (1A).

An expression for correcting rotary drum operating pressure for static head of slurry is derived by taking the time averaged head of slurry above the drum. Letting β as before be the central angle subtending the arc of the submerged portion of drum and ϕ the central angle subtending the segment of arc between the surface of the slurry and a differential area of drum surface dA as shown in Figure (1B) the height of slurry above dA is h where h is given by

$$h = R\cos(\beta/2 - \phi) - R\cos(\beta/2)$$

and average h is

$$h_{av} = \frac{\int_0^\beta h\,d\phi}{B} = \frac{R\int_0^\beta \left[\cos(\beta/2 - \phi) - \cos(\beta/2)\right] d\phi}{\beta}$$

$$= \frac{R}{\beta} \sin(B/2) - \beta/2 \cos(\beta/2)$$

Using the expression for average height of slurry, the average correction for pressure of filtration is given by p_s

$$p_s = \rho_f\, h_{av} = \rho_f \left[\frac{R}{\beta} \sin(\beta/2) - \beta/2 \cos\, (\beta/2)\right] \tag{29}$$

The rate of solids filtration from a slurry by rotary drum filtration can be calculated by integrating for the volume of filtrate per unit area of a section of drum surface passing through the slurry from which

$$w_{max} = \frac{s\rho}{1 - ms} v_{cycle}$$

The rate of solids recovery for the drum is then

$$W = 2\pi\, R\, \omega\, L\, w_{max} \tag{30}$$

where W is weight of solids filtered per minute, ω is drum rotation rate in radians per second and L is drum width. For simplified calculations v is obtained using Equation (26) for time $\theta = \frac{\beta}{\omega}$. The continuous filtrate flow rate can be obtained by material balance using Equations (20) and (30).

Rotary disc filtration calculations for time rate of solids recovery require numerical methods of mathematics to obtain solutions. The disc can be considered to consist of an infinite number of concentric rings of differential thickness each having different residence times in the slurry in which the disc continuously rotates. The time of submergence of a thin ring of width dr at radius r as indicated in Figure (1A) is

$$\theta = \frac{\phi}{\omega} \frac{2\left[\frac{\beta}{2} - \arccos \frac{r}{R \cos\, (\beta/2)}\right]}{\omega}$$

where ϕ is the central angle subtending the points on the arc of radius r at the slurry surface. Using the form of Equation (26) in which the constant terms are lumped into K and medium resistance is neglected, the volume of filtrate is given by

$$v = (2K\theta)^{1/2} = 2\sqrt{\frac{K}{\omega}}\left[\frac{\beta}{2} - \text{arcos}\,\frac{r}{R\cos(\beta/2)}\right]^{1/2}$$

Following this expression the total volume filtered and solids recovery may be obtained by integrating for all r from R to R cos(β/2)

$$W = 2\pi R\omega\,\frac{s\rho}{1-ms}\int_{R\cos(\beta/2)}^{R} v\,dr = R\omega\pi\,\frac{4s\rho}{1-ms}\sqrt{\frac{K}{\omega}}\int_{R\cos(\beta/2)}^{R}\left[\frac{\beta}{2} - \text{arcos}\,\frac{r}{R\cos(\beta/2)}\right]^{1/2} dr \qquad (31)$$

to which numerical methods can be applied to obtain solutions. This analysis assumes that the disc sectors are closely spaced to produce a vacuum differential uniformly on each element of surface as it enters the slurry. The error of this approach depends on the ability of the vacuum pump to produce operating vacuum in sectors in the time interval of partial submergence.

Hydraulic pressure losses due to friction in pipe connections, fittings, feed lines, and filtrate draw off lines have been considered negligible. Usually flow conduits in filtration equipments are of ample size for the volume of flow being carried and hydraulic losses can safely be neglected. For this requirement to be met, ample clearance must be provided between the downstream side of the medium and the support screen to carry filtrate into drawoff lines without appreciable pressure drop.

Constant Rate Filtration

Length of constant rate filtration cycles are determined by a cutoff pressure. When a certain pressure is reached the flow of slurry is stopped and cake washed or discharged from the filter. Feed is constant rate filtration is supplied at a positive pressure by reciprocating or diaphram pumps. Assuming filtrate is discharged to atmospheric pressure and pressure losses in the filtrate conduits are negligible the batch constant rate filtration is terminated when the maximum discharge pressure of the pump is attained or the maximum operating pressure of the filtration equipment is reached.

The time required to reach a given pressure drop across the filter cake is given by Equation (32) combined from Equations (3), (20), and (25)

$$\theta = \int \frac{dv}{q} = \frac{v}{q} = \frac{1}{q}\left[\frac{1 - ms}{s\rho} w\right] = \frac{1}{q^2} \; \frac{1 - ms}{s\rho} \, \frac{g_c}{\mu} \; \frac{\Delta p}{\alpha_{av}} \tag{32}$$

If medium resistance is known and assumed constant the pressure p_1 at the medium calculated from Equation (18) is subtracted from the maximum filtration pressure for Δp in Equation (32). Average specific resistance and average porosity to calculate m are evaluated at Δp.

Plots of specific resistance data from compression-permeability cell measurement are found to be linear with pressure on log-log plots over wide pressure ranges as shown in Figures (11) and (12). Taking n as the slope in the log-log relationship an empirical expression for many compressible materials can be written in the form

$$\alpha = \alpha_o \, p_s^{\,n} \tag{33}$$

Equation (33) can be substituted into Equation (17) in the integral for α for use in calculating filtrations of compressible materials when α is approximated by the logarithmic relationship over the applicable range of filtration pressure. Integration of the substituted equation following the form of Equation (32) results in

$$\theta = \frac{v}{q} \quad \frac{1 - ms}{s\rho} \frac{1}{q^2} \frac{g_c}{\mu} \int_{p_i}^{p-p_1} \frac{dp_s}{\alpha_o p_s^{\,n}} = \frac{1-ms}{s\rho} \frac{1}{q^2} \frac{g_c}{\mu} \frac{1}{\alpha_o(1-n)} \left[(p-p_1)^{1-n} - p_i^{\,1-n} \right] \quad (34)$$

where the upper limit $(p - p_1)$ represents the maximum pressure of filtration and p_i represents some arbitrary lower limit below which integration is carried out assuming α is constant and equal to $\alpha_o p_i^{\,n}$. The lower limit is necessary because $\frac{dp_s}{\alpha_o p_s^{\,n}}$ will approach ∞ for p_i approaching zero. The form of Equation (34) is similar to the expression determined empirically from constant rate filtration data by Luke.[41] The exponent n in Equation (33) has been calculated from compression-permeability cell measurement to range in value up to about 2.0, but the empirical relationship is probably not valid for values of of n greater than 0.7. Experimental values of n provide a measure of relative compressibility of filterable solids.[62] Magnitudes of n greater than 0.5 are regarded as being indicative of highly compressible materials whereas below 0.2 is characteristic of relatively incompressible cakes.

The final volume of filtrate v in Equation (32) is obtained from a material balance at the final pressure differential across the cake, final mass of solids, and final filtrate rate. The filtrate rate is taken as constant in Equation (32) through the entire filtration. When average cake porosity varies over a wide range up to the maximum pressure of filtration the value of m will vary appreciably with the result that q_{feed} will not equal $q_{filtrate}$ during the filtration. Tiller has pointed out that it is necessary to have information relating rate of change of m with time to calculate the true filtrate flow rate during filtration.[62] During filtration of compressible materials, q will vary from point to point in the cake thickness as a function of the rate of change of point porosity with time. Differentiating the material balance of Equation (20) with time yields

$$q = \frac{dv}{d\theta} = \frac{d}{d\theta}\left(\frac{1 - ms}{s\rho} w\right) = \frac{1 - ms}{s\rho} \frac{dw}{d\theta} - \frac{w}{\rho} \frac{dm}{d\theta} \tag{35}$$

to account for variation in porosity on filtrate rates during constant rate filtration. It is therefore not possible to accurately use the expression $\theta = v/q$ for calculations for constant rate filtration of compressible materials until m and w are determined as functions of time by trial and error. Filtrate volume is related to the constant slurry feed rate q_{feed} by volume balance

$$v = q_{feed}\,\theta - \frac{w}{\rho}(m - 1) = q_{feed}\,\theta - \frac{s\rho}{1 - ms}\frac{v}{\rho}(m - 1) \tag{36}$$

which can be solved for v

$$v = \frac{q_{feed}\,\theta}{1 + \frac{s\,(m - 1)}{1 - ms}} \tag{37}$$

Example 3. is provided to demonstrate the use of approximate calculations for time of constant rate filtration assuming negligible change in over-all filtrate velocity through the cake. The results found in Example 3. show good agreement between calculations based on the empirical equation used in Equation (34) and those using final cake properties from Equation (32).

It has been observed that under practical filtration conditions rapid feed rates of the same slurry will produce a greater volume of filtrate before a maximum pressure is reached as compared to slow feed rates. Tiller investigated this behavior in a series of constant rate filtrations of Kaolin slurry.[62] Analysis of data following Equation (34) yielded values of n for the series of filtrations conducted at different rates, the values of n being found ranged from about 0.25 for two minute filtrations to 0.44 for a twenty minute filtration. Above this time of filtration the value of n remained constant, the plot of n vs. time being parabolic from zero time to twenty minutes after which n became constant. Since the value of n indicates the relative rate of change of specific resistance with pressure it is evident that filtrations conducted at high rates with compressible solids result in greater filtrate per unit area because of the lower rate of increase of cake resistance as solids accumulate. Tiller interpreted these data as indicating that equilibrium consolidation of the particles was not being attained during the high rate filtrations.

Example 3. Constant Rate Filtration of Talc

A talc slurry for which the solids have resistance and porosity properties shown in Figures (11), (12) and (18) is to be filtered with an enclosed pressure leaf filter having two hundred square feet of surface. The maximum pressure of filtration is 50 p.s.i. being limited by the maximum operating pressure of the filter shell. The slurry is 10.0% solids by weight (s = 0.10) and physical properties of solids and filtrate identical to those given in Example 1. A feed rate of 0.25 gallons per minute per square foot is to be supplied by a reciprocating pump. To dampen the pump pulsations an air chamber is provided on the feed line. The total change in volume of air space in the chamber is small enough to neglect correcting the total volume of feed for the volume delivered to the air chamber.

Curve A of Figure (20) shows average specific resistance plotted as a function of pressure drop across the cake and Curve B indicates the variation in average cake porosity. To determine the pressure drop across the cake it is necessary to determine the pressure at the filter medium at the specified flow rate. Assuming that medium resistance remains constant medium pressure drop is calculated from Equation (18). It is also necessary to convert the filtrate rate to units cu.ft./(sq.ft.)(sec.)

$$q = 0.000557 \text{ cu.ft./(sq.ft.)(sec.)}$$

$$R_m = 10^{10} \text{ 1/ft.}$$

$$p_1 = \frac{(0.001)\ (10^{10})\ (0.000557)}{(32.2)\ (144)} = 1.22 \text{ p.s.i.}$$

Cake pressure drop is then 48.8 p.s.i., significant in calculations. Average cake porosity is 0.779 for this pressure and m is calculated from Equation (23) to be 2.317. Average specific resistance is read from Figure (20) for 50 p.s.i. as 3.35 (10^{11}). Substituting these terms into Equation (32) results in

$$\theta = \frac{(32.2)\ (1 - 0.10 \cdot 2.317)(48.8)\ (144)}{(0.001)(0.000557)^2\ (0.10)\ \ (62.4)\ (3.35)(10^{11})} = 275 \text{ seconds}$$

The volume of filtrate is calculated from Equation (37)

$$v = \frac{(0.000557)\ (275)}{1 + \dfrac{0.10(2.317 - 1)}{1 - (2.317)(0.10)}} = 0.131 \text{ cu.ft./sq.ft.}$$

which compares to 0.1529 cu.ft./sq.ft. based on the feed rate only.

Tiller determined the slope of talc compression-permeability cell specific resistance data vs. pressure shown in Figure (11) and found a value of n = 0.5/8. A value for α_o at one pound per square inch is read from Figure (18) as 0.85 (10^{11}). Substituting terms into Equation

$$\theta = \frac{(32.2)(1 - 2.317 \cdot 0.10)(144)\ (48.8^{0.492})}{(0.001)\ (0.10)\ (62.4)(0.85)(10^{11})\ (0.492)} = 286 \text{ seconds}$$

Variable Pressure-Variable Rate Filtration

The most common method for charging feed to a batch filter is by means of a centrifugal pump. Each centrifugal pump has a characteristic pumping rate for a given back pressure. During filtration, resistance to flow builds up as cake is deposited. The pumps act against a continuously increasing pressure and the rate of feed supply

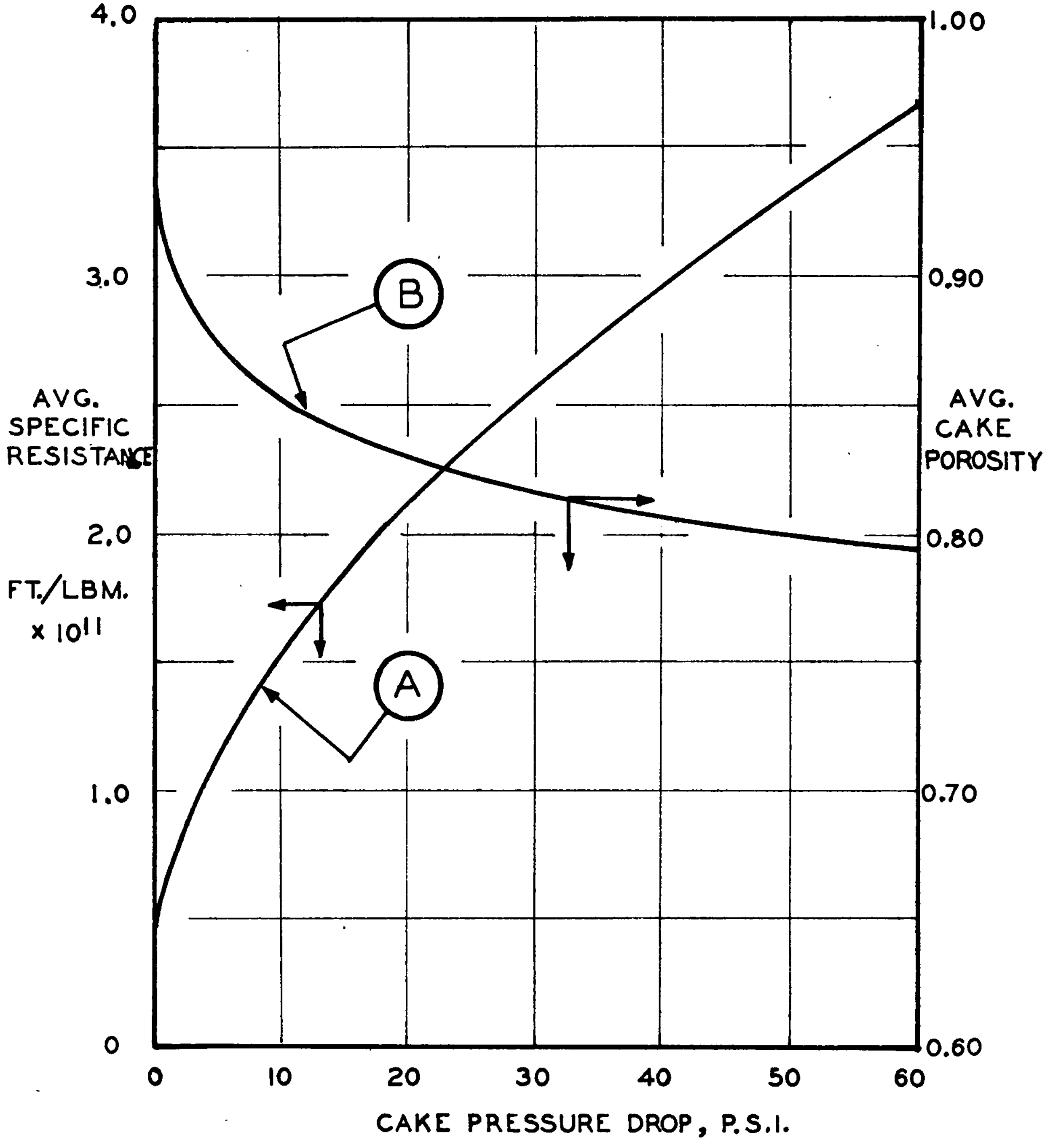

FIGURE 20.

AVERAGE SPECIFIC RESISTANCE AND AVERAGE POROSITY VS. SOLIDS PRESSURE TO 60 P.S.I. FOR TALC C

to the filter gradually decreases to the pump output rate corresponding to the pressure drop across the cake and medium. Centrifugal pump output is highest when the back pressure on the pump is least and decreases to zero when the maximum or shutoff pressure of the pump is reached. Pump manufacturers supply performance curves relating the pumping rate vs. pressure. A typical curve is shown in Figure (21).

Calculations for batch filtrations using centrifugal pumps as a feed supply require knowledge of the pressure vs. rate characteristics of the pump given in the performance curve.[63] Numerical methods are applied in the general case filtering compressible solids. Example 4. illustrates use of the pump performance curve shown in Figure (21) for filtration of talc slurry in a plate and frame filter. A filtration cycle is completed when the frame volume is filled with solids. Filtration takes place through both faces of the frame under ideal conditions. The thicknesses of the oppositely faced cakes are assumed uniformly thick and equal for calculation purposes until the end of the filtration when the faces merge into one cake. Numerical integration is more convenient using an altered form of Equation (25) in integrating for time

$$\theta = \int \frac{dv}{q} = \frac{v}{q} - \int v \, d\left(\frac{1}{q}\right) \tag{38}$$

The incremental size of $1/q$ is chosen to supply the required accuracy in integrating for time in Equation (38). For each q, pressure drop is obtained from the pump performance curve. Evaluation of average specific resistance and average cake porosity as a function of pressure permits calculation of v by Equation (24) with m being evaluated by Equation (23).

Numerical evaluation of filtration rates using centrifugal pumps may be carried out more rapidly for estimating performance by substituting an expression relating q vs. p in the fundamental equation, Equation (17). Pump performance curves may be approximated by an elliptical equation of the form

$$a^2p^2 + b^2q^2 = r^2 \tag{39}$$

For conservative estimate specific resistance and porosity evaluated at the maximum pressure can be inserted as constants into Equation (17). Medium resistance can be neglected since the pump output provides a maximum initial flow rate. The fundamental equation becomes after substitution

$$dv = \frac{1 - ms}{s\rho} \frac{g_c}{\mu\,\alpha} \frac{\quad}{\sqrt{r^2 - a^2p^2}} \tag{39a}$$

Time to reach a given pressure can be obtained by integration

$$\theta = \int \frac{dv}{q} = \frac{1 - ms}{s\rho} \frac{g_c}{\mu\,\alpha} \frac{b^2}{a} \int \frac{a\,dp}{r^2 - a^2p^2} = \frac{1 - ms}{s\rho} \frac{g_c}{\mu\,\alpha} \frac{1}{2r} \ln\frac{r + ap}{r - ap} \tag{40}$$

Filtrations conducted at constant pressure result in greater output per unit time on stream as compared to filtration of the same slurry at constant rate to a given maximum pressure. This is shown by the simplified form of the fundamental equation

$$q = \frac{g_c}{\mu} \frac{1 - ms}{s\rho} \frac{1}{v} \frac{1}{\alpha} \frac{p}{v} = \frac{dv}{d\theta} \tag{41}$$

Integration and solution for v for constant pressure performance results in

$$v = \sqrt{\frac{2\theta}{pK}} \tag{41a}$$

where $K = \frac{1 - ms}{s\rho}\frac{g_c}{\mu\alpha}$, constant terms. Constant rate performance is obtained from Equation (41) for $v = q\theta$

$$v = \sqrt{\frac{\theta}{pK}} \tag{42}$$

Comparing filtrate volume per unit time for constant pressure and constant rate operation by dividing Equation (41a) by Equation (42) produces

$$\frac{v_{\text{constant pressure}}}{v_{\text{constant rate}}} = \sqrt{2}$$

When using centrifugal pump feed supply, performance advantage is obtained if constant pressure operation is approximated rather than constant rate as determined by the pump curve.

Example 4. Filtration in Plate and Frame Press with Centrifugal Pump Feed Supply

An open impeller centrifugal pump having performance indicated by the curve in Figure (21) is to supply slurry to a plate and frame filter press having eight 4 x 4 feet frames with cake space two inches thick. The slurry is ten per cent by weight fine talc, filtration data for which is given in Figure (20). The time required to fill the press with solids is to be calculated using this data and pump curve.

The increment of 1/q to be used in the integration for time using Equation (38) is 100 sec./ft., this size increment being chosen by rough approximation of time and volume of filtrate beforehand to provide a convenient set of points for numerical computation. Values of q read from Figure (21) are converted from g.p.m. to cu.ft./(sq.ft.) (sec.) by the multiplier 8.70 (10^{-6}) based on total filtration area of the press of 256 sq.ft. Filtrate density and viscosity during the filtration and solids density are the same as given in Example 1. For each incremental increase in 1/q the volume of filtrate is calculated from

$$v = \frac{(32.2)\ (1 - 0.10m)(1.149 \cdot 10^5)(144)}{(0.001)\ (62.4)\ (0.10)\ q}\ \frac{\Delta p}{\alpha_{av}}$$

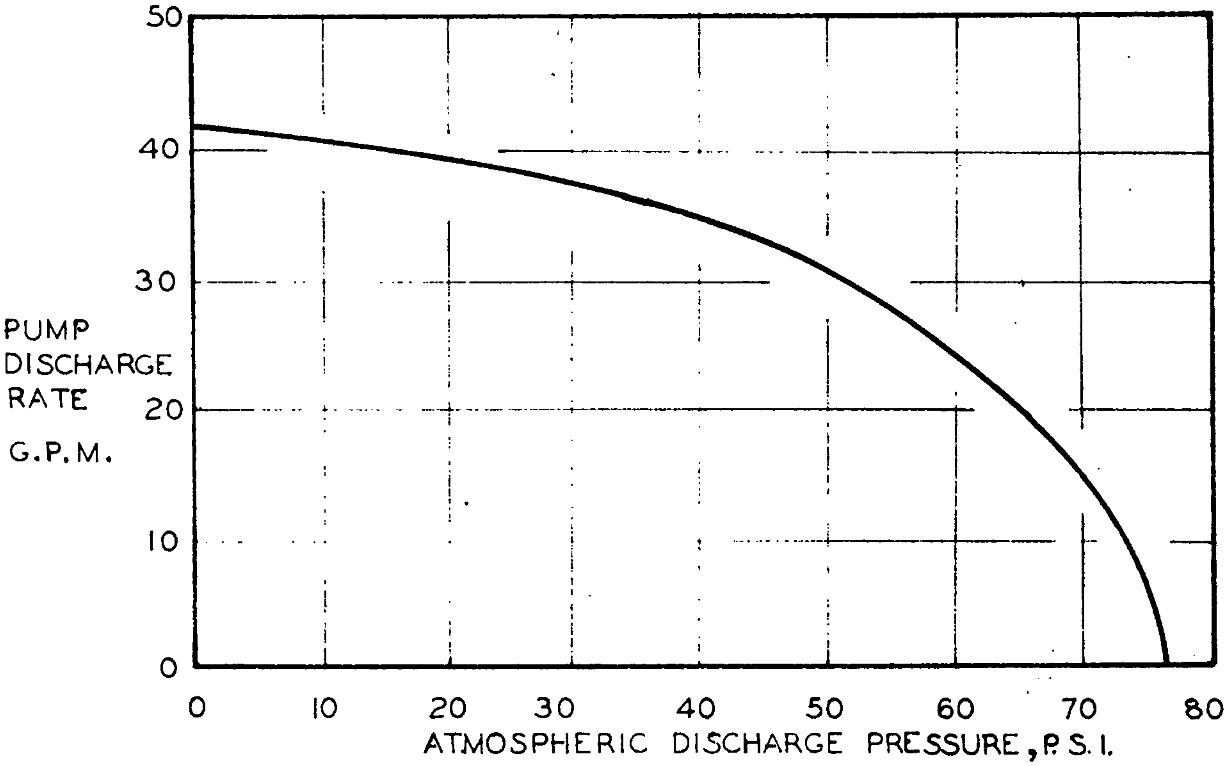

FIGURE 21.

PERFORMANCE CURVE OF TYPICAL OPEN IMPELLER CENTRIFUGAL PUMP

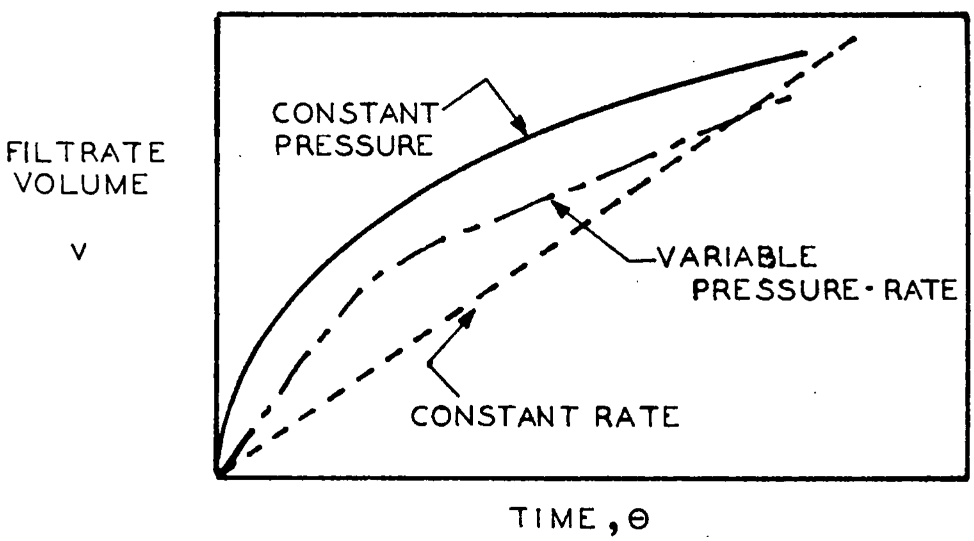

FIGURE 22.

VOLUME OF FILTRATE VS. TIME FOR TYPICAL FILTRATION OPERATIONS

where for convenience q is substituted in gallons per minute total flow and Δp in pounds per square inch. The calculations are completed when for an incremental increase in $1/q$ the thickness of cake L exceeds one inch where L is calculated in

$$w = \rho_s (1 - \epsilon_{av}) L$$

altering Equation (4). The initial value of q is obtained for pump pressure equal to the pressure drop across the medium at initial maximum flow. Assuming constant medium resistance and no loss of pressure due to friction in filtrate outlet conduits in the press

$$p_i = \frac{(0.001)(10^{10})}{(32.2)(144)(2736)} \text{ p.s.i.} = 0.79 \text{ p.s.i.}$$

by Equation (18) for $R_m = 10^{10}$ 1/ft. To obtain cake properties the pressure drop across the cake taken as the pump pressure corresponding to the flow rate minus the medium pressure drop. The incremental calculation results are given in Table II.

The number of incremental points including v = 0 in Table II up to the cake thickness of one inch is an even integer. Numerical integration by Simpson's rule for the total time will be accomplished in two parts since an odd number of points are summed according to the derivation of the rule. The time to filter to v = 0.2889 cu.ft./sq.ft. by the first integration is

$$\theta = (0.2889)(3536) - \frac{100}{3}(14.634) = 859 \text{ seconds}$$

and the filtration time from 0.2889 to 0.3871 cu.ft./sq.ft. filtrate volume is

$$\theta = (0.3871)(4236) - (0.2889)(3536) - \frac{100}{3}(20.517) = 390 \text{ sec.}$$

the total time being the sum of these, 1249 seconds or 20.8 minutes.

Time vs. volume of filtrate for the variable pressure-variable rate filtration calculated in Example 4. is illustrated in Figure (22) along with typical constant rate and constant pressure filtration data. The tangent to the slope at any point on the curves is the filtrate rate. Constant pressure data plotted in this manner is always parabolic as indicated by Equation (41). In constant rate filtration when the filtrate rate does not materially differ from the feed rate volume vs.

TABLE II

FILTRATION IN PLATE AND FRAME PRESS
WITH CENTRIFUGAL PUMP FEED SUPPLY

$1/q$	q	Δp_{pump}	Δp_{cake}	ϵ_{av}	α_{av}	v	w	L
(sq.ft.)(sec.)/(cu.ft.)	g.p.m.	p.s.i.	p.s.i.		ft./lbm.	cu.ft./sq.ft.	lbm./sq.ft.	inches
2736	41.9	0.8	0.0	0.871	0.32 (10^{11})	0.0	0.0	0.0
2836	40.5	14.6	13.8	0.815	1.78	0.1213	1.027	0.4
2936	39.1	23.7	22.9	0.801	2.26	0.1667	1.385	
3036	37.8	29.8	29.0	0.794	2.54	0.1955	1.613	
3136	36.6	34.4	33.6	0.791	2.73	0.2187	1.795	
3236	35.5	37.8	37.0	0.788	2.87	0.2370	1.940	
3336	34.4	41.1	40.3	0.785	2.99	0.2560	2.090	0.70
3436	33.4	43.9	43.1	0.783	3.09	0.2729	2.228	
3536	32.5	46.0	45.2	0.782	3.16	0.2889	2.350	0.77
3636	31.6	48.2	47.6	0.781	3.24	0.3043	2.472	
3736	30.7	50.4	49.8	0.780	3.32	0.3196	2.593	
3836	30.0	51.8	51.0	0.779	3.37	0.3329	2.697	
3936	29.2	53.5	52.7	0.778	3.42	0.3483	2.818	
4036	28.5	54.7	53.9	0.777	3.46	0.3615	2.921	0.94
4136	27.8	55.7	54.9	0.776	3.51	0.3719	3.005	0.96
4236	27.1	57.0	56.2	0.776	3.54	0.3871	3.124	1.00

time data will approximate a straight line from Equation (42). Variable pressure-variable rate data fall between these limiting curves.

Washing of Filter Cakes

Necessity for washing of filter cakes arises when (a) valuable cake solids are to be freed of residual filtrate in cake pores (b) processing requirements specify replacement of residual filtrate in filter cake by a second liquid (c) filtrate is valuable and economics dictate recovery of residual liquid in cake. Washing of sulfates from filtered nickel reduction slurry to reduce corrosion in subsequent processing is an example of case (a). Elimination of solubles for purity requirements is essential in filtering crystalline aluminum trihydrate from alumina leach solution, this application demonstrating case (b). Processes in which residual filtrate left in the cake is worth the cost of recovery by washing are filtration of gypsum from crude phosphoric acid in the wet phosphate process and in silicate gangue filtration from uranium pentoxide leach liquor. Volume of cake accumulation in these processes is large and recovery of product left in the cake is economically justified.

The efficiency with which washing can be carried out is highly dependent on the design of filtration equipment in addition to cake characteristics. Filter cakes are washed by (a) total submergence of the cake in the wash stream and (b) spray washing. Spray washing is commonly utilized on vacuum and centrifugal filters and is not regarded as being as effective as submerged washing due to inefficient contacting of the wash fluid with the cake solids. Usually considerable amounts of air are pulled through the cake with spray wash in vacuum filtration and the resulting two phase flow gives rise to much higher friction losses per unit mass of liquid passing through the cake to reduce the mass rate of flow. Correlations describing flow of air and liquid through packed beds have been applied to vacuum filtration in washing and dewatering of cakes.[5,6,44] The mechanism operating in dewatering the cake in this manner is displacement and entrainment of liquid by gas. Vaporization of filtrate into the air stream has also been investigated.[20]

Filter cake washing by total submergence is carried out with maximum efficiency in equipment such as plate and frame press and enclosed pressure and vacuum leaf filters. In rotary drum filtration it is possible by proper design to approximate total submerged washing. Filter cake washing can be treated theoretically through principles of hydraulics in flow through porous media and consideration of mass transfer by diffusion through films. These two operations are acting when wash fluid flow is forced through a filter cake. The initial effect of washing involves the contents of the pores being swept out by influx of wash fluid. This process is known as displacement washing. Surface films of filtrate adhering to the solid particles are replaced by wash fluid through turbulent and molecular diffusional exchange in the secondary effect. Prediction of washing requirements by theoretical means is at present impractical but test data taken in the range of operating conditions can be interpreted with knowledge of fundamentals for making extrapolations.

Displacement washing was treated theoretically by Ruth in reducing the problem to a simplified model involving laminar flow in straight circular capillaries with no mixing taking place at the interface of the displacing and displaced fluids.[51] Figure (23) shows a longitudinal section of a straight circular capillary through a filter cake of length L. The velocity distribution in an immiscible fluid displacing the capillary is given by means of integrating the Poiseuille equation

$$u = U \left[1 - (r/r_o)^2\right] \tag{43}$$

in which u is the velocity component of the fluid at radius r in the capillary of radius r_o and U is the maximum velocity (at r = 0) of flow. Figure (23) illustrates the parabolic form assumed by the interface of displacing fluid in the capillary. Complete displacement of original liquid in the cake by the wash stream occurs at infinite time. The distance x in Figure (23a) representing the position of the interface of displacing fluid at r for some time θ is

$$x = \theta\, u = \theta\, U \left[1 - (r/r_o)^2\right] \tag{44}$$

in which θ represents the elapsed time of washing. In Figure (23b) x = L/U at the instant the displacing fluid interface has just reached the end of the capillary. At this time the displaced volume of filtrate equals the volume of wash fluid V_w

$$V_w = - \int_0^L \pi r^2 dx = \pi \int_0^L r^2\, d\left[L - L(r/r_o)^2\right] = \frac{2\pi L}{r_o^2} \int_0^{r_o} r^3 dr = \frac{\pi L r_o^2}{2} = \frac{V_c}{2} \tag{45}$$

where V_c represents the capillary volume or cake voids. By the derivation the effluent from the cake after this instant will contain mixed wash fluid and filtrate. If the wash fluid is water and the filtrate in the cake is water with solute, the solute concentration in the wash effluent will begin diminishing at this point.

Integration of the Poiseuille equation produces the relationship for flow in circular conduits

$$U_{av} = \frac{U}{2}$$

The total volume of wash for θ is then

$$V_w = \pi\, r_o^2 \frac{U}{2} \theta \tag{46}$$

and the ratio of wash volume to void volume, β

$$\beta = \frac{V_w}{V_c} = \frac{\pi\, r_o^2\, U\, \theta}{\pi\, r_o^2\, 2\, L} = \frac{U\, \theta}{2\, L} \tag{47}$$

For an arbitrary time θ the interface of wash fluid will have reached a distance L_i in its maximum extension in a capillary extended to any given length, Figure (23c). The displaced volume V_b of the capillary at θ is

$$V_b = \frac{2\, \pi\, L_i}{r_o^2} \int_{r_i}^{r_o} r^3\, dr = \frac{\pi\, (r_o^4 - r_i^4)\, U\, \theta}{2 r_o^2} \tag{48}$$

where $L_i = U\, \theta$. The value of r_i is such that

$$u_i\, \theta = L = U\, \theta\, \left[1 - (r_i/r_o)^2\right]$$

Solving for r_i and substituting the result in Equation (48) yields

$$V_b = \pi\, r_o^2\, L\, (1 - \frac{L}{2\, U\, \theta}) = \pi\, r_o^2\, L\, (1 - \frac{1}{4\beta}) \tag{49}$$

Material balances can be written for calculating weight fraction of filtrate remaining in the cake and weight fraction of filtrate in cumulative and instantaneous wash effluent as a function of time using Equations (46) through (49). The weight fraction of filtrate in total cake fluid at time θ assuming equal wash and filtrate density is

$$W_c = \frac{V_c - V_b}{V_c} \quad \frac{\pi \, r_o^2 \, L}{4\beta \, L \, \pi r_o^2} = \frac{1}{4\beta} \tag{50}$$

The average weight fraction of filtrate in total exit wash is expressed is

$$W_{av} = \frac{V_b}{V_w} = \frac{\pi \, r_o^2 L (1 - \frac{1}{4\beta})}{\pi \, r_o^2 \, \frac{U}{2} \, \theta \, (\frac{L}{L})} = \frac{1 - \frac{1}{4\beta}}{\beta} = \frac{1}{\beta} - \frac{1}{4\beta^2} \tag{51}$$

and the instantaneous weight fraction in a given wash effluent at θ is given by

$$W_i = \frac{dV_b}{dV_w} = \frac{d \left[\pi \, r_o^2 \, L \, (1 - 1/4\beta)\right]}{d \left[\pi \, r_o^2 \, \frac{U}{2} \, \theta \right] \frac{L}{L}} = - \frac{d(1/4\beta)}{d\beta} = \frac{1}{4\beta^2} \tag{52}$$

The displacement washing theory developed by Ruth is of interest for its easily grasped heuristic description but assumption of no mixing across fluid interfaces leave little hope for its being dependable for application to practical problems. A wash volume predicted by the simple displacement theory for washing a filter cake to some specified extent can be regarded as a lower limit. Faster washing rates should increase the accuracy of the equations developed for displacement washing since diffusion effects would become proportionately less significant in laminar flow.

Other investigations have been published in which molecular and turbulent exchange between displaced and displacing fluids is taken into account.[59,60,64] These references are primarily developments in studies directed toward oil reservoir displacement problems based on fundamental hydrodynamics. Dahlstrom pointed out that assumptions in these analyses limit application of the equations to very slow flow velocities in thick sections of porous media whereas high velocities and thin sections are encountered in filtration.[16] Taylor published a solution to the partial differential equation describing laminar flow and diffusion in a circular capillary for the case of no forward diffusion and complete lateral diffusion.[60] The solution altered to the nomenclature being used here is

$$W_i = \frac{1}{2} - \frac{1}{2} \operatorname{erf} \left[L(1 - \beta)\left(\frac{24 \pi D}{V_c U \beta} \right) \right] \tag{53}$$

where D is the molecular diffusion coefficient. Composition would be uniform throughout each cross section by these assumptions.

Complete mixing of wash fluid and filtrate throughout a cake cross section is the limiting case for maximum volume required to accomplish a given wash duty. The tenet on which an assumption of complete mixing is based is as unlikely as a hypothesis of immiscible displacement, the actual representation being somewhere between these limiting conditions. A system having fine particles and thin sections would seem to favor complete mixing treatment over the displacement washing concept.

Rhodes first introduced equations treating filter cake washing based on complete mixing.[47] The assumption basic to the analysis is that concentration of filtrate in wash effluent at any instant is proportional to filtrate concentration in the cake. Using the previous nomenclature on basis of one unit area filter surface

$$w_i = \frac{dV_b}{dV_w} = k\, W_c = k\,\left(\frac{V_c - V_b}{V_c}\right) \tag{53}$$

Assuming k constant the time rate of change of instantaneous effluent concentration is

$$\frac{dW_i}{d\theta} = k\,\frac{d}{d\theta}\left(\frac{V_c - V_b}{V_c}\right) = -\,\frac{k}{V_c}\,\frac{dV_b}{d\theta} = -\,\frac{k}{V_c}\,\frac{dV_b}{dV_w}\,\frac{dV_w}{d\theta}$$

If the wash rate is constant

$$\frac{dV_w}{d\theta} = \text{constant} = F$$

and substitution in above results in

$$\frac{dW_i}{d\theta} = -\,k\,W_i\,F \tag{54}$$

using the equality given in Equation (53). Integration of Equation (54) results in

$$W_i = e^{-k\,F\,\theta} \tag{55}$$

The constant of integration is unity since $W_i = 1$ for $\theta = 0$. For constant wash rate $F = U/2 = \frac{L\,\beta}{\theta}$ and Equation (55) can be given in terms of wash ratios

$$W_i = e^{-k\,L\,\beta} \tag{56}$$

The empirically derived constant k varies with the difficulty of washing, the higher the washing efficiency the larger the value of k. Rhodes presented data for which higher values of k were found with faster washing of filter cakes in a plate and frame press. Presumably k increased with increased wash rates because diffusion from small pores into the main wash stream took place more rapidly. In this derivation the assumption of the constancy of k has no theoretical validation.

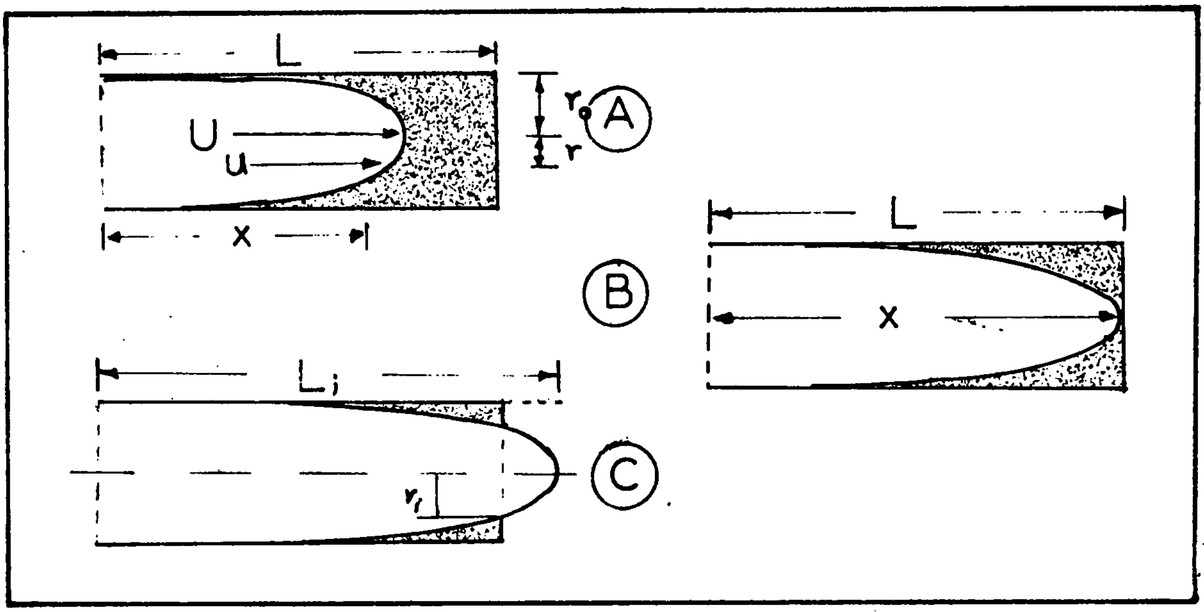

FIGURE 23.

WASHING BY IMMISCIBLE DISPLACEMENT IN CAPILLARY

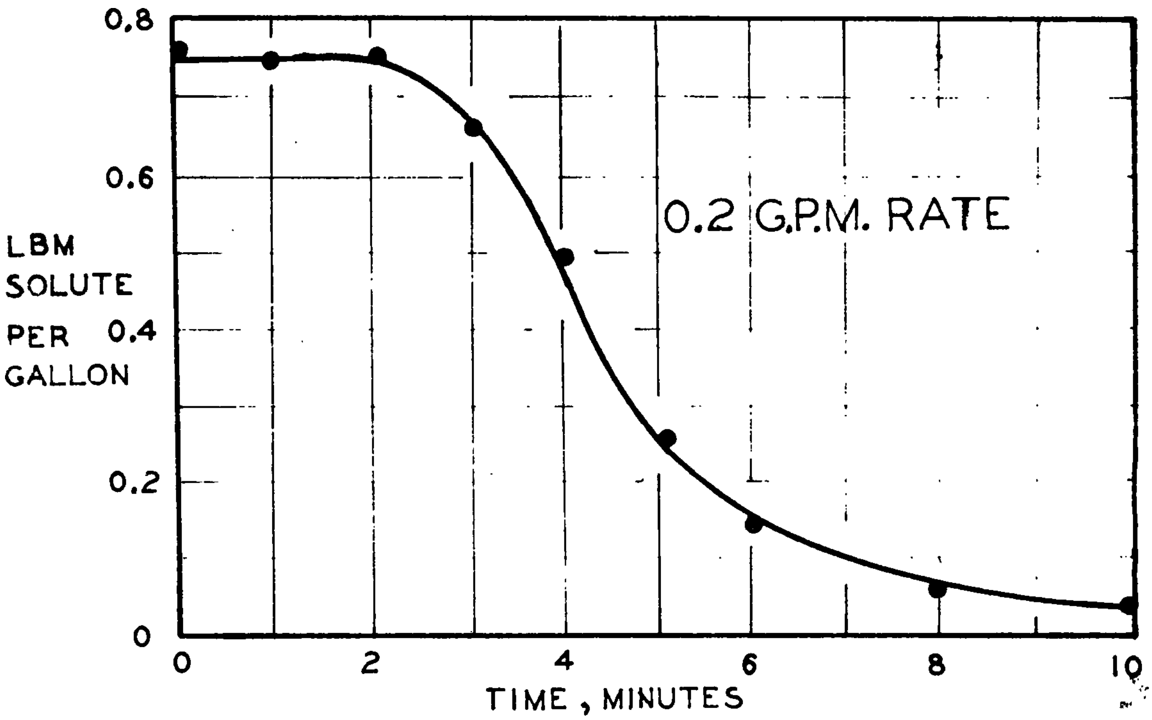

FIGURE 24.

EFFLUENT CONCENTRATION VS. VOLUME OF WASH -- DATA FROM WASHING SALT FROM FILTER CAKE

The data used by Rhodes to substantiate his hypothesis were faulty apparently due to filtrate in the wash lines which indicated more soluble material was washed out than was originally in the cake.[51] Dahlstrom studied washing problems in industrial applications and published data correlated by the complete mixing equation.[16] Reasonably good fits were obtained within the accuracy of the data. Equation (56) can be integrated again to relate the weight fraction filtrate remaining in the cake as a function of time in terms of k. By Equations (53) and (55)

$$\frac{dV_b}{dV_w} = e^{-k\,F\,\theta}$$

and

$$\int_{V_c}^{V_b} dV_b = \int_0^{F\theta} e^{-k\,V_w}\,dV_w$$

which for constant wash rate is integrated to

$$V_b - V_c = -\frac{1}{k}\,e^{-k\,F\,\theta}$$

Rearrangement results in

$$W_c = \frac{V_c - V_b}{V_c} = \frac{1}{k\,V_c}\,e^{-k\,L\,\beta} \qquad (56)$$

Dahlstrom called the fraction of filtrate removed from the cake for a volume of wash corresponding to one wash ratio ($\beta = 1$) the per cent wash efficiency E

$$W_c = \left(1 - \frac{E}{100}\right)^{\beta} \qquad (57)$$

and found values of E ranging from 35% to 86%.[16] Data taken from washing aluminum trihydrate cakes free from sodium hydroxide yielded E = 80%.

In calculating the length of a wash cycle by these equations the wash fluid flow rate through the cake is usually assumed equal to the filtrate flow rate at the last moment of filtration when the flow of wash fluid is through the same cake thickness as the last filtrate flow. Cake resistances have been observed to increase, however, during the washing process thus causing a reduction in the volumetric flow rate during the washing cycle when centrifugal pump or constant pressure feed is used. McMillen and Webber cite 70 to 90% reductions in beginning wash rates in a series of constant pressure tests.[42] Reduced electrolyte concentrations and different particle environments can appreciably alter cake structures to bring about resistance changes as discussed previously under "Filtration Resistance." Correction for viscosity in the rate equation must also be observed especially if the wash fluid is at a different temperature than the temperature at which filtration is carried out.

Example 5. Calculation of Filter Cake Wash Requirements

A test carried out to establish washing requirements yielded the following data for washing at a constant rate of 0.2 gallons/(sq.ft.)(min.):

Time, minutes	0	1	2	3	4	5	6	8	10
Lbm. solute/ gallon	0.740	0.739	0.740	0.687	0.480	0.266	0.144	0.0575	0.0313

This data is plotted in Figure (24). After the test was made it was desired to extrapolate this data to estimate the solute removal for twice the volume of wash, for twenty minutes wash at the indicated constant rate.

The cake had the following properties: thickness, 2.0 inches; solids density, 125 lbm./cu.ft.; filtrate density, 64.4 lbm./cu.ft.; weight per cent soluble salts in filtrate, 4.96%; volume per cent moisture in fresh cake, 55.9%.

Because the precision of the measurements were not high it will be assumed that (a) filtrate and wash densities are equal, (b) temperatures of wash and filtrate are constant and equal, and (c) wash rate remained constant during the test. The data will be analyzed by means of the displacement and mixing equations. Extrapolations to the specified volume of wash will be made by both methods and results compared to an expermental value.

Table III contains the results of calculations. Weight fraction of filtrate in the effluent is obtained from solute concentration in lbm. per gallon of effluent by the following steps

$$\text{Avg. cake density} = (0.40)(125.0) + (0.60)(62.4) = 88.6 \text{ lbm/cu.ft.}$$

$$\text{Mass solute/sq.ft.} = (L)(\text{avg. density})(0.0496) = 0.733 \text{ lbm./sq.ft.}$$

$$\text{Wgt. fraction solute in filtrate} = \frac{\text{mass solute/sq.ft.}}{(\text{avg.density})(L)(0.60)} = 0.0827$$

$$W_i = \frac{(\text{lbm. solute in effluent/gal.})}{(8.33 \text{ lbm/gal.})(\text{w.f.solute in filtrate})} = 1.355(\text{lbm.sol/gal.})$$

The second column in Table III contains values of W_i converted from data. The wash ratio β for displacement washing is calculated from Equation (52). The constant k for the mixing theory is obtained from Equation (56) using the theoretical wash ratio.

The displacement theory predicts wash ratios increasing out of proportional to the theoretical amount based on cake void volume. In order to compare the calculated to theoretical values, the ratio is obtained and given in Table III. Extrapolation to twice the volume of wash will be made using the final β value of 2.43

$$W_i = \frac{1}{(4)(4.86)^2} = 0.0.06 \text{ lb. filtrate/lb. effluent}$$

The effluent salt concentration then is 0.0078 lbm. salt/gal. The concentration of filtrate remaining in the cake is calculated using Equation (50)

$$W_c = \frac{1}{(4)(4.86)} = 0.0516 \text{ lb. filtrate/lb. cake fluid}$$

$$= 0.0379 \text{ lbm salt/gal. cake fluid}$$

Extrapolation in the mixing theory is made using k = 14.4, this being the average of apparent constant values of k, the magnitude of k increasing rapidly up to β = 1 with the two values after that point being about the same. Calculations result in

$$W_i = e^{-(14.4)(1/6)(2.68)} = 0.00166 \text{ lb. filtrate/lb. effluent}$$

$$W_c = \frac{0.00166}{(14.4)(0.10)} = 0.00115 \text{ lb. filtrate/lb. cake fluid}$$

$$= 0.00085 \text{ lbm. salt/gal. cake fluid}$$

Integration of the curve in Figure (24) according to

$$V_b = \int W_i \, dV_w = 0.675 \text{ lbm. salt/sq.ft. for 2.0 gal. wash}$$

$$= 0.708 \text{ lbm. salt/sq.ft. for 4.0 gal. wash}$$

yields a value for W_c after 4.0 gallons of wash

$$W_c = \frac{\text{lbm. salt in original cake - lbm. salt in cake at } \theta}{\text{lbm. filtrate in cake}}$$

$$= \frac{0.733 - 0.708}{(0.60)(1/6)(62.4)} = 0.0401$$

based on one square foot.

The calculated value of concentration after 4.0 gallons of wash by the displacement theory is in good agreement with the measured value, but this agreement may be fortuitous as a result of the value of β chosen. The diffusion-mixing theory results for this data are seen to be very misleading. Dahlstrom pointed out that his data showed little agreement with data in low residual concentrations of solubles for values of β above 2.0.[16]

V. EXPERIMENTAL METHODS

Laboratory methods for evaluating filtration resistance of filter cakes offer a practical means of obtaining technical information on filterability of slurries. Alternates to the use of laboratory evaluation techniques are the use of full scale equipment for test runs or the employment of fundamental theory to predict flow resistance in a given application. Installing plant size equipment is costly and frequently the mechanical difficulties in reaching steady state operation overshadow the effect of many variables with reduction in accuracy of resulting data. Correlation of fundamental properties of materials into a means of predicting resistance still remains to be demonstrated.

TABLE III

CALCULATION OF FILTER CAKE WASH REQUIREMENTS

Time minutes	W_i lbm.filt./lbm.effl.	$\beta_{theoretical}$	$\beta_{displacement}$	$\beta_{displ}/\beta_{theor}$	k
0	1.00	0.000	0.50	-	-
1	1.00	0.134	0.50	-	-
2	1.00	0.268	0.50	-	-
3	0.93	0.400	0.52	-	-
4	0.65	0.534	0.62	1.15	4.85
5	0.360	0.668	0.834	1.25	9.18
6	0.1945	0.800	1.13	1.41	12.25
8	0.0776	1.068	1.79	1.68	14.65
10	0.0423	1.34	2.43	1.81	14.20

Laboratory or small scale filtration techniques for evaluating resistance characteristics have been described and evaluated extensively. Four experimental methods are used to approach the problem of obtaining resistance data; these are filtration bomb techniques, constant rate filtrations, compression-permeability cell evaluation of cake characteristics, and variable pressure-variable rate evaluation methods.

Bomb Filtration Tests

Laboratory bomb filters have long been a source of data in evaluation of filtration characteristics.[58] This technique consists of confining the slurry to be filtered in a sealed vessel (bomb or montejus) and maintaining a known gas pressure in the vessel during filtration. A filter leaf of known size is submerged in slurry and filtrate is carried out for measurement.

Hoffing and Lockhart used a laboratory bomb filter in a series of constant pressure filtration tests and reported data for fifty-six filtrations at one pressure with a precision of 4.63%.[32] The material used in these tests, mixtures of keiselguhr and silica, was incompressible. The experimental procedure consists simply of charging the slurry sample into the bomb, quickly raising the bomb pressure to the desired level using a gas pressure regulator, and measuring the volume of expelled filtrate at intervals of time. Figure (25) illustrates the bomb filter used by Hoffing and Lockhart, this particular apparatus being designed and supplied by the

Dicalite Division of the Great Lakes Carbon Corporation. The constant pressure bomb filtration method may be used to obtain average specific resistance of compressible cakes by conducting a series of tests at different pressures over a desired range.[25] When medium resistance can be neglected data treated according to the form of Equation (27) yield specific resistance of cake solids by evaluating slopes either graphically or by least squares curve fitting. Example 6. illustrates the calculation procedure.

Data obtained during the initial periods of the test will usually be uncertain and be of little value in the overall analysis for several reasons. These reasons may be enumerated as follows: (a) the time factor inherent in the development of flow rates across the medium to generate the pressure differential of the test, (b) high velocities of flow through the filtrate draw-off lines at the start of filtration tends to result in excessive pressure loss, (c) air in filtrate draw-off lines is being displaced during the first stages of the test, (d) the greater difficulty in accurately measuring volume of filtrate vs. time during initial high rates. During the period of high rates in test filtrations of compressible materials data must also be examined for the possibility that solids had not attained equilibrium consolidation.

Example 6. Constant Pressure Bomb Filtration

The following data were obtained in a bomb filter test on a

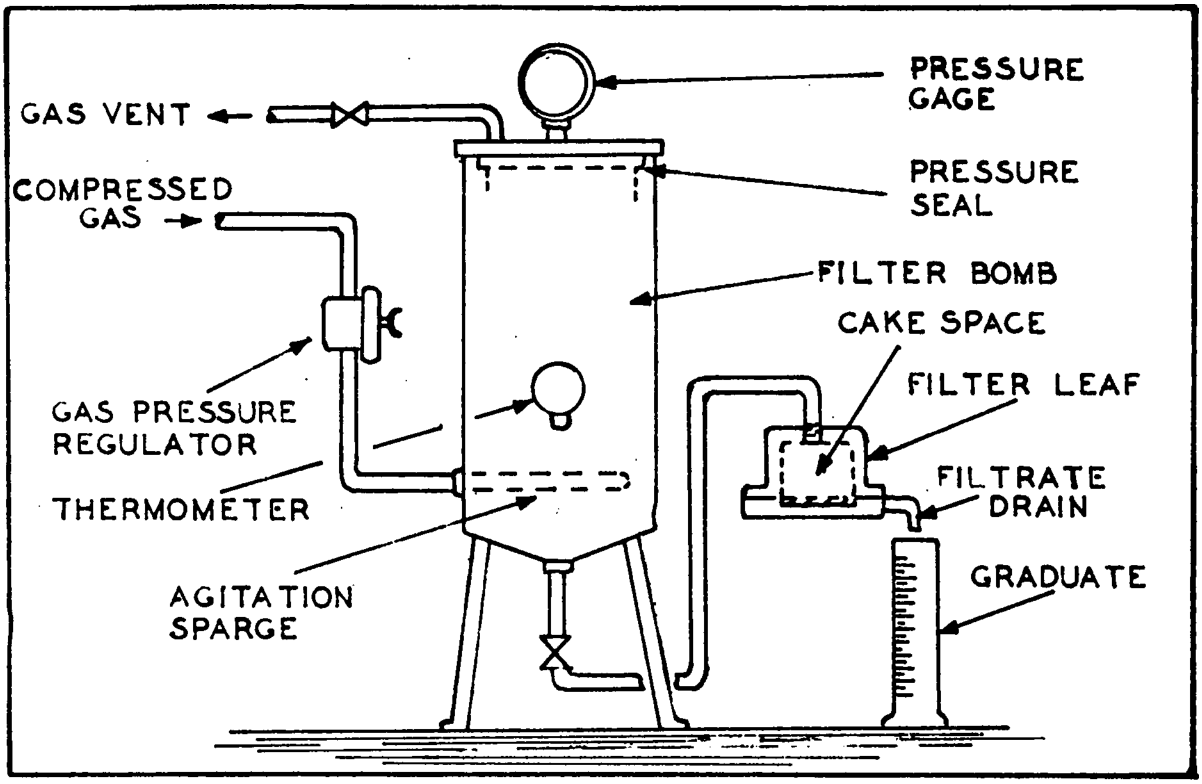

FIGURE 25.

DICALITE BOMB FILTER

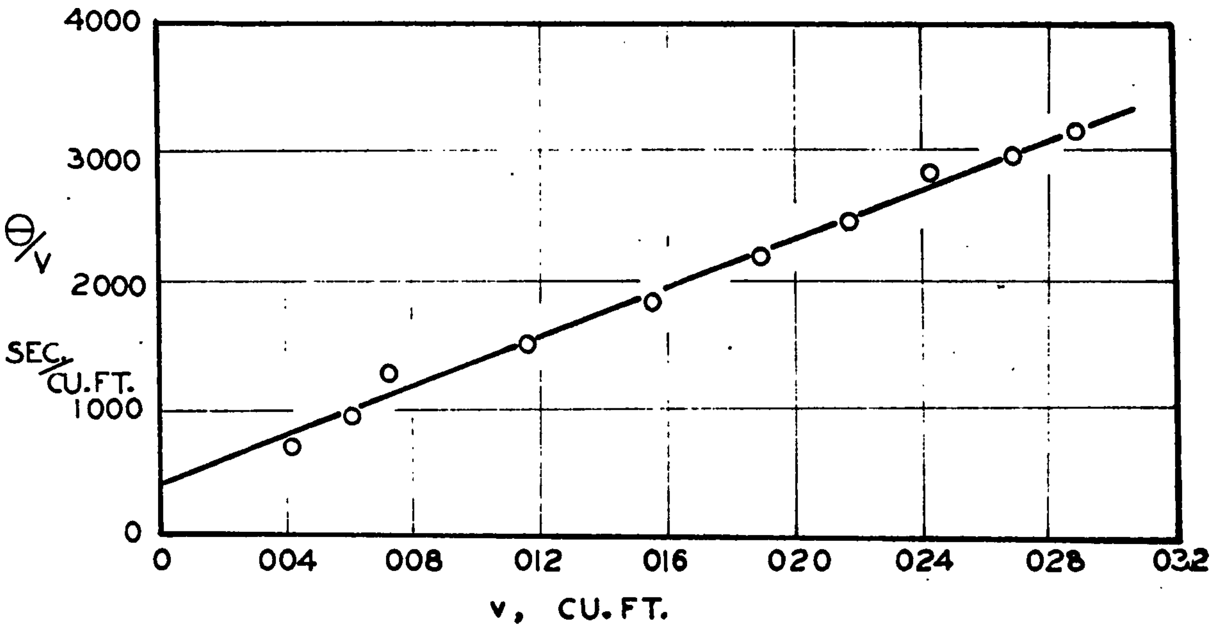

FIGURE 26.

PLOT OF DATA FROM CONSTANT PRESSURE BOMB FILTRATION

slurry containing 0.2% by weight solids.[32] The solids in the slurry consisted of a mixture of 25% by weight diatomaceous earth (keiselguhr) and 75% silica of 5-10 micron size. These materials were slurried in pure water. The test was conducted at ten pounds per square inch gage pressure.

Time, minutes	0.5	1.0	2.0	3.0	5.0	7.0	9.0	11.0	13.0	15.0
Filtrate volume, c.c.	117	181	269	337	450	538	617	689	756	818

The ambient temperature during the test was 22.5° C. at which temperature water has a viscosity of 0.947 centipoise. Measurement of the cake for porosity after filtration yielded $\epsilon = 0.718$.

The first step in the calculation procedure is to plot θ/v vs. v, shown in Figure (26). In order to obtain specific resistance in the English engineering notation, ft./lbm., all terms are converted to (lbm.)(ft.)(sec.) units.

$$\frac{\theta}{v} = \frac{\text{sec.}}{\text{cu.ft.}} = \frac{(60)(38320)}{(1.699)(10^6)} \frac{\text{min.}}{\text{cc.}};\ v = \text{cu.ft.} = 3.531\ (10^{-5})\ \text{c.c.}$$

Filter area cancels out in obtaining the slope. No regular deviation in observed in the plotted points in Figure (26) from a straight line relationship, indicating satisfactory agreement with theory is exhibited.

θ/v (x1000 sec./cu.ft.)	0.727	0.937	1.264	1.511	1.886	2.210	2.479	2.710	2.919	3.118
v (x1/100 cu.ft.)	0.413	0.640	0.950	1.191	1.590	1.901	2.179	2.435	2.670	2.891

The slope of the best straight line through the points is obtained in the final calculation step and by Equation (27) is set equal to

$$\text{slope} = \frac{1}{2} \frac{\mu}{g_c} \frac{s\rho}{1 - ms} \frac{\alpha_{av}}{p}$$

The slope, obtained graphically, is 0.981 (10^7). In evaluating the average specific resistance from the slope, the term (1 - ms) can be considered equal to unity because of the dilute slurry being filtered (s = 0.002).

$$0.981\ (10^7) = \frac{1}{2} \frac{(0.002)(62.4)}{(10)(144)} \frac{0.947}{1488} \alpha_{av}$$

from which average specific resistance is calculated to be 3.70 (10^{11}) ft./lbm.

Constant Rate Test Filtrations

Laboratory filtration tests in which feed is supplied to a test filter at constant rate are described by Bonilla, Luke, Tiller, and Walas.[4,41,62,65] It has generally been the objective in constant rate filtration tests to evaluate the exponent n in the empirical equation

$$\alpha = \alpha_o \ p^n \tag{33}$$

through use of the integrated rate expression, Equation (34). Equation (34) is utilized for treatment of data and calculation of n and α_o.

In carrying out tests at constant rate, reciprocating and diaphram pumps have been used most often for slurry feed. Reciprocating and diaphram pumps produce a surge in line pressure with each stroke which is relieved as filtrate passes through the cake. The rate therefore will vary slightly during each cycle of pump action. Rapid stroking and air chambers to dampen pump pulsations tend to reduce the effect of this mechanical problem but small fluctuations in rates are magnified by the time-pressure relationship Equation (34) since the slope is proportional to the rate squared. The method used to analyze constant rate data is demonstrated by Example 7.

Example 7. Calculations for Constant Rate Filtration Test

Tiller obtained constant rate filtration data using a Milton-Roy positive displacement adjustable stroke pump operating at 100 cycles per minute.[62] The pump charged a slurry containing 0.05% kaolin in water to a horizontal pressure test leaf eight inches in diameter. The constant flow rate for the run, for which data is given in Table IV, was 0.493 liters per minute. The filtrate temperature during the test was 87° F.

By Equation (34) data plotted in the form $\ln\theta = \ln k + (1-n)\ln(p-p_1)$ should result in a straight line if resistance of the cake solids behaves according to the empirical power function expression, Equation (33), where p will be given in units of pounds per square inch. The term K in Equation (34) is

$$K = \frac{1 - ms}{s\rho} \frac{g_c}{\mu} \frac{1}{q^2} \frac{144}{\alpha_o (1 - n)}$$

the multiplier 144 being inserted to convert pounds per square inch to pounds per square foot in order to obtain α_o in units ft./lbm.

If the assumption of negligible medium resistance is made in analyzing the data slight deviations from linear form will occur in the first portion of the plotted points, as noticeable in Figure (27). The constant pressure drop through the medium will become proportionately smaller as the filtration pressure increases and deviations from a straight line due to medium pressure drop become negligible. The initial points showing poor agreement to the linear form can therefore be ignored in treating the data, all points being plotted with medium resistance considered negligible.

Analysis of the data proceeds as follows: the data are plotted Table IV on log-log coordinates as indicated in Figure (27). The slope is evaluated graphically over the linear portion, deviations from the straight line below 8 p.s.i. not being considered. With time given in minutes the slope is 0.0095. Converting this to seconds to maintain consistent units (lbm.)(ft.)(sec.), 1 - n = 0.57 and n = 0.43. K is calculated using a data point indicated by Figure (27) as having a good fit to the least squares straight line. Using Θ = 70 minutes and p = 16.3 lbf./sq.in.

$$K = \frac{(70)(60)}{16.3^{0.57}} = 858$$

Substitution of terms in the expression given for K by Equation (34) is made, converting liters per minute to cu.ft./(sq.ft.)(sec.) for the filter of area 0.349 sq.ft. Viscosity of water at 87° F. is converted from 0.79 centipoise to English engineering units. For the dilute slurry (1 - ms) can be considered unity.

$$K = \frac{1}{(0.0005)(62.4)} \frac{144}{(0.000832)^2} \frac{(32.2)(1488)}{(0.79)} \frac{1}{\alpha_o (0.57)} = 858$$

Solving the above yields $\alpha_o = 9.05\ (10^{11})$ ft./lbm.

Compression-Permeability Cell Analysis

Description of this instrument and its operation were discussed in detail in part III. of Chapter II., mechanical features of the device as modified by Grace having been shown in Figure (10). Typical data taken from compression-permeability cell measurements are used to calculate point specific resistance in Example 8.

TABLE IV

CALCULATIONS FOR CONSTANT RATE FILTRATION TEST

TIME-PRESSURE DATA

Time minutes	Pressure lbf./sq.in.
20	3.0
25	3.9
30	4.9
35	5.8
40	7.0
45	8.0
50	9.1
55	10.4
60	11.6
65	14.7
70	16.3
75	18.0
80	20.2
85	23.5
90	25.1
100	30.0
102	31.5
104	31.6
106	33.7
108	35.0
110	35.0

Example 8. Point Specific Resistance Calculation Using Data From Compression-Permeability Cell

Specific resistance is calculated in consistent units ft./lbm. by Equation (10). Data is substituted into this expression in units as follows: pressure in lbf./sq.ft., viscosity in lbm./(ft.)(sec.), filtrate rate q in cu.ft./(sq.ft.)(sec.), solids density ρs in units lbm./cu.ft. and cake thickness L in feet.

Grace reported experimental data for a sample of talc filter cake under 1.10 p.s.i. mechanical pressure in a compression-permeability cell[24]

filtrate constant head	21.3 cm.
average filtrate flow rate	0.368 c.c. per min.
viscosity of filtrate	0.854 centipoise
area of filter leaf	11.35 sq. cm.
density of talc solids	2.68 gm. per c.c.
porosity of cake	0.856
volume of cake	18.50 c.c.
medium resistance	0.012 (10^{11}) 1/ft.

To perform the calculation q is converted to cu.ft./(sq.ft.)(sec.) from metric units of cubic centimeter per minute

$$q = \frac{Q}{A} = \frac{0.368 \text{ c.c. per min.}}{60 \text{ sec. per min.}} \; \frac{1}{11.35 \text{ sq.cm.}} \; \frac{1}{30.5 \text{ cm. per ft.}}$$

$$= 1.775\,(10^{-5}) \text{ cu.ft./(sq.ft.)(sec.)}$$

Correction for medium pressure drop is obtained by

$$p_1 = \frac{u}{g_c}\, q\, R_m = \frac{(0.859)(1.775)(10^{-5})(0.012)(10^{11})}{(1488)(32.2)} = 0.38 \text{ lbf./sq.ft.}$$

Calculation for α follows converting cm. filtrate head to lbf./sq.ft.

$$p = \frac{21.3 \text{ cm.}}{30.5 \text{ cm./ft.}} \; \frac{62.4 \text{ lbm.}}{\text{cu.ft.}} \; \frac{g}{g_c} = 43.6 \text{ lbf./sq.ft.}$$

$$\alpha = \frac{43.6 - 0.4}{\dfrac{(0.859)(1.775)(10^{-5})(62.4)(2.68)(18.50)(0.144)}{(1488)\qquad\qquad(11.35)(30.5)}}$$

$$= 1.06\,(10^{11}) \text{ ft./lbm.}$$

The result of a series of runs is data such as that plotted in Figures (11) and (12). Recalling the definition for α_{av}

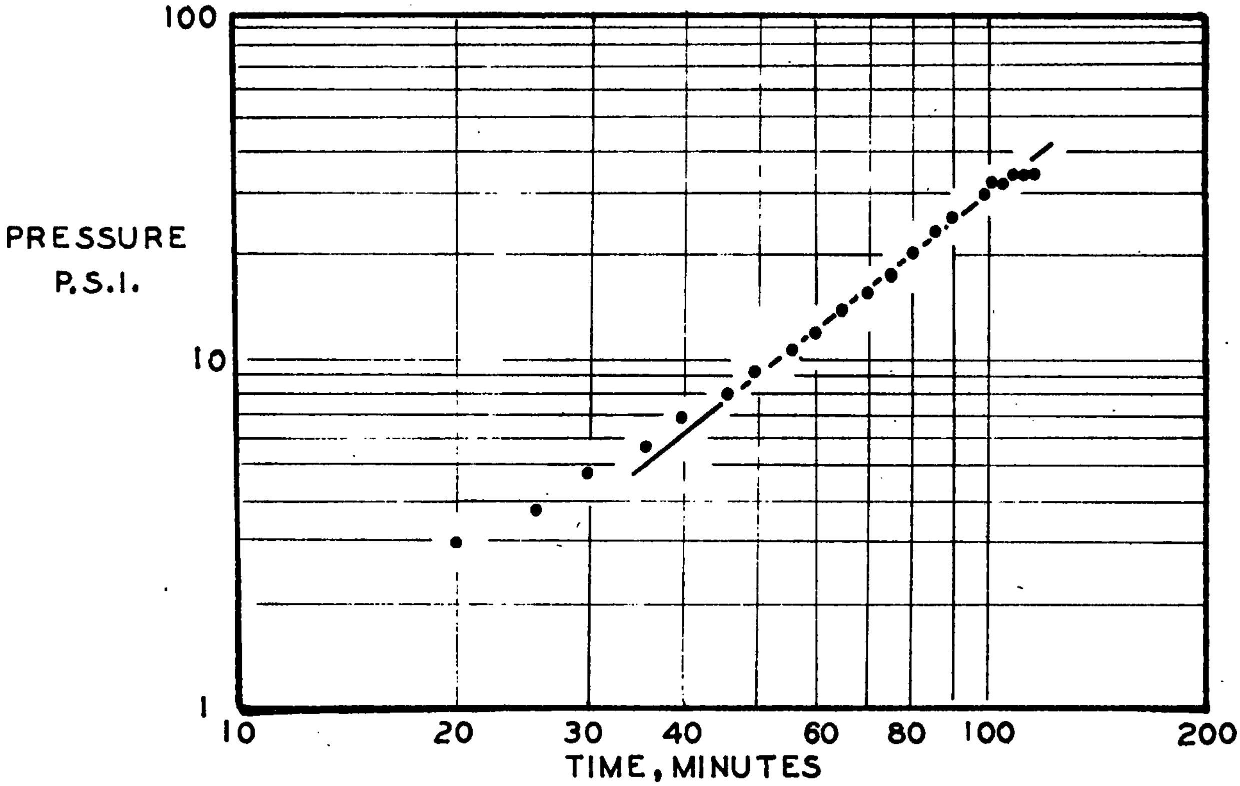

FIGURE 27.

LOGARITHMIC PLOT OF DATA FOR EVALUATION OF COMPRESSIBILITY CONSTANT FROM CONSTANT RATE FILTRATION TEST

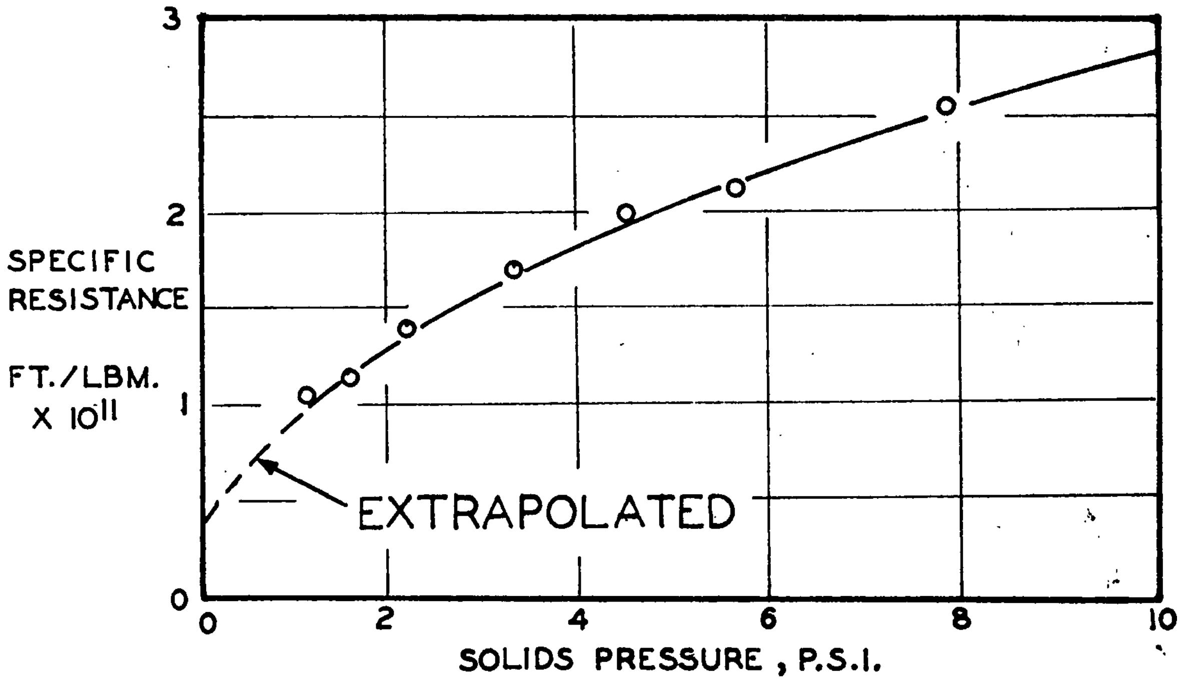

FIGURE 28.

POINT SPECIFIC RESISTANCE VS. SOLIDS PRESSURE FOR TALC C

TABLE V

INTEGRATED VALUES OF AVERAGE SPECIFIC RESISTANCE FOR TALC

Pressure lbf./sq.in.	Point Specific Resistance ft./lbm.	$\int \frac{dp_s}{\alpha}$ lbf.lbm./sq.in.ft.	Average Specific Resistance ft./lbm.
0.0	0.32 (10^{11})	0.0	0.32 (10^{11})
0.8	0.79	1.442 (10^{-11})	0.55
2.0	1.29	2.568	0.77
6.0	2.18	4.831	1.24
10.0	2.80	6.443	1.55
14.0	3.36	7.731	1.81
18.0	3.83	8.844	2.03
26.0	4.63	10.76	2.42
34.0	5.46	12.35	2.75
42.0	6.20	13.72	3.06
50.0	6.94	14.94	3.35
58.0	7.63	16.05	3.61

$$\alpha_{av} = \frac{p - p_1}{\int_0^{p-p_1} \frac{dp}{\alpha}} \qquad (22)$$

numerical integration of the integral in the denominator yields values for α_{av} as a function of pressure in the range of measurement. Example 9. illustrates the procedure used to calculate α_{av} vs. pressure for the talc data plotted in Figures (18) and (20). Compression-permeability cell measurements below approximately one pound per square inch were not reported by Grace in the data on which the integration for talc average specific resistance was made.[24] In order to perform the integration from zero solids pressure to a given pressure it is necessary to extrapolate the α vs. p data to zero from the lowest experimental points. The extrapolation in the integrations of Example 9. was accomplished by plotting the experimental points on linear coordinate paper and extending the curve to the zero ordinate. The extrapolation is shown by the dotted line in Figure (28).

<u>Example 9.</u> Integration of Compression-Permeability Cell Data for Average Specific Resistance

Figures (11) and (28) contain plotted values of point specific resistance vs. solids pressure data resulting from compression-permeability cell tests conducted by Grace.[24] To determine average specific resistance by Equation (22) values of the integral are calculated for the limits zero and $(p - p_1)$. Numerical integration by Simpson's rule is carried out in the same manner as illustrated for Example 1. Calculations for the value of the integral between zero and 0.8 p.s.i. and zero and 2.0 p.s.i. are made as follows

p (p.s.i.)	0.0	0.2	0.4	0.6	0.8	1.0	1.2	1.4	1.6	1.8	2.0
α $(x10^{11})$	0.32	0.50	0.60	0.71	0.79	0.88	0.96	1.11	1.14	1.21	1.29
$\frac{1}{\alpha}$ $(x10^{-11})$	3.13	2.00	1.67	1.41	1.28	1.14	1.04	0.902	0.877	0.826	0.776

$$(p - p_1) = 0.8; \; \alpha_{av} = \frac{0.8}{\int_0^{0.8} \frac{dp}{\alpha}} = \frac{0.8}{\frac{\Delta p}{3} \Sigma \, n(\frac{1}{\alpha})} = \frac{0.8}{1.442 \; (10^{-11})} = 0.55 \; (10^{11})$$

$$(p - p_1) = 2.0; \; \alpha_{av} = \frac{2.0}{2.569 \; (10^{-11})} = 0.77 \; (10^{11}) \text{ ft./lbm.}$$

The intervals for p were chosen small in this integration because of the rapid change in α over this pressure range.

Table V contains values of α_{av} for talc integrated up to 58 p.s.i. used to plot Figures (18) and (20).

Variable Pressure-Variable Rate Methods

Rearrangement of Equation (21) and substitution of α_{av} results in

$$\frac{g_c}{\mu} \frac{(p - p_1)}{q} = \alpha_{av} \, v \left(\frac{s\rho}{1 - ms} \right) \tag{21}$$

which is also identical with

$$\frac{g_c}{u} \; \frac{p}{q} = \alpha_{av} \, w + R_m \tag{58}$$

When centrifugal pump feed is used, the left hand member of this equation is a fixed function of pressure since q is known for all p from the pump performance curve. Feeding slurry to a filter leaf with a centrifugal pump taking suction on volumetric measuring tank or weight tank provides the means for measuring total volume of flow (or mass of solids delivered to the filter) and pressure simultaneously. With the pump performance curve ordinates p/q in Equation (58) are plotted against w on the abscissa. The slope at any point on the resulting curve represents α_{av} and numerical differentiation of data at various points on the curve will yield a complete evaluation of average specific resistance vs. pressure up to the maximum pump pressure with all necessary data being obtained in one experimental run.[63] Point specific resistance data can be determined also by the following mathematical treatment. Differentiating Equation (22) with respect to solids pressure produces

$$\frac{d\alpha_{av}}{dp_s}\int_0^{p_s}\frac{dp_s}{\alpha} - \frac{\alpha_{av}}{\alpha} = 1 \tag{59}$$

On substituting the integral in Equation (59)

$$\frac{d\alpha_{av}}{dp_s}\,\frac{p_s}{\alpha_{av}} - \frac{\alpha_{av}}{\alpha} = 1$$

and solving for α

$$\alpha = \frac{\alpha_{av}}{1 - \dfrac{p_s}{\alpha_{av}}\,\dfrac{d\alpha_{av}}{dp_s}} = \frac{\alpha_{av}}{1 - \dfrac{d\ \ln\ \alpha_{av}}{d\ \ln\ p_s}} \tag{60}$$

this derivation being due to Tiller.[63]

CHAPTER III

FILTRATION OF CONCENTRATED SLURRIES AT CONSTANT PRESSURE

In treating constant pressure cake filtration by differential analysis two approximations are made which may be invalid under certain circumstances.[25,63] In the Ruth filtration equation

$$\frac{dv}{d\Theta} = \frac{1}{\mu} \frac{g_c\ p}{\left(\frac{\alpha\ s\ \rho}{1 - ms} + R_m \right)} \tag{24b}$$

it is generally assumed for constant pressure operation that the filtration resistance α and the ratio m of the mass of wet cake to dry cake are constant. Analysis of the basic phenomena indicates that these assumptions must modified for thick slurries of highly compressible materials filtered for abbreviated periods of time. In rotary filtration and in experimental determination of cake characteristics, the time of filtration is frequently short and the employment of constant values of α and m may lead to erroneous results. Use of conventional filtration equations requires the assumption that equilibrium porosities are attained instantaneously which may not always be true.[62]

In Figures (2) and (3) a filter cake is illustrated schematically in which flow of fluid takes place from left to right, and distance is measured from the surface of the cake. At a distance x the hydraulic pressure is p_x, and the solid compressive pressure is p_s. As the liquid flows frictionally through the compressible, porous cake, p_x drops until it reaches the value p_1 at the interface of the cake and filter medium.

The relationship of time to pressure p_1 at the medium and the pressure drop across the cake $(p - p_1)$ are illustrated in Figure (29) where pressure at the medium is defined by

$$g_c \, p_1 = \mu \, R_m \, q = \mu \, R_m \frac{dv}{d\theta} \tag{18}$$

where $q = dv/d\theta$ is the rate of flow in (cu.ft.)/(sq.ft.)(sec.) and R_m is the medium resistance.* Initially when there is no cake, the entire pressure drop is across the medium; and $p = p_1$. As the filtrate rate decreases with time, p_1 falls in accord with Equation (18); and the pressure drop $(p - p_1)$ across the cake builds up.

In constant pressure filtration the average value of α used in Equation (24b) has in some cases been defined by

$$\alpha = \frac{p}{\int_0^p \frac{dp_s}{\alpha_x}} \tag{61}$$

where α_x is the point resistance at a solid pressure p_s.[32] In general the relation between α_x and p_s is obtained in a compression-permeability cell or by direct calculations based upon actual filtration data.[37,57,63] Equation (61) is valid when the medium resistance is negligible or when the rate has dropped to a point where p_1 is small. A more exact expression for an average α is given by

$$\alpha = \frac{p - p_1}{\int_0^{p - p_1} \frac{dp_s}{\alpha_x}} \tag{22}$$

where $(p - p_1)$ represents the pressure drop across the cake.[24] Whereas α is a function of p alone in Equation (61), α is a function of p and

* Calculations shown in Appendix II

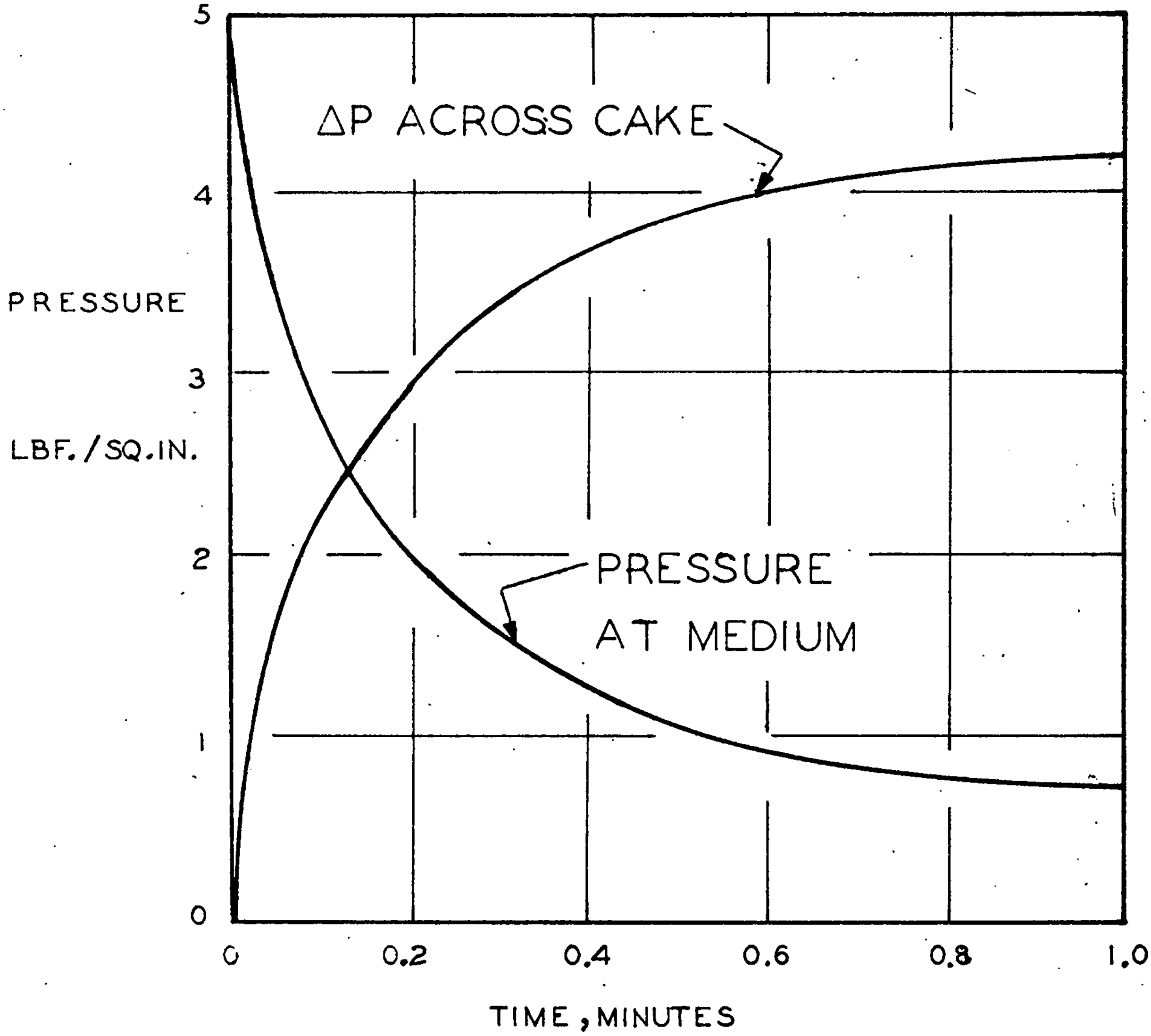

FIGURE 29.

PRESSURE VARIATION WITH TIME IN FILTRATION OF TALC AT 5 P.S.I.

$dv/d\theta$ in Equation (22) in addition to the parameters μ and R_m.

Porosity varies throughout the cake as a function of time and thickness as illustrated in Figure (30).* The first infinitesimal layer has a porosity and specific resistance corresponding to zero compressive pressure. As the pressure drop across the cake increases the porosity at the medium decreases and eventually reaches a minimum value equal to a porosity determined by the maximum applied pressure p.

It is instructive to replot the data showing the porosity as a function of the distance (L - x) from the medium as indicated in Figure (31). The first layer of solids deposited on the medium has a porosity corresponding to point A. As time proceeds the porosity at the medium decreases and eventually reaches a minimum value at B which is determined by the total filtration pressure. The average value of the porosity represented by the dotted line approaches a limiting value as the cake becomes infinitely thick. A replot of the data showing ϵ as a function of x/L is presented in Figure (32).

The ratio m of the mass of wet cake to mass of dry cake is

$$m = 1 + \frac{\rho\ \epsilon_{av}}{\rho_s\ (1 - \epsilon_{av})} \tag{23}$$

where ϵ_{av} is the average of porosity of the cake, or the over-all cake porosity. Obviously as ϵ_{av} decreases, m will also decrease. In Figure (33) a plot of m vs. θ for the filtration of several materials is shown.** The value of m at time equal to zero is calculated from the value of ϵ

* Calculations shown in Appendix II

** Calculations shown in Appendix III

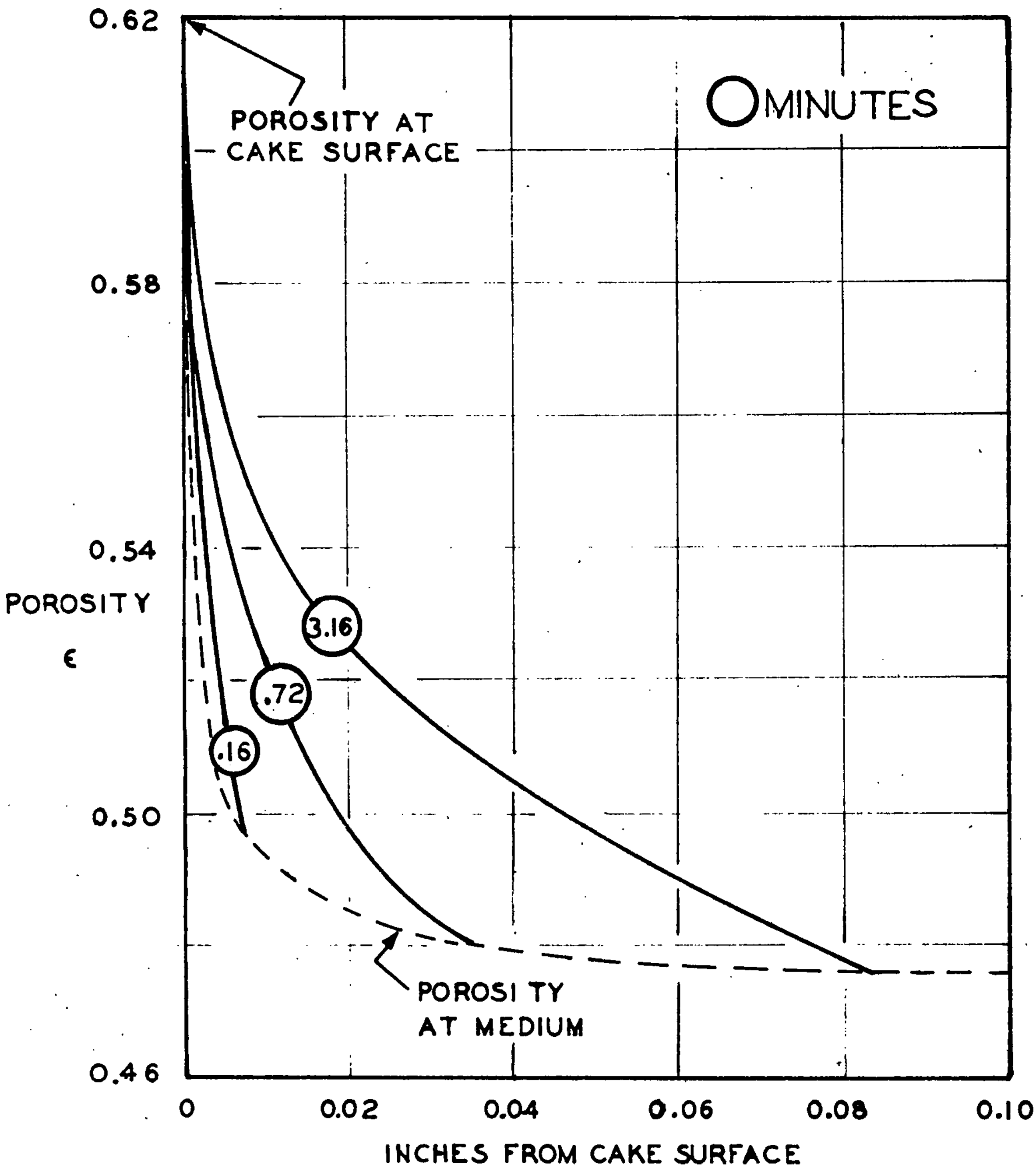

FIGURE 30.

VARIATION OF POROSITY IN KAOLIN FILTER CAKE
DURING CONSTANT PRESSURE FILTRATION AT 100 P.S.I.

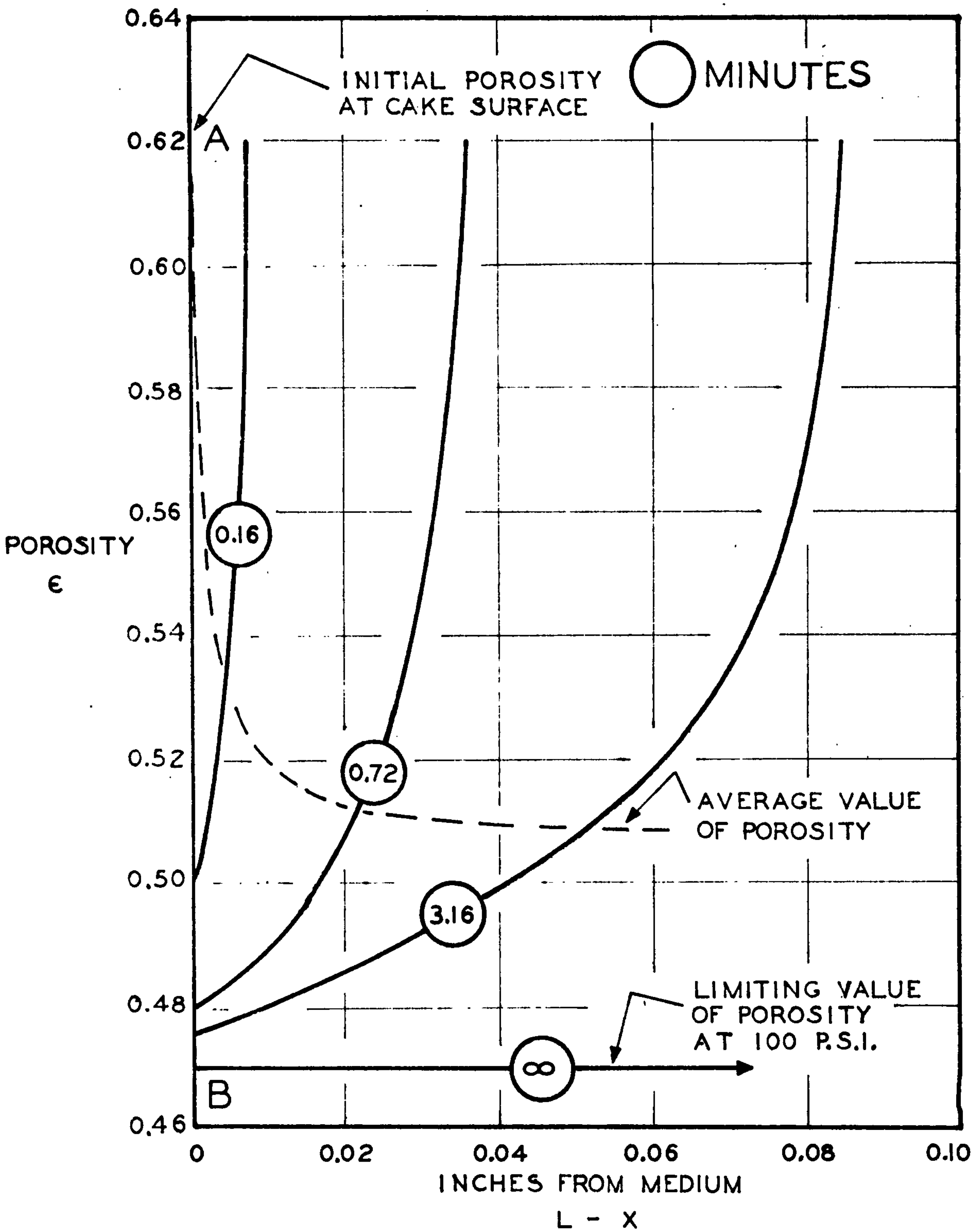

FIGURE 31.

POROSITY OF KAOLIN FILTER CAKE SHOWN IN RELATIONSHIP TO DISTANCE FROM FILTER MEDIUM DURING CONSTANT PRESSURE FILTRATION AT 100 P.S.I.

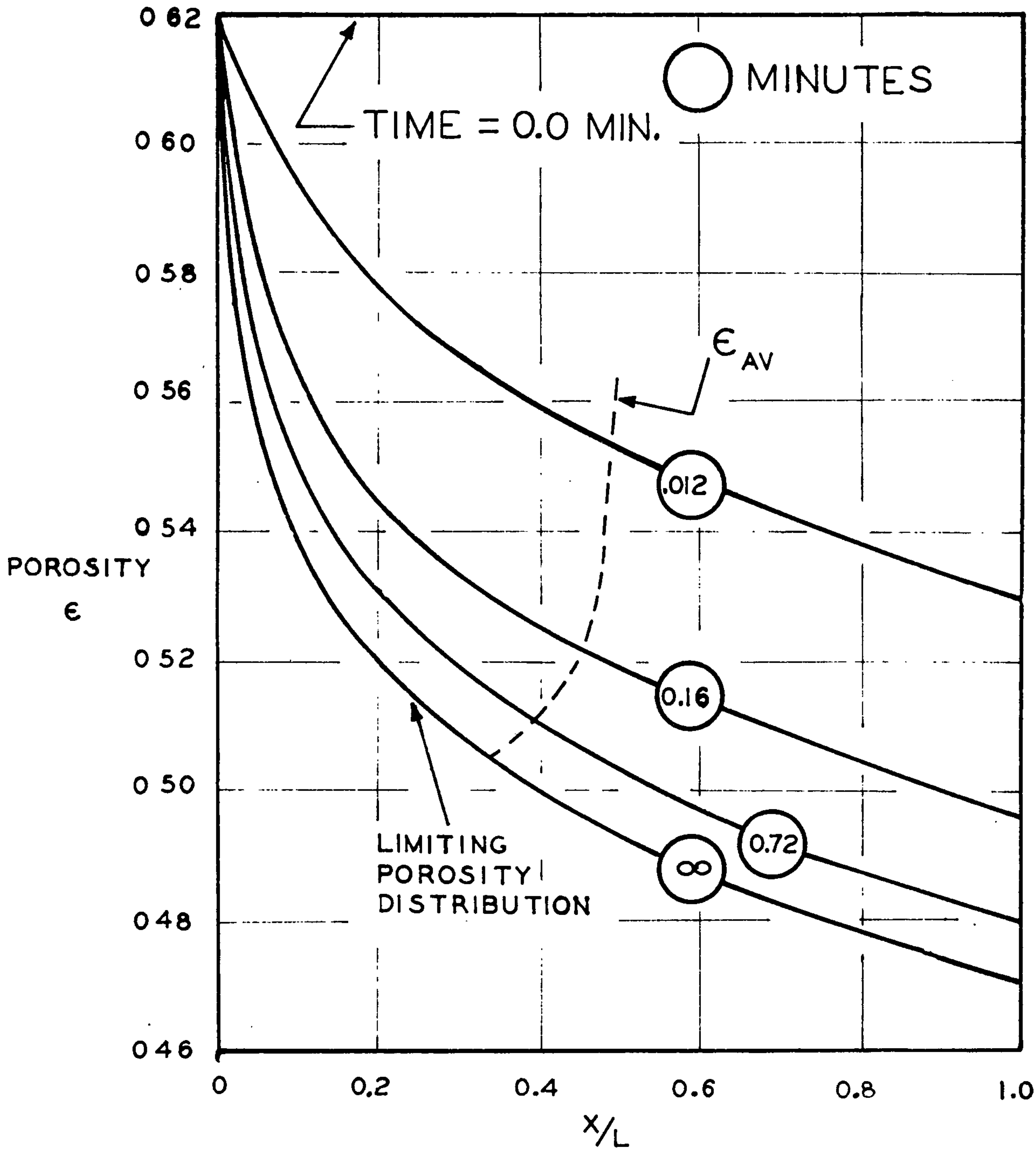

FIGURE 32.

POROSITY OF KAOLIN FILTER CAKE GIVEN AS FUNCTION OF X/L DURING CONSTANT PRESSURE FILTRATION AT 100 P.S.I.

at the cake surface under zero compressive stress. The limiting value of m usually is rapidly approached and is determined by the limiting porosity distribution curve as illustrated in Figure (33).*

A material balance applied to the filtration results in the expression

$$w = \frac{sp}{1 - ms} v \tag{20}$$

based on the volume of filtrate v. Another expression can be derived on the basis of volume of liquid per square foot passing into the cake from the slurry v_o

decrease in mass of liquid in slurry = mass of liquid in cake + mass of filtrate

$$\frac{w}{s}(1 - s) = \rho v_o = (m - 1)w + \rho v \tag{62}$$

Equation (62) can be rewritten in terms of v_o

$$v_o = \frac{1 - s}{1 - ms} v \tag{63}$$

If the value of m is constant, w and v_o will be proportional to v. Similarly the rate of flow into the solid, $q_o = dv_o/d\theta$, will be proportional to the rate of flow from the cake, $q = dv/d\theta$, and may be written in the form

$$q_o = \frac{dv_o}{d\theta} = \frac{1 - s}{1 - ms}\frac{dv}{d\theta} = \frac{1 - s}{1 - ms} q \tag{64}$$

If the average porosity is not constant, this equation must be modified by permitting m to vary. If Equation (63) is solved for v and then differentiated with respect to time, there results

* Calculations shown in Appendix IV

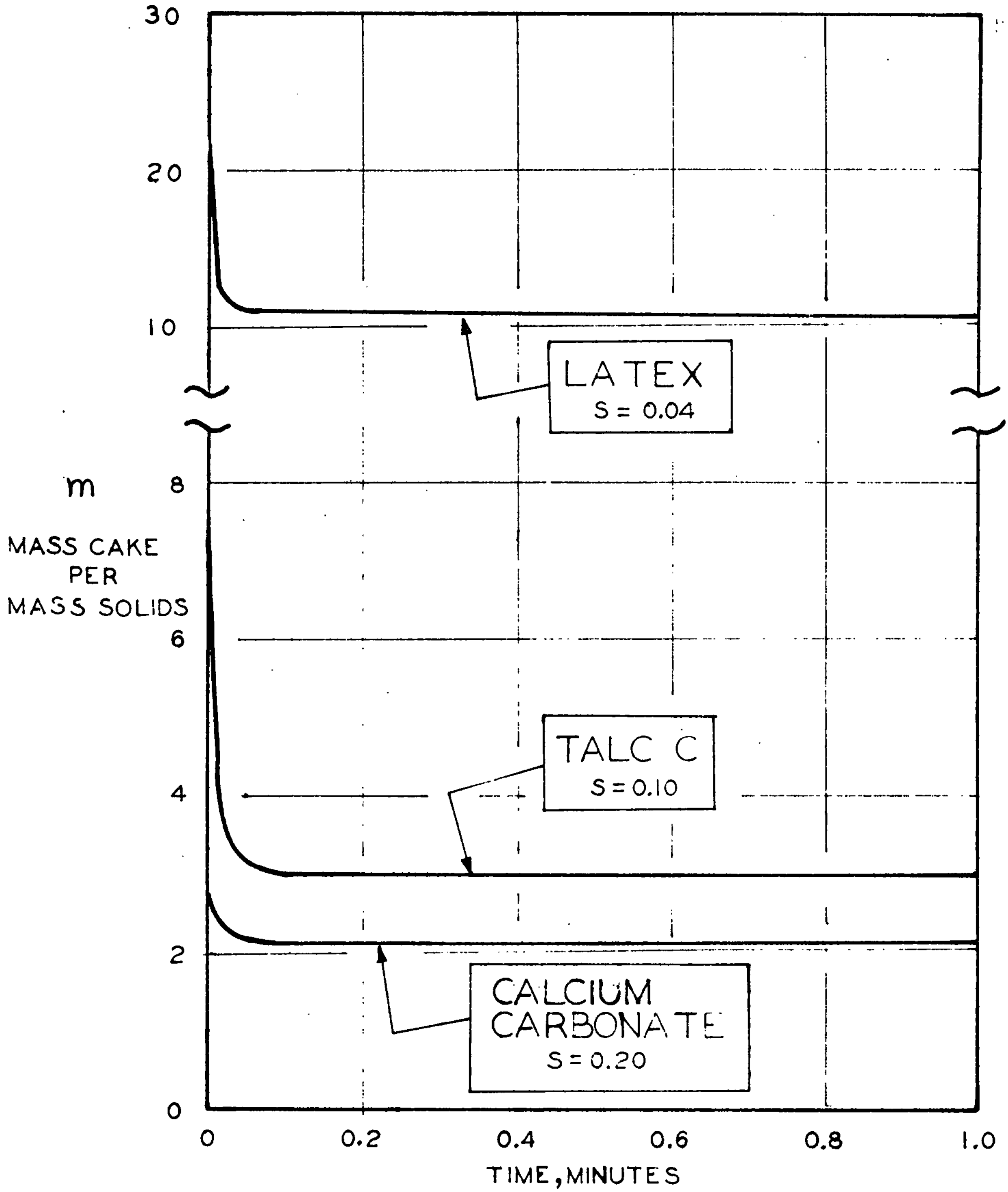

FIGURE 33.

MASS RATIO OF WET TO DRY CAKE VS. TIME DURING FILTRATION AT 15 P.S.I.

$$\frac{dv}{d\theta} = q = \frac{1 - ms}{1 - s} q_o - \frac{s}{1 - s} v_o \frac{dm}{d\theta} \tag{65}$$

When $dm/d\theta$ becomes small as m approaches constancy the last term in Equation (65) can be omitted. As can be seen in Figure (33) $dm/d\theta$ is negative; and the last term in Equation (65) represents a positive correction which decreases with time.

It is possible to find the minimum value of q at the surface of the cake, as illustrated by point B in Figure (34). Letting q_i be the value of q at the surface corresponding to m_i, the maximum ratio of wet to dry cake attained at zero compressive pressure, a differential material balance based on Equation (63) can be written

$$\frac{dv_o}{d\theta} = q_o = \frac{1 - s}{1 - m_i s} q_i \tag{66}$$

Eliminating q_o between Equations (65) and (66) yields

$$q_i = \frac{1 - m_i s}{1 - ms} q + \frac{s(1 - m_i s)}{(1 - s)(1 - ms)} v_o \frac{dm}{d\theta} \tag{67}$$

When the equilibrium porosity is nearly reached and $dm/d\theta$ is quite small, q_i is given by

$$q_i = \frac{1 - m_i s}{1 - ms} q \tag{68}$$

Thus even when m becomes essentially constant, q_i is less than q, and the flow rate throughout the cake is variable.

The basic empirical equation describing flow through a porous compressible solid can be written as[62]

$$-g_c \frac{dp_x}{dx} = g_c \frac{dp_s}{dx} = \alpha \mu \rho_s (1 - \epsilon) q \tag{5}$$

or eliminating dx by $dw_x = \rho_s (1 - \epsilon)dx$

$$-g_c \frac{dp_x}{dw_x} = g_c \frac{dp_s}{dw_x} = \alpha \mu q \tag{3}$$

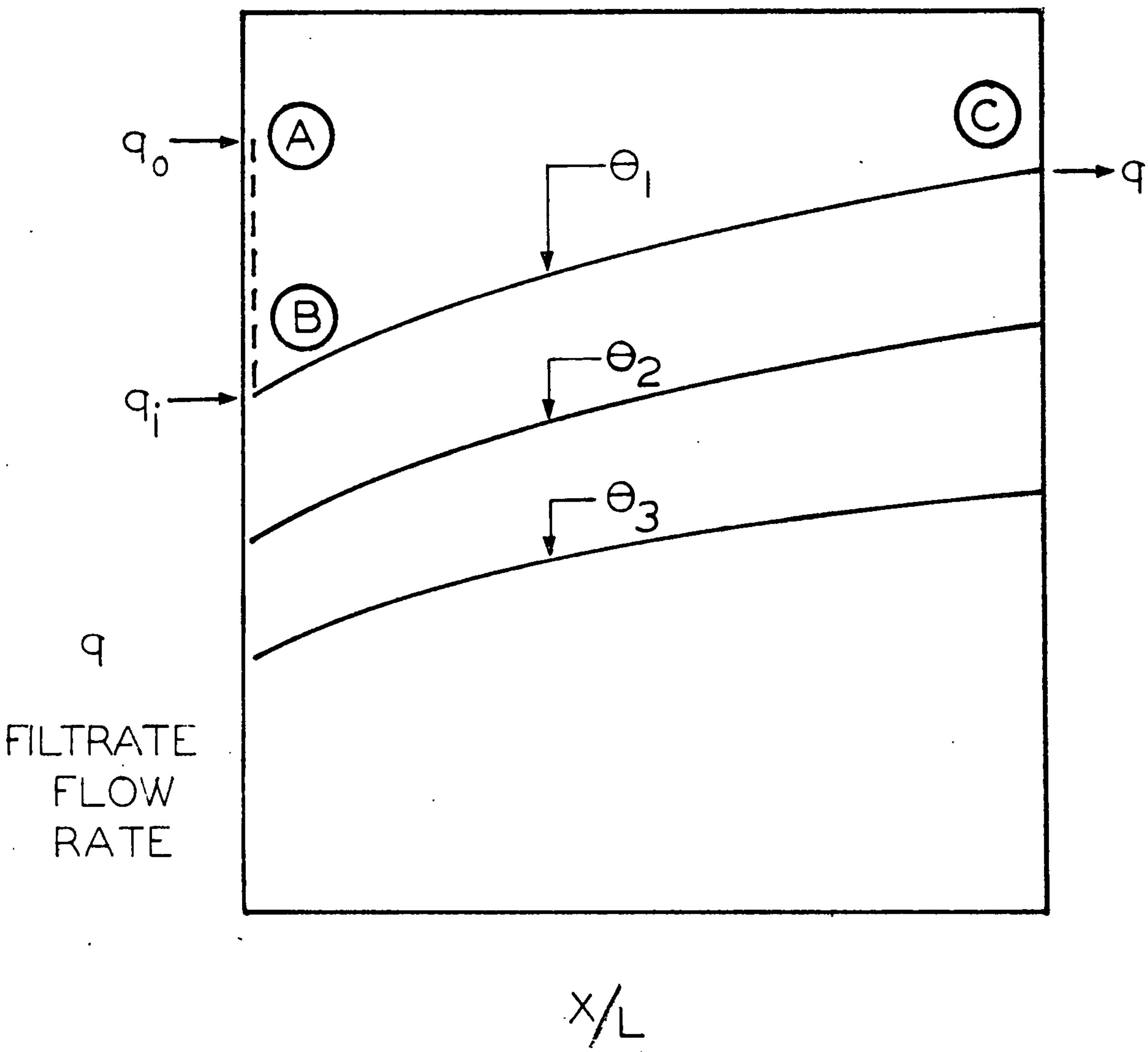

FIGURE 34.

FLOW THROUGH COMPRESSIBLE FILTER CAKE

In past investigations, Equations (3) and (5) have been integrated on the basis of q being constant throughout the cake at any instant, i.e., q has been assumed to be a function of the time θ but not the distance x.[25,61,62,63] However if the average porosity of the cake is decreasing then some of the liquid is being squeezed out of the cake; and q will be varying from the cake surface through the solid reaching its maximum value at the interface between the solid and supporting medium.

A liquid material balance over a differential section of the cake on a unit area basis yields

$$\frac{\text{Rate out}}{\text{area}} - \frac{\text{Rate in}}{\text{area}} = (\text{rate of change of porosity}) \times \frac{(\text{volume})}{\text{area}}$$

$$q_{out} - q_{in} = \Delta q = \frac{\epsilon\ (\text{initial}) - \epsilon\ (\text{final})}{\Delta\theta}\ \Delta x \tag{69}$$

or in the limit

$$\frac{\partial q}{\partial x} = - \frac{\partial \epsilon}{\partial \theta} \tag{70}$$

This equation may also be obtained by writing the hydrodynamical equation of continuity. Since ϵ is a function of p_s alone, Equation (70) may be rewritten as

$$\frac{\partial q}{\partial x} = - \frac{d\epsilon}{dp_s} \frac{\partial p_s}{\partial \theta} \tag{71}$$

The quantity $\partial \epsilon/\partial\theta$ is negative since the porosity decreases at each point with respect to time; consequently $\partial q/\partial x$ is positive, indicating that q increases with x. In Figure (34) the flow rate is illustrated as a function of time and distance. At point A just prior to entry into the cake the flow rate of the slurry is q_o. Immediately on depositing the surface layer of high moisture content material the rate drops to B.

With decreasing porosity the flow rate increases until it reaches the value of q at C.

Equations (5) and (71) represent simultaneous equations with q and p_s as dependent variables and x and θ as independent variables. To eliminate q between Equations (5) and (71) the latter equation is first differentiated with respect to x

$$g_c \frac{\partial^2 p_s}{\partial x^2} = \mu \, p_s \frac{d}{dp_s} \left[\alpha \, (1 - \epsilon)\right] \frac{\partial p_s}{\partial x} q + p_s \, \mu \, \alpha \, (1 - \epsilon) \frac{\partial q}{\partial x} \quad (72)$$

Eliminating q and $\partial q / \partial x$ leads to

$$g_c \frac{\partial^2 p_s}{\partial x^2} = \frac{g_c}{\alpha(1-\epsilon)} \left(\frac{\partial p_s}{\partial x}\right)^2 \frac{d}{dp_s} \left[\alpha(1-\epsilon)\right] - p_s \, \mu \, \alpha \, (1-\epsilon) \left(\frac{d\epsilon}{dp_s}\right)\left(\frac{\partial p_s}{\partial \theta}\right) \quad (73)$$

Equation (73) may be rewritten as

$$g_c \frac{\partial^2 p_s}{\partial x^2} = g_c \frac{d \ln \left[\alpha \, (1-\epsilon)\right]}{dp_s} \left(\frac{\partial p_s}{\partial x}\right)^2 - p_s \, \mu \, \alpha \, (1-\epsilon) \frac{d\epsilon}{dp_s} \left(\frac{\partial p_s}{\partial \theta}\right) \quad (74)$$

If w_x is used as an independent variable replacing x, Equation (74) becomes

$$g_c \frac{\partial^2 p_s}{\partial w_x^2} = g_c \frac{d \ln \left[\alpha \, (1-\epsilon)\right]}{dp_s} \left(\frac{\partial p_s}{\partial w_x}\right)^2 - \frac{\mu \, \alpha}{p_s \, (1-\epsilon)} \frac{d\epsilon}{dp_s} \left(\frac{\partial p_s}{\partial \theta}\right) \quad (75)$$

A solution for mass of cake corresponding to time and pressure of filtration is obtainable by integrating the non-linear partial differential equation given in Equation (75), the coefficients of which are obtained from experimental data. Numerical procedures must be used since analytical solutions for boundary conditions describing cake behavior have not been discovered for this equation, the variables of which are not separable.

An upper limit on the variation of p_s in the filter cake can be obtained by assuming that the flow rate remains constant throughout the cake and equals q or q_o. Since q is larger than the rate at any point within the solids, use of q throughout the cake will lead to conservative values of pressure drop or mass of filter cake, a low value for cake mass and corresponding filtrate volume resulting from the calculation.

If the value $q(x,\theta)$ in Equation (3) is replaced by $q = q(L,\theta) = q(w,\theta)$, the value of the rate at the septum, it is possible to integrate the equation treating q as a constant. Solving for dw_x and integrating yields

$$\int_0^w dw_x = w = \frac{g_c}{\mu q}\int_0^{p - p_1} \frac{dp_s}{\alpha} \tag{17}$$

where w is the total mass of solid per unit area contained in the distance zero to L. In terms of filtrate volume, Equation (17) can be written

$$v = \frac{g_c\ (1 - ms)}{\mu\ \rho\ s\ q}\int_0^{p - p_1} \frac{dp_s}{\alpha} \tag{76}$$

by substitution of Equation (20). A changing value of m must be used in Equation (76) for each pressure drop across the cake $(p - p_1)$.

In order to calculate m it is necessary to obtain the average porosity. If L is the thickness of the cake then

$$\epsilon_{av} = \frac{1}{L}\int_0^L \epsilon dx \tag{77}$$

or changing the variable of integration

$$\epsilon_{av} = \frac{1}{L}\int_0^{p - p_1} \epsilon\ (\frac{dx}{dp_s})\ dp_s \tag{78}$$

The term dx/dp_s can be obtained from Equation (5) and substituted in Equation (78) to yield

$$\epsilon_{av} = \frac{g_c}{\mu \rho\ sq}\ \frac{1}{L}\int_0^{p - p_1} \frac{\epsilon dp_s}{\alpha\ (1 - \epsilon)} \tag{79}$$

The thickness of the cake can be found by integrating dx from zero to L in Equation (5) as follows

$$\int_0^L dx = L = \frac{g_c}{\mu \rho sq} \int_0^{p - p_1} \frac{dp_s}{\alpha (1 - \epsilon)} \tag{80}$$

Dividing Equation (76) by (77) leads to

$$\epsilon_{av} = \frac{\int_0^{p - p_1} \frac{\epsilon \, dp_s}{\alpha (1 - \epsilon)}}{\int_0^{p - p_1} \frac{dp_s}{\alpha (1 - \epsilon)}} \tag{81}$$

For convenience of calculation, Equation (81) may be rewritten as

$$\epsilon_{av} = \frac{\int_0^{p - p_1} \frac{dp_s}{\alpha (1 - \epsilon)} - \int_0^{p - p_1} \frac{dp_s}{\alpha}}{\int_0^{p - p_1} \frac{dp_s}{\alpha (1 - \epsilon)}} \tag{82}$$

Since the integral of dp_s/α must be determined prior to use of Equation (82) only the integral $dp_s/\alpha (1 - \epsilon)$ need be found instead of the two additional integrals in Equation (81). The value of m may be found by substituting ϵ_{av} from Equation (82) into Equation (23).

To solve a problem involving a short filtration with a concentrated slurry the following procedure may be conveniently followed:

1. The value of the pressure at the medium p_1 is calculated as a function of q, the exit flow rate.

2. The integrals

$$\int_0^{p - p_1} \frac{dp_s}{\alpha} \qquad \int_0^{p - p_1} \frac{dp_s}{\alpha (1 - \epsilon)}$$

are calculated as functions of q.

3. The average value of porosity θ_{av} is calculated using Equation (82). The value of m is found by means of Equation (23).

4. The value of v as a function of q is found by employing Equation (76).

5. With the volume of filtrate known as a function of q. the time may be obtained by integrating the expression

$$dv = q\,d\theta \tag{19}$$

in the following manner

$$\theta = \int_0^v \frac{dv}{q} \tag{25}$$

This procedure is illustrated by Example 10.

Example 10. Calculations for Talc Filtration with Exit Flow Rate

Talc is to be filtered at a constant pressure of 15 lb. force/sq. in. under the following conditions:

μ = 0.001 lb. mass/(ft.)(sec.)

ρ = 62.4 lb. mass/cu.ft.

ρ_s = 167.0 lb. mass/cu.ft.

s = 0.10 mass fraction solids in slurry

R_m = 1.0 (10^{10}) reciprocal feet

The following porosity and filtration resistance data of Grace will be assumed to apply:[10]

p lb.force/sq.in.	α ft./lbm.	ϵ
0.0	0.32 (10^{11})*	0.900*
0.5	0.66*	0.859*
1.0	0.90	0.848
2.0	1.29	0.828
4.0	1.80	0.802
6.0	2.18	0.784
8.0	2.52	0.772
10.0	2.80	0.762
15.0	3.43	0.747

*Obtained by arithmetic extrapolation. Calculations are quite sensitive to different methods of extrapolation.

In Table VI the results of the calculations are shown. Following the procedure which was suggested, values of q are assumed as given in column (1). The values of pressure at the medium are calculated using Equation (18) as listed in column (2). With the limits of integration known as $(15 - p_1)$, numerical integration of the two required integrals is accomplished, the values listed in columns (3) and (4).

The average porosity and ratio of mass of wet to mass of dry cake are calculated with Equations (23) and (82), the results being presented in columns (5) and (6). With the preceding values the volume of filtrate is calculated employing Equation (24). Finally the time in seconds is obtained from an integration of Equation (25).

The data as calculated in the example are shown in Figure (35) along with curves for talc at 5 lb. force/sq.in. and polystyrene latex at at 10 lb. force/sq.in.* The curves are plotted in the form of $d\theta/dv$ vs. v; and according to conventional theory such curves should yield straight lines if α, and R_m are constant. These calculations illustrate that marked deviation from linear form result when variation of cake pressure drop is taken into consideration in filtration of compressible materials.

The time rate of filtration may be calculated using the minimum q during filtration, the flow into the cake from surface solids deposited

* Calculations shown in Appendix V.

TABLE VI

TALC FILTRATION WITH EXIT FLOW RATE

q (cu.ft.)/(sq.ft.)(sec.)	p_1 lb.force/sq.in.	$\int_0^{p-p_1} \frac{dp_s}{\alpha}$ $\frac{(\text{lb.mass})(\text{lb.force})}{(\text{ft.})(\text{sq.in.})}$	$\int_0^{p-p_1} \frac{dp_s}{\alpha\ (1-\theta)}$	θ_{av}	m	v cu.ft./sq.ft.	θ seconds
6.96 (10^{-3})	15.0	0	0	0.945	7.42	0	0
6.00	12.9	2.73 (10^{-11})	25.75 (10^{-11})	0.894	4.15	0.00198	0.31
5.50	11.8	3.40	29.06	0.883	3.83	0.00284	0.46
5.00	10.7	4.06	32.48	0.875	3.62	0.00386	0.65
4.50	9.7	4.57	35.15	0.870	3.50	0.00491	0.87
4.00	8.6	5.04	37.33	0.865	3.40	0.00619	1.17
3.50	7.5	5.51	39.36	0.860	3.30	0.00785	1.62
3.00	6.5	5.94	41.25	0.856	3.22	0.00988	2.28
2.50	5.4	6.36	43.26	0.853	3.17	0.01293	3.36
2.00	4.3	6.86	45.73	0.850	3.12	0.01756	5.44
1.50	3.2	7.15	46.43	0.846	3.05	0.02463	9.56
1.00	2.2	7.44	47.69	0.844	3.02	0.03864	21.25
0.75	1.6	7.61	48.47	0.843	3.00	0.05282	37.80
0.50	1.1	7.77	49.18	0.842	2.99	0.18107	84.90
0.25	0.8	7.85	52.02	0.841	2.98	0.16395	333.50

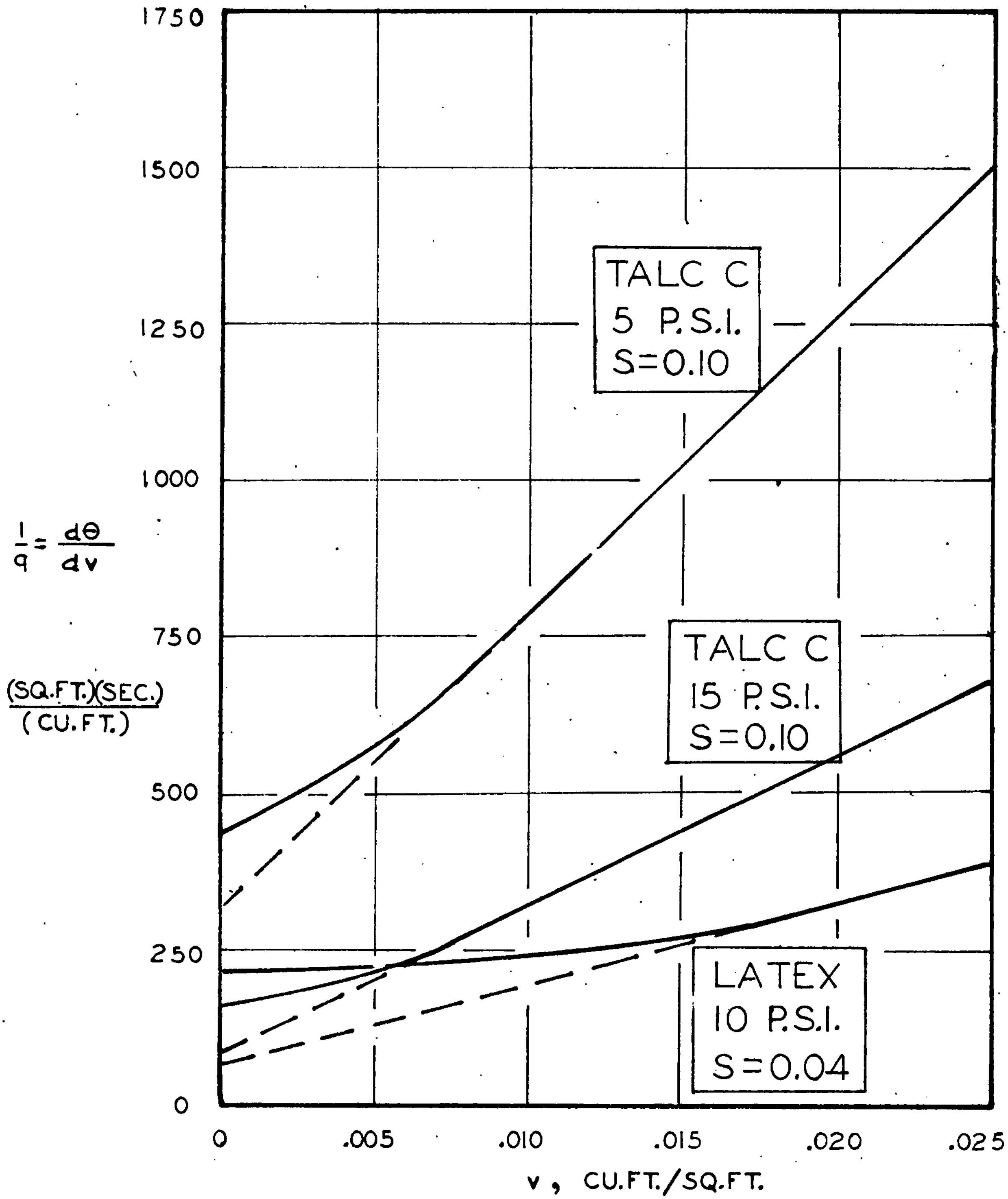

FIGURE 35.

DEVIATION FROM CONVENTIONAL FILTRATION EQUATION
IN CALCULATIONS FOR COMPRESSIBLE MATERIALS

at an initial porosity. When the flow of filtrate through the medium, q_1, is used in the integrated equation for filtration rates, a low value of filtrate volume is calculated per unit time compared to calculations based on maximum flow rate. The filtrate flow rate in a filter cake, highest at the medium due to progressive compression of the cake from surface to medium, is of minimum magnitude at the point of initial flow into the cake as indicated in Figure (34). In a differential section of cake, resistance to flow is directly proportional to mass of cake and inversely proportional to superficial filtrate rate. Equation (25) indicates that a low volume of filtrate v will be obtained in a given time θ in the integrated result when a low value of flow rate is used.

Comparison of computations obtained using minimum filtrate flow rate with those from the maximum exit rate demonstrates how the assumption of filtrate flow velocity effects results of filtration rate estimates by illustrating the limiting cases. From Equations (63) and (67) v_o (volume of liquid removed from slurry) and q_i (minimum flow into cake from surface solids) can be calculated for a given pressure drop across the cake. It is necessary to have information on the rate of change of average porosity with time to perform this calculation. The volume of filtrate calculated using q_i for filtration of talc at 15 lb.force/sq.in. under the same conditions as used in the illustration of Example 10. as shown in Table VI. Example 11. indicates the calculation procedure. The resulting time vs. filtrate volume calculated in Examples 10. and 11. are compared in Figure (36).

<u>Example 11</u>. Calculation for Talc Filtration with Inlet Flow Rate

Table VII contains the calculated results taking values of q_1 from column (1) in Table VI as a basis for computing q_i. The medium pressure p_1 is calculated using Equation (18) and values of q in column (1). For each cake pressure drop $(p - p_1)$ a value of average specific resistance and average cake porosity corresponding is utilized to calculate m given in column (3) and v shown in column (4), using Equations (23) and (76).

Calculation of q_i requires knowledge of v_o, volume of liquid removal from the slurry, and $dm/d\theta$ following Equation (67). Equation (63) using m provides the basis for v_o in column (5). The differential term $dm/d\theta$ corresponding to each term q_i is obtained from the results shown in Table VI relating m to θ based on time integration for the maximum filtrate rate q. The calculations shown in Table IV are plotted in Figure (33). To numerically differentiate m vs. θ orthogonal polynomials are fitted to portions of the curve and the resulting least squares equation being treated analytically, the results being given in column (6). Appendix X describes the application of this technique.

The estimated surface porosity of talc, 0.945, is the basis for m_i given as 7.42. Results of numerical integration for time are shown in column (8), where the expression is utilized

$$\theta = \int_0^v \frac{dv}{q_i} \qquad (25a)$$

TABLE VII

TALC FILTRATION WITH INLET FLOW RATE

q	p_1	m	v	v_o	-dm/dθ	q_i	θ
(cu.ft.)/(sec.)(sq.ft.)	lb.force/sq.in.		cu.ft./sq.ft.		1/sec.	cu.ft./(sec.)(sq.ft.)	seconds
6.96 (10^{-3})	15.0	7.42	0	0	7.12	6.96 (10^{-3})	0
6.00	12.9	4.15	1.98(10^{-3})	3.05 (10^{-3})	3.25	2.36	0.56
5.50	11.8	3.83	2.84	4.67	1.18	2.√4	0.95
5.00	10.7	3.62	3.86	5.44	0.67	1.86	1.47
4.50	9.7	3.50	4.91	6.78	0.35	1.69	2.06
4.00	8.6	3.40	6.19	8.42	0.25	1.47	2.87
3.50	7.5	3.30	7.85	10.52	0.17	1.27	4.09
3.00	6.5	3.22	9.98	13.27	0.12	1.07	5.92
2.50	5.4	3.17	12.04	17.04	0.10	0.88	8.97
2.00	4.3	3.12	17.56	22.97	0.08	0.67	15.03
1.50	3.2	3.05	24.63	31.90	0.07	0.47	27.82
1.00	2.2	3.02	38.64	49.81	0.05	0.27	68.66
0.75	1.6	3.00	52.82	167.93	0.02	0.22	127.11
0.50	1.1	2.99	81.07	104.09	0.00	0.18	268.92
0.25	0.8	2.98	163.95	210.18	0.00	0.09	956.82

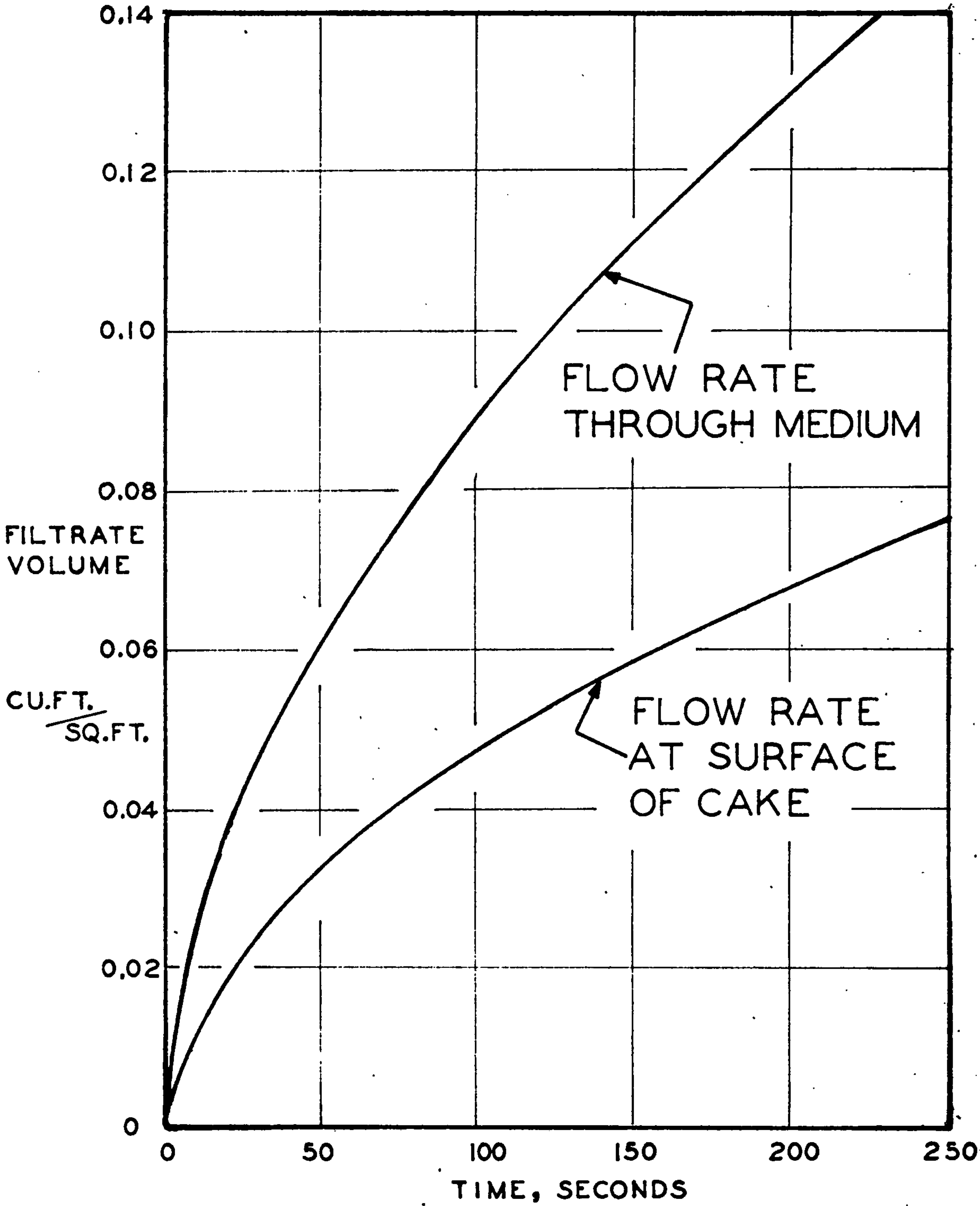

FIGURE 36.

COMPARISON OF CALCULATED FILTRATE VOLUMES FOR MINIMUM AND MAXIMUM FILTRATE RATES FOR TALC AT 15 P.S.I.

CHAPTER IV

ROTARY DRUM FILTRATION

Rotary drum filtration is a method of continuous filtration carried out by means of a drum covered by a permeable medium rotating partially submerged in a solid-liquid slurry. A pressure driving force is provided across the permeable medium causing mass flow of slurry into the medium. Solids are separated on the drum surface with filtrate passing through into the drum and continuously carried out. The solid cake formed on the medium surface is removed in a continuous manner by reversing the pressure vector by air pressure on a sector inside the drum or by cutting the bulk of cake off with a scraper blade mounted close to the drum surface.

Rotary filtration taken as a unit operation is a continuous process of separation of solids and liquid from a steady stream of slurry. In order to analyze the process to estimate rates, the operation is approached from a discontinuous standpoint since the output of one segment of the drum is taken as a basis. Each segment can be thought to be performing a short batch filtration during a drum rotation cycle beginning with the entry of a unit segment into the slurry and ending with emergence of the segment. In the remaining portion of the drum rotation cycle washing may be performed and solids are discharged.

Calculations for rotary drum filtration have generally been made in the past by considering the pressure drop across the cake to be constant.[52,55] The effect of constant p is that specific resistance during filtration is treated as constant and the Ruth equations can be applied. One form of the Ruth equation is Equation (27),

$$\frac{\theta}{v} = \frac{1}{2} \frac{\mu}{g_c} \frac{s\rho}{1 - ms} \frac{\alpha_{av}}{p} v + \frac{\mu}{g_c} \frac{R_m}{p} \tag{27}$$

Constant cake pressure drop occurs in constant pressure filtration only when medium resistance is negligible in comparison to cake resistance. Medium resistance has been shown to be a more significant portion of total flow resistance in continuous rotary filtration than is normally encountered in batch pressure filtration.[43] When medium resistance is significant, specific resistance of compressible cakes will vary throughout the filtration cycle because of the changing cake pressure drop and the Ruth equations become fundamentally in error. Previous analysis of constant pressure filtration has shown that errors in assuming constant specific resistance become progressively greater as slurry concentration increases and filtration pressure decreases. Rotary drum filtrations are often carried out under low pressures as the pressure differential across the drum is usually supplied by a vacuum pump drawing from the drum interior. In addition applications of rotary drum filtration are more economical when concentrated slurries are filtered since drum surface is costlier than filter area in other commonly used equipment designs.

Vacuum rotary drum filtration is frequently carried out at differentials as low as five inches of mercury head in applications in which filtrate vapor pressure is high. If large sized drums are used at high submergence the magnitude of static pressure of slurry above the drum surface may be great enough to be equivalent to the vacuum supplied by the pump at the point of maximum submergence. Figure (36) indicates variation of total pressure (sum of static pressure and pressure difference delivered by a vacuum pump) in curve A and pressure differential across the cake, curve B, calculated for filtration of compressible solids.* When static head is large in comparison to pump pressure differential, accurate mathematical representation of the filtration process requires consideration of the variable total pressure.

Analysis of rotary filtration is made most conveniently by considering one unit rotation cycle of the filter. A rotation cycle of a drum filter is the movement of a section of drum surface from its point of entry into the slurry to its point of emergence. The volume of filtrate removed from the slurry and the mass of cake held on the medium referred to unit area represents the filter performance per unit area per revolution. The time per filtration cycle is dependent upon the rate of drum rotation. In Figure (1B) a segment of drum $\Delta \phi$ enters the slurry at A with the drum rotating at a constant rate ω, defining rate of rotation as

$$\omega = \frac{\Delta \phi}{\Delta \theta} \tag{83}$$

Assuming a constant pressure differential p_o maintained between the downstream side of the medium and the atmosphere, the pressure driving force for filtration is the sum of p_o and the static head. The height of slurry above any point on the submerged drum, h as shown in Figure (1B), is dependent on ϕ. The angle ϕ denotes the arc measured on the drum axis between the point A where the filtration cycle commences at the point of entry into the slurry and the position of the incremental arc subtended

* Based on calculations given in Appendix IX

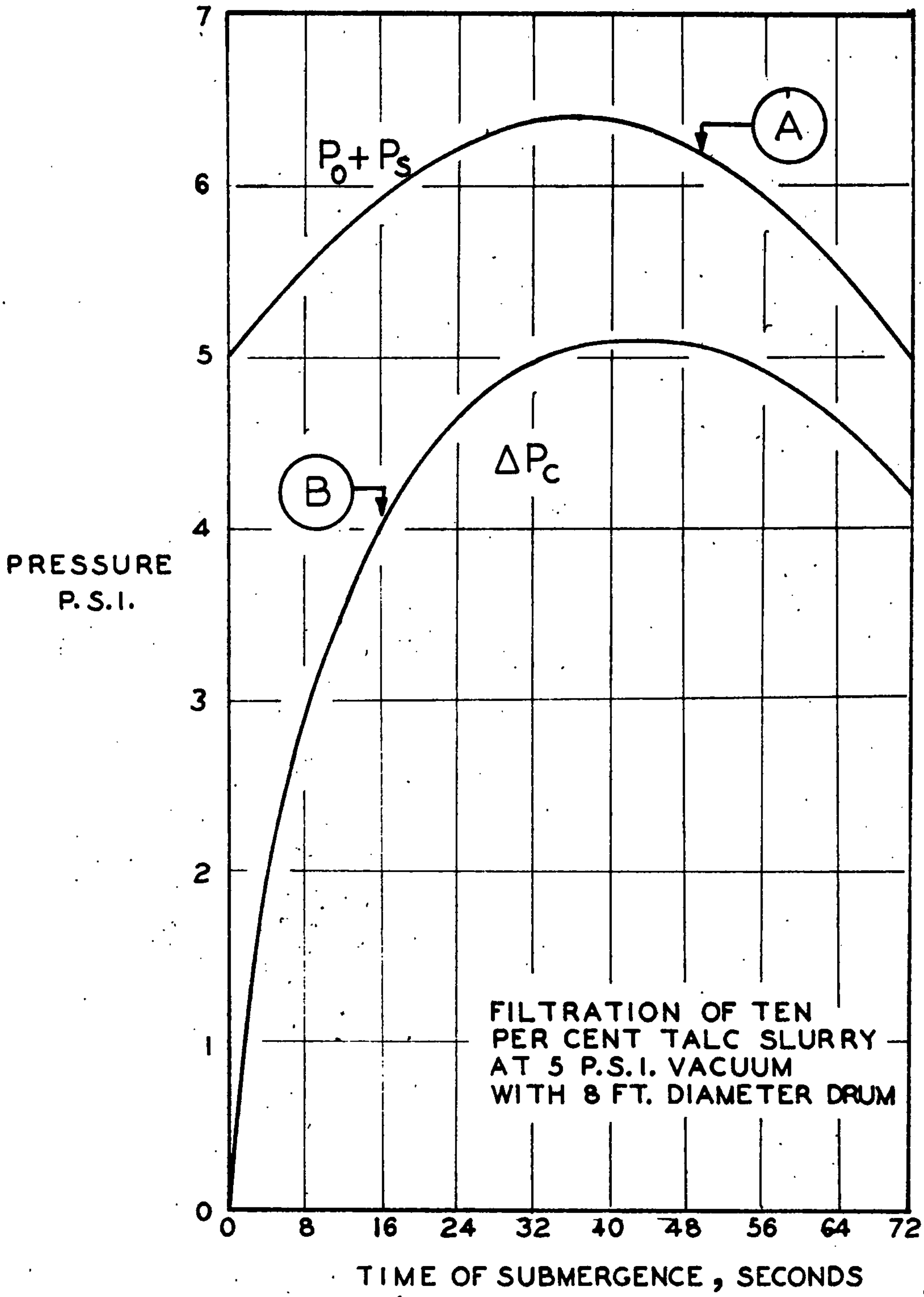

FIGURE 37.

PRESSURE VARIATION IN ROTARY DRUM
FILTRATION OF COMPRESSIBLE SOLIDS

by the sector $\Delta\phi$. A maximum value of ϕ equal to β is reached when the sector $\Delta\phi$ emerges from the slurry at B. β is the angle of submergence of the drum. Figure (1B) is utilized to show that the height of slurry above a point on the drum at the arc given by the angle ϕ on the drum axis from the slurry surface is

$$h = R\left[\cos\left(\beta/2 - \phi\right) - \cos\left(\beta/2\right)\right] \tag{29a}$$

and the corresponding static pressure p_s becomes

$$p_s = \rho_f h = \rho_f R\left[\cos\left(\beta/2 - \phi\right) - \cos\left(\beta/2\right)\right] \tag{84}$$

where ρ_f is density of the slurry and R is drum radius.

The surface of a drum filter is formed by a number of segments composing the periphery of a circle on the axial plan of the drum, each segment corresponding to a sector $\Delta\phi$. Internal rotary valve ports are arranged to pull vacuum on each sector in turn as it becomes completely submerged upon entering the slurry. The working filtration area is therefore smaller than indicated by the angle of submergence β. To simplify mathematical treatment applied to large diameter drums, the assumption is made that $\Delta\phi$ approaches a differential value $d\phi$ in the limit, or $\Delta\phi$ is considered small in comparison to β. An expression synomomous to Equation (83) can then be written

$$d\phi = \omega d\theta \tag{85}$$

Substituting Equation (85) in the fundamental equation of filtration, Equation (21), produces

$$q = \frac{dv}{d\theta} = \frac{\omega dv}{d\phi} = \frac{g_c\ s\ \rho}{\mu\ v\ (1 - ms)}\int_0^{p-p_1}\frac{dp}{\alpha} \tag{86}$$

Solution of this expression for v when $\phi = \beta$ yields the filtrate volume per unit rotation cycle.

The upper limit of the integral term in Equation (86) is a variable in ϕ since the medium pressure p_1 is given by

$$p_1 = \frac{\mu}{g_c} qR_m = \frac{\mu}{g_c} R_m \omega \frac{dv}{d\phi} \tag{18a}$$

and

$$p - p_1 = p_o + \rho_f R[\cos(\beta/2 - \phi) - \cos(\beta/2)] - \frac{\mu}{g_c} R_m \omega \frac{dv}{d\phi} \tag{87}$$

Equation (86) thus contains two variables, v and ϕ, since α and m are functions of $(p - p_1)$ given by Equation (87). Analytical solution for filtration of compressible materials using Equation (86) cannot be accomplished in the absence of an expression for ϵ_{av} and α_{av} in terms of $(p - p_1)$. A numerical procedure used to approximate solutions of Equation (86) is given in Appendix VIII.

Simplified solutions for variable static head obtained by neglecting the change in pressure drop across the cake can be derived by direct integration of the Ruth equation, substituting Equation (87) for p into Equation (86) with the terms α and m considered constants.[33] The result of this treatment is

$$\frac{\omega}{2} \frac{\mu \ \alpha_{av} \ s \ \rho}{g_c \ (1 - ms)} v^2 + R_m \omega \frac{\mu}{g_c} v = p_o \phi - \rho_f R\left[(\phi + 1)\cos(\beta/2) - \cos(\beta/2 - \phi)\right] \tag{88}$$

Another simplification is the use of an integrated average static head correction added to the pressure of filtration, p_o. The correction term obtained by integration of Equation (84) from $\phi = 0$ to $\phi = \beta$ is[52]

$$p_{s_{av}} = \rho_f h_{av} = \rho_f \left[\frac{R}{\beta} \sin(\beta/2) - \frac{\beta}{2} \cos(\beta/2)\right] \tag{29c}$$

A solution is then obtained for Equation (86) for constant p in the upper limit of the integral.

Estimating rates for rotary drum filtration is more exact using Equation (86) which takes into account variable static head on a segment of filter surface as the drum moves through a cycle in addition to variable cake pressure drop due to medium resistance. Results of the calculations using simplified expressions are compared with the results of the more precise procedure in Figure (37).* Curve A indicates filtrate volume vs. time of submergence during filtration of a compressible material based on a segment of an eight foot diameter drum 40% submerged moving through one rotation in two minutes. The effect of variation in static head and cake pressure drop are taken into account in the calculations on which curve A is based. The Ruth equation (constant cake pressure drop) with variable static head is the basis of curve B, using Equation (88). Specific resistance for the compressible solids is evaluated for maximum cake pressure drop for curve B calculations. Average static head correction, Equation (29c) is utilized with the basic exact equation for constant pressure filtration, Equation (86), to determine curve C to illustrate difference in results based on average static head correction and variable static head.

It is to be noted that in the solution of Equation (86) for filtration of talc slurry at five pounds per square inch vacuum differential, the cake pressure drop as plotted in Figure (36) reaches a maximum and decreases to a final value lower than the maximum. It has been shown experimentally that compression of solids in filter cakes is

* Calculations and discussion given in Appendix IX

irreversible, or the filter cake dimensions do not return elastically to their original magnitudes after release of the compressing force.[61] The numerical solution of Equation (86) carried out as given in Appendix IX is based on the assumption that cake specific resistance and solids porosity do not decrease from maximum cake pressure drop values.

The results of calculations based on Equations (86), (88), and (27) are dependent on attainment of equilibrium values of specific resistance and porosity instantaneously with application of compression forces. The results will be conservative if the solids being filtered compress slowly into equilibrium consolidation since compressive stresses are operative over relatively short time intervals in rotary drum filtration.

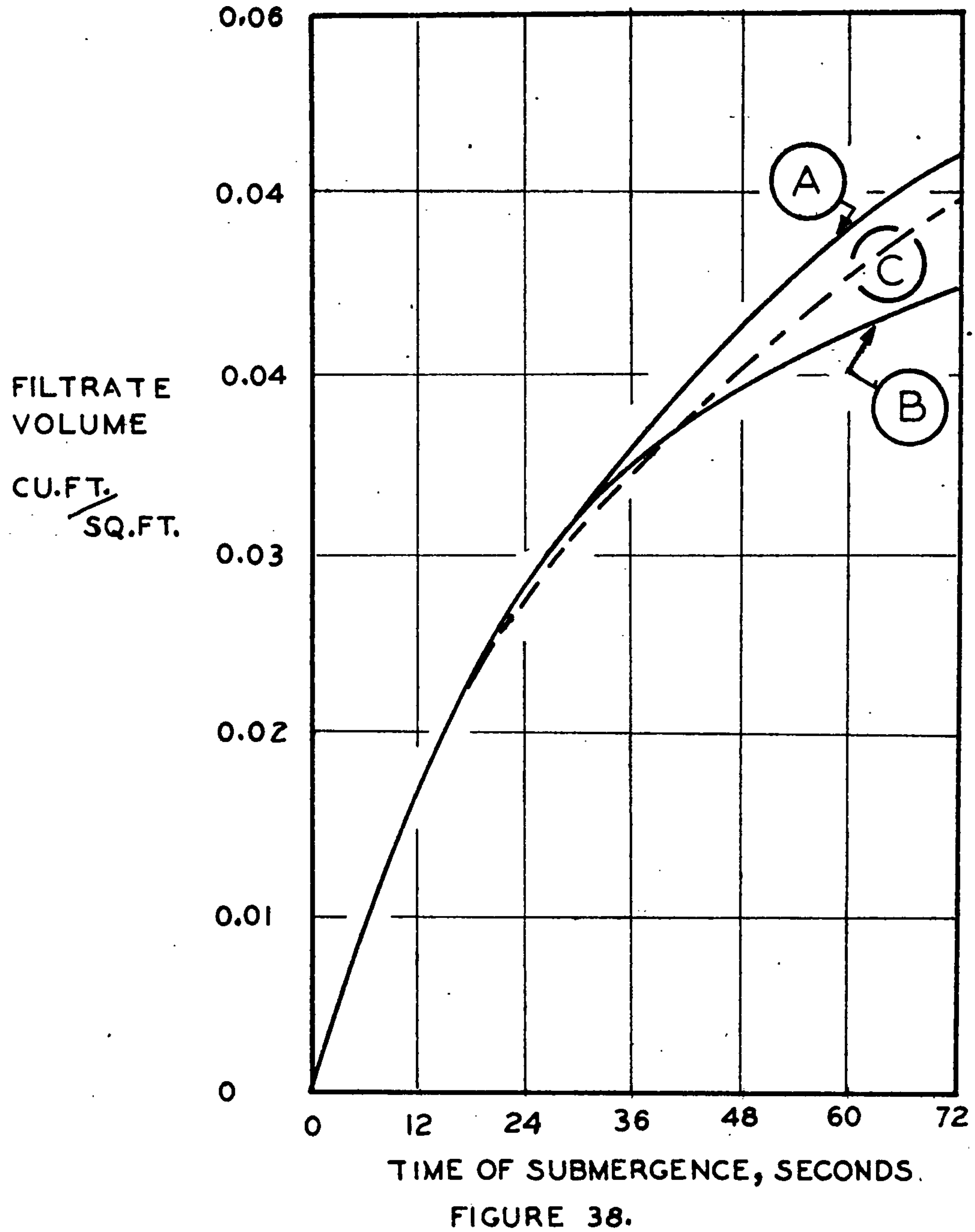

FIGURE 38.

FILTRATE VOLUME VS. TIME FOR
ROTARY DRUM FILTRATION OF TALC
AT 5 P.S.I. FOR DRUM DIAMETER OF EIGHT FEET

CHAPTER V

VARIATION OF POROSITY IN FILTER CAKES

Porosity variation in filter cakes has been the subject of a number of experimental investigations.[24,35,48,68] Hutto has made the most extensive study of porosity variations using a unique banding technique.[35] In discussing data in the literature, Hutto was concerned about different slopes of porosity vs. distance from surface of cake reported by different investigators. Figure (39) shows porosity curves that have been reported in the literature, plotting porosity vs. the ratio x/L which represents relative distance through the cake for x/L = 0 at the cake surface. It was stated by Hutto that data in which porosity decreased most rapidly at the septum, $\frac{d^2\epsilon}{dx^2} > 0$, could not be harmonized with data in which porosity decreased most rapidly at the cake surface, $\frac{d^2\epsilon}{dx^2} < 0$.[11,24,61,68] Analysis of compression-permeability cell data demonstrates that both types of variation are possible. In addition it was found that it is possible to encounter rapidly changing porosity gradients at the surface and medium which indicates that the direction of the slope is changing within the cake.

Porosity and specific resistance data are customarily obtained in a compression-permeability cell developed by Ruth and improved by Grace and Hutto.[24,35,50] In filtration theory it is assumed that porosity and specific resistance found in compression-permeability measurement at a given mechanical stress are the same as the values of ϵ and α at a point in the cake where the compressive pressure, defined by Equation

(10), is equal to the mechanical pressure.

$$p_s = p - p_x$$

In Equation (10) p_s is compressive pressure, p total pressure at surface, and p_x hydraulic pressure. Data obtained in a compression-permeability cell may be used to predict ϵ vs. x for different filtration conditions.

The basic equation employed for filtration is

$$-g_c \frac{dp_x}{dw_x} = g_c \frac{dp_s}{dw_x} = \alpha \mu q \tag{3}$$

where w_x is the mass of dry solids at the distance x measured from the cake surface, α_x the specific resistance, μ the viscosity, q the superficial velocity of fluid through the cake per unit area, g_c the dimensional constant relating force to mass, and p_s and p_x defined previously. The differential dw_x can be eliminated by Equation (4) to yield Equation (5)

$$dw_x = (1 - \epsilon) \; \rho_s \, dx \tag{4}$$

$$g_c \frac{dp_s}{dx} = \mu \rho_s (1 - \epsilon) \alpha_x q \tag{5}$$

Rearranging and integrating to x and p_x, the hydraulic pressure at x

$$\int_0^x dx = x = \frac{g_c}{\mu \; \rho_s q} \int_0^{p_x - p_1} \frac{dp_s}{\alpha (1 - \epsilon)} \tag{80a}$$

where p_1 is given by the limit to flow due to resistance of the medium,

$$g_c \; p_1 = \mu \; R_m \; q \tag{18}$$

If the integration is carried out over the entire cake, x = L, Equation (80a) becomes

$$L = \frac{g_c}{\mu \; \rho_s \; q} \int_0^{p - p_1} \frac{dp_s}{\alpha \; (1 - \epsilon)} \tag{80}$$

where p_1 is defined as the pressure at the interface of cake and medium. The ratio x/L can be obtained from Equations (80a) and (80) in the form

$$\frac{x}{L} = \frac{\displaystyle\int_0^{p_x} \frac{dp_s}{\alpha\,(1 - \epsilon)}}{\displaystyle\int_0^{p - p_1} \frac{dp_s}{\alpha\,(1 - \epsilon)}} \tag{80b}$$

where p_x varies from zero to $(p - p_1)$. In the discussion that follows p_1 will be neglected.

Equation (80b) yields a functional relationship between x/L and p_s. As ϵ is known as a function of p_s by compression-permeability measurement, ϵ may be related directly to x/L by treating p_s as a parameter.

The denominator of Equation (80b) is a constant for any given total pressure drop and will be represented by the symbol 1/C, leading to Equation (80c) as a simplification of Equation (80b) for evaluating the pressure at any point in the cake

$$x = LC \int_0^{p_x} \frac{dp_s}{\alpha\,(1 - \epsilon)} \tag{80c}$$

The curves of Figures (41, (42), and (43) were calculated by numerical integration of Equation (80c) using compression-permeability cell data reported by Grace.[24] Average cake porosity can be calculated by integrating the porosity distance curves by the expression

$$\epsilon_{av} = \frac{1}{L} \int_0^L \epsilon dx \tag{77}$$

Grace reported that a filter cake formed during constant pressure filtration of calcium carbonate slurry at 350 p.s.i. was sliced into sections with each section being weighed and dried to determine its average porosity. By this means a series of data points were obtained representing average porosity of each section of the cake from which the experimental curve in Figure (40) was constructed. Integration of this crudely obtained curve by Equation (77) resulted in a calculated average porosity of 0.72.

The calculated curve in Figure (40) was determined with compression-permeability cell data from the same calcium carbonate slurry as was used in the 350 p.s.i. filtration following Equation (80c).* A rapid rate of change of porosity with distance is indicated at the surface and medium in the filter cake. Any rapid changes in porosity present in the experimental cake would not be shown in the data obtained by Grace due to the averaged values in the section. Integration of the calculated curve yielded an average value of 0.72 for porosity which checked the experimental data. A dried filter cake of the same material obtained at 369 p.s.i. measured 0.70 porosity by material balance, providing further evidence for the validity of Equation (80c) and its method of derivation.

The slope of ϵ vs. x can be written in the following form

$$\frac{d\epsilon}{dx} = \frac{d\epsilon}{dp_s} \frac{dp_s}{dx} \tag{83}$$

The derivative dp_s/dx can be eliminated by means of Equation (5)

* Calculations shown in Appendix VII

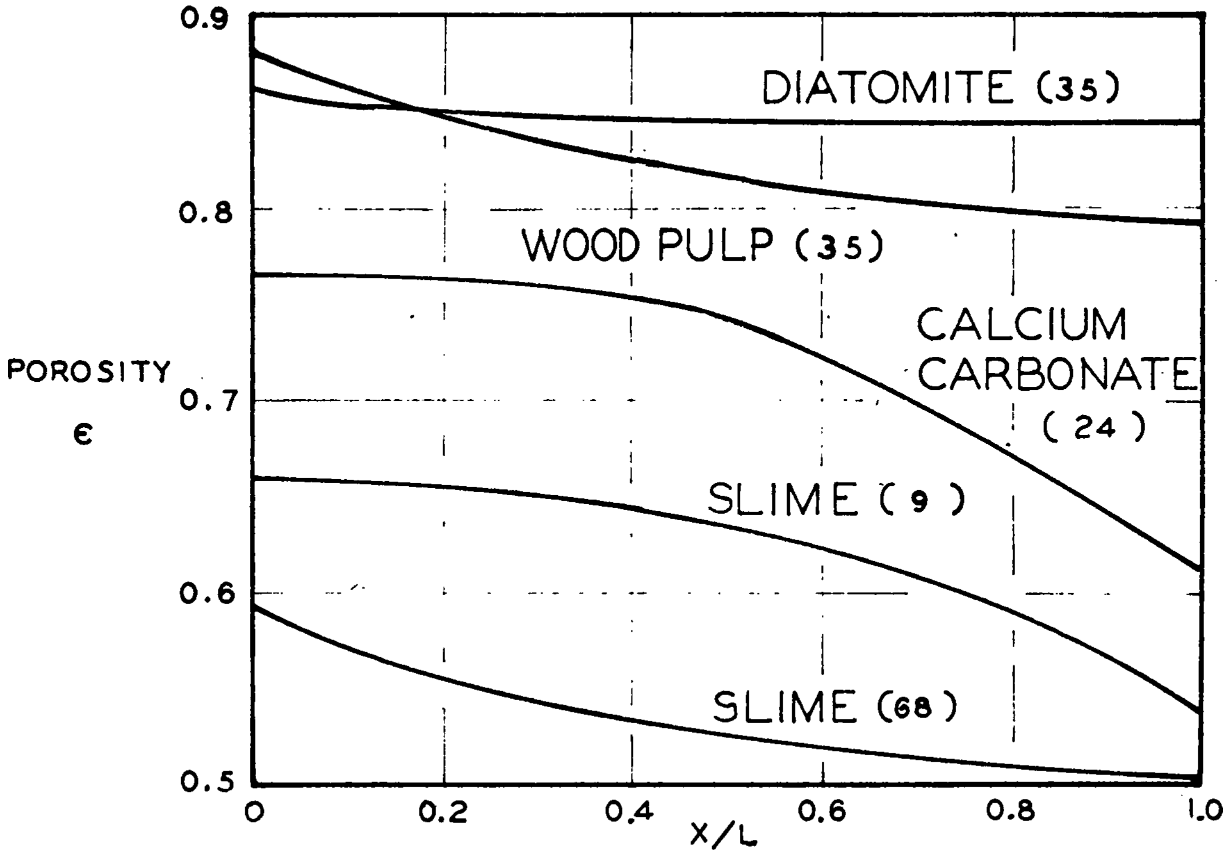

FIGURE 39.

POROSITY VARIATION IN FILTER CAKES FOUND EXPERIMENTALLY

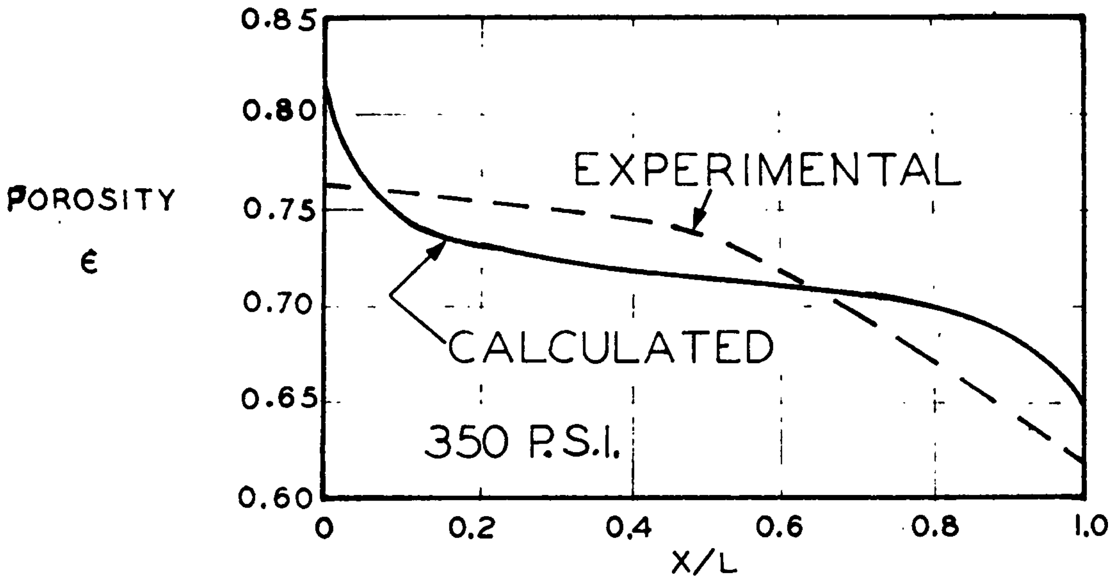

FIGURE 40.

POROSITY DISTRIBUTION CURVES FOR CALCIUM CARBONATE leading to

$$\frac{d\epsilon}{dx} = \frac{\mu \rho_s q}{g_c} (1 - \epsilon) \frac{d\epsilon}{dp_s} \alpha_x \tag{84}$$

Since $d\epsilon/dp_s$ is always negative, $d\epsilon/dx$ will be negative. In order to calculate $d\epsilon/dx$ it is necessary to have α_x and ϵ as functions of p_s.

The second derivative determines which of the curves of Figure (39) will be followed. Differentiating Equation (83) yields

$$\frac{g_c}{\mu \rho_s q} \frac{d^2\epsilon}{dx^2} = \frac{d}{dp_s}\left[\alpha (1 - \epsilon) \frac{d\epsilon}{dp_s}\right] \frac{dp_s}{dx} \tag{85}$$

For a particular material the nature of the porosity-distance curve is determined by the differential of ϵ with respect to x. Compression-permeability cell data reported in the literature were analyzed by fitting least squares polynomials to ϵ vs. p_s data and differentiating the resulting expressions.*

Plots are shown of the term $\alpha_x(1 - \epsilon) \frac{d\epsilon}{dp_s}$ vs. p_s in Figure (41). If the slope of $\alpha_x(1 - \epsilon) \frac{d\epsilon}{dp_s}$ vs. p_s is positive, the second derivative is positive and porosity gradients will be steepest at the surface of the cake. Data for flocculated calcium carbonate and kaolin seen in Figure (41) indicate that cake porosity will decrease rapidly at the surface of the cake and approach a constant value at the filter medium in filter cakes obtained at pressures up to 100 p.s.i. Curves relating ϵ vs. x/L calculated by Equation (80c) are given in Figure (43). The slope of the calculated curves for flocculated calcium carbonate and kaolin agree with the form predicted by the second derivative in

* Results are presented in Appendix VI.

Equation (85) as the data in Figure (41) illustrate.

Figure (42) contains ϵ vs. x/L plotted for materials predicted by the curves of Figure (41) to have steepest porosity gradients at the medium. Agreement between results of calculations based on compression-permeability cell data using Equation (80c) and gradients indicated by Equation (85) is shown in the curves for silica, zinc sulfide B, and Solka-floc. These three materials having greatest porosity change at the medium are representative of highly compressible materials whereas flocculated calcium carbonate and kaolin are relatively incompressible.

Porosity gradients reversing in direction are shown in Figure (43) for latex, zinc sulfide A and talc. The change in curvature of the porosity-distance relationship for these materials is indicated by the reverse in sign in the slope $\alpha_x(1 - \epsilon) \frac{d\epsilon}{dp_s}$ as can be determined from Figure (41).

In summary it is seen by these analyses that materials forming highly compressible cakes can be expected to decrease in porosity slowly in the direction of flow until the filter medium is approached. Compression increases with distance most rapidly close to the medium. Less compressible filter cakes are subject to the highest rate of compression close to the surface of the cake, shown in Figure (43). Between the extremes of highly compressible and less compressible materials, several materials are observed by analysis of compression-permeability cell data to exhibit steep porosity distance gradients at both surface and medium of the cake. An exception to this behavior is polystyrene latex, the data for which indicate that porosity variation with distance approaches a slower rate of change at both surfaces and is most rapid at the center of the cake.

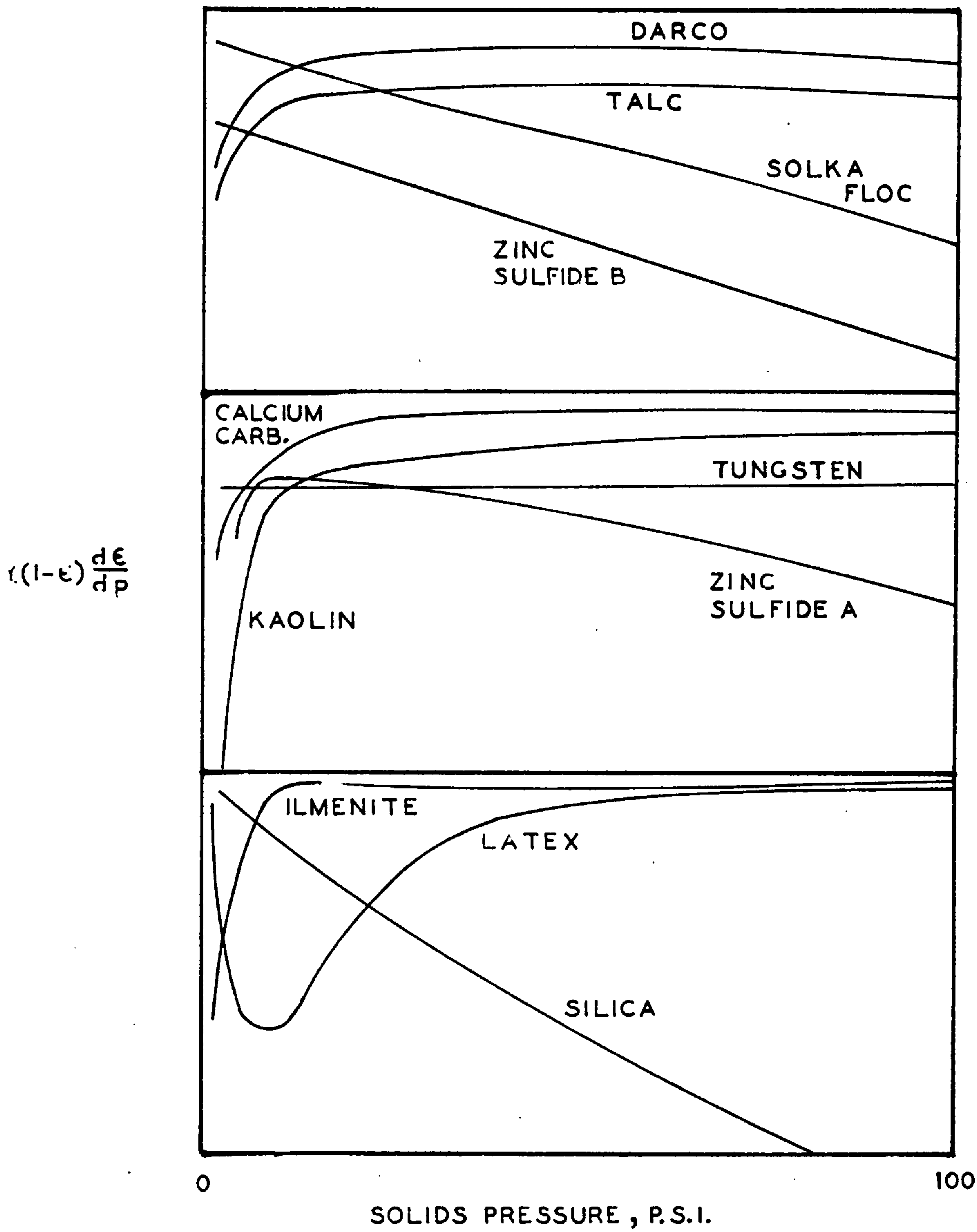

FIGURE 41.

POROSITY VARIATION -
RESULTS OF NUMERICAL ANALYSIS OF GRACE DATA

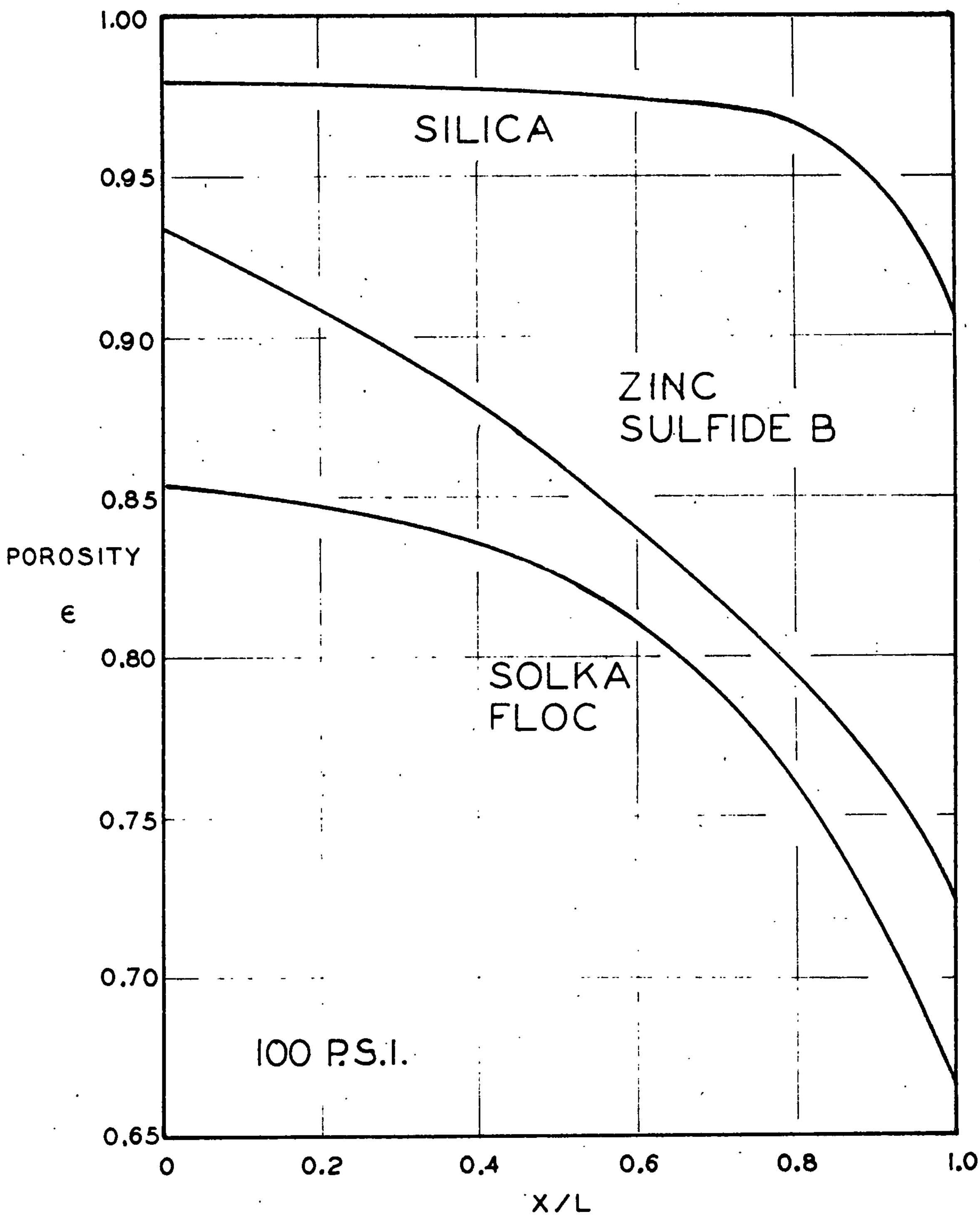

FIGURE 42.

CALCULATED POROSITY VARIATION - GREATEST CHANGE OF SLOPE AT MEDIUM

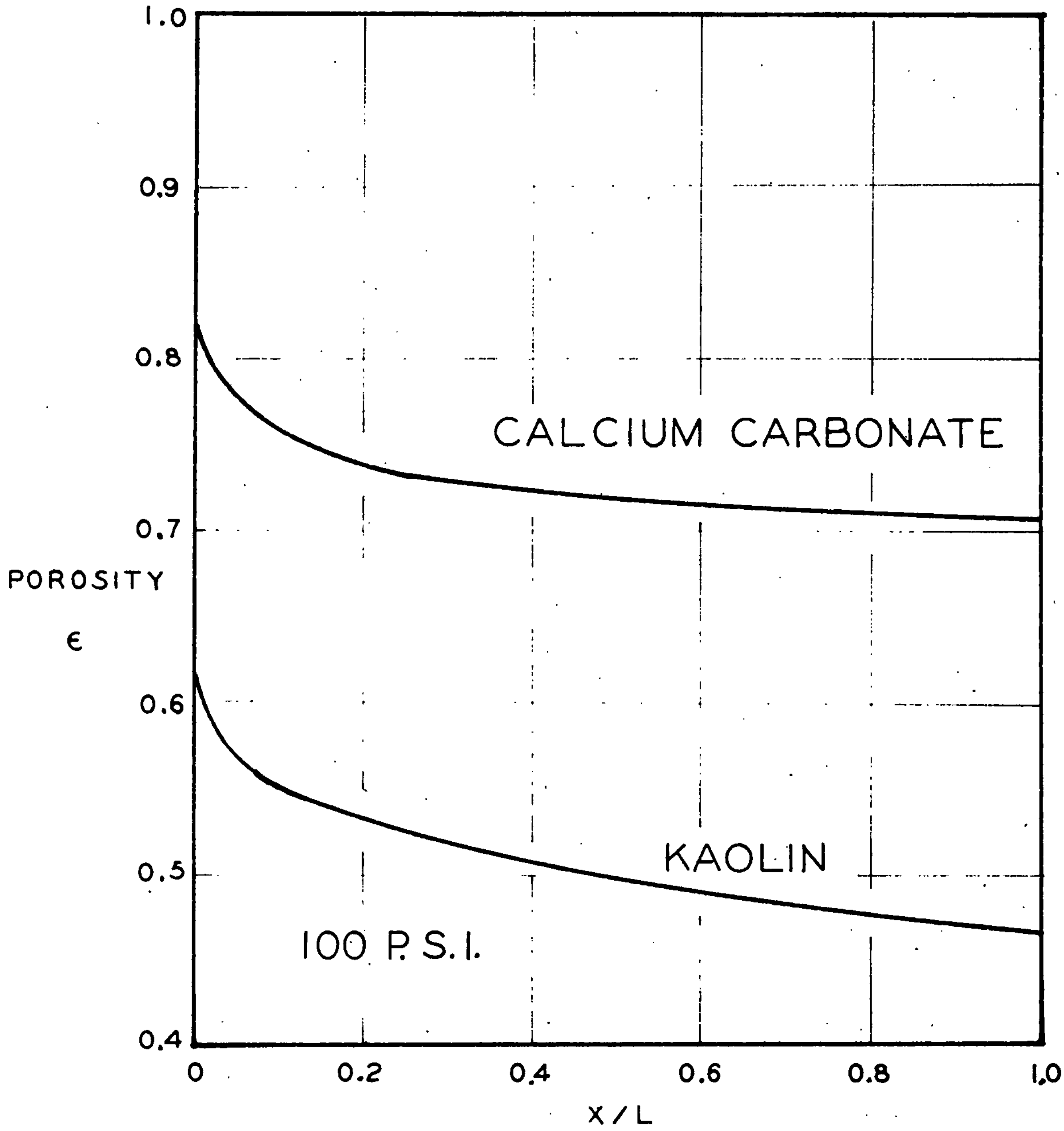

FIGURE 43.

CALCULATED POROSITY VARIATION -
GREATEST CHANGE OF SLOPE AT SURFACE

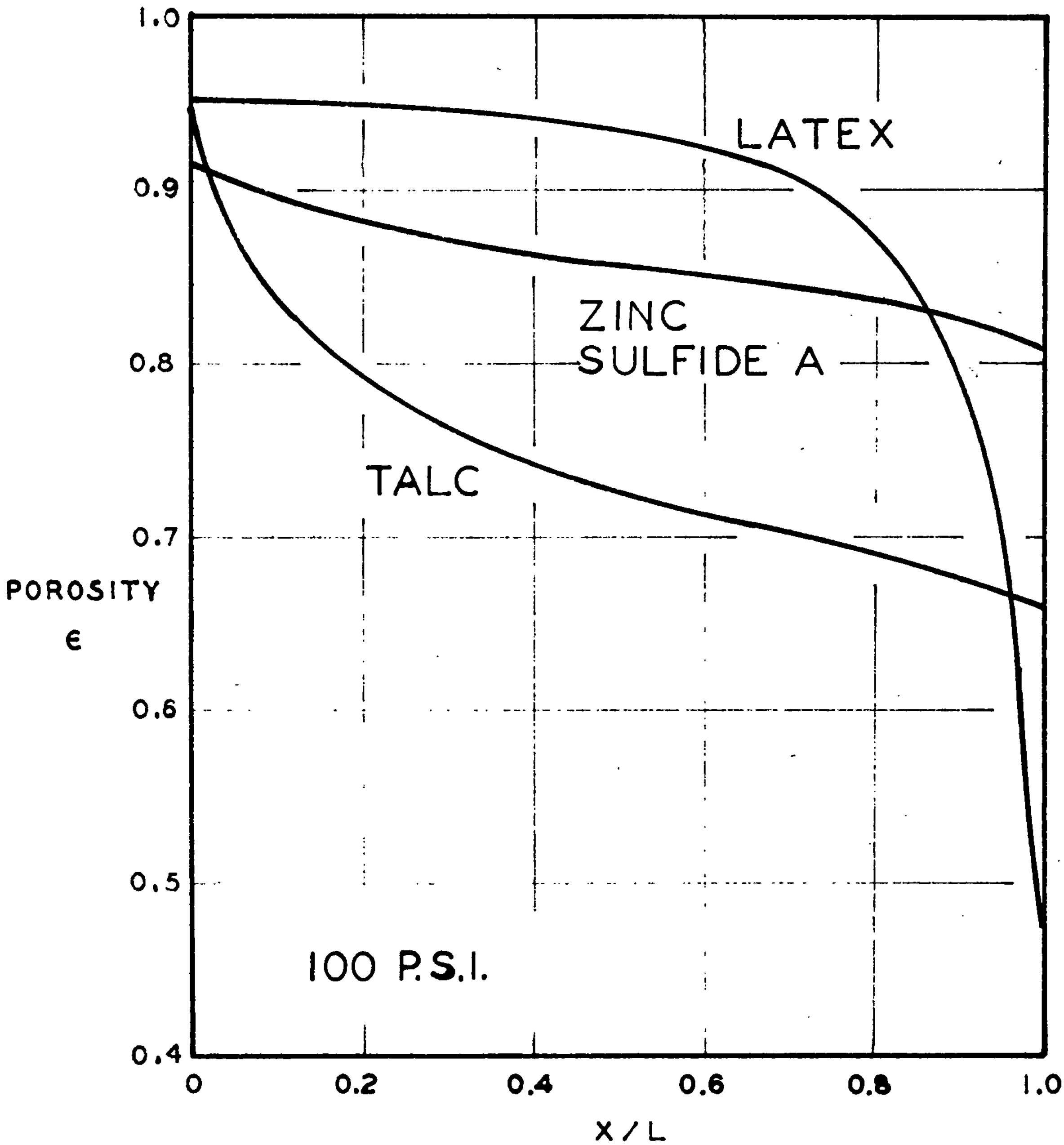

FIGURE 44.

CALCULATED POROSITY VARIATION -
REVERSAL OF SLOPE WITHIN CAKE

CHAPTER VI

CRITICAL ANALYSIS OF COMPRESSION-PERMEABILITY CELL DATA IN APPLICATION TO THE FUNDAMENTAL EQUATION

In the fundamental equation of filtration specific resistance is defined as a multiplier of the mass of solids in a filter cake through which a pressure drop occurs at a known rate of flow of filtrate at a given viscosity. Specific resistance α appears in the filtration rate equation

$$q = \frac{g_c\ (-)dp_x}{\mu\alpha_x\ dw} = \frac{g_c\ \Delta p_c}{\mu\ \alpha_{av} w} \tag{3}$$

where the point value corresponding to a section of cake is α_x and the average value for the cake in the integrated form is α_{av}. Bloomfield, Carman, Ruth, and Tiller recognized that for a compressible porous structure α varied with the hydraulic pressure throughout the cake.[3,11,24,50] Defining solids pressure in the filter cake as the compliment to hydraulic pressure by the expression $dp_s = -dp_x$ and assuming point contact between the particles packed in the cake, a correlation can be obtained relating specific resistance to external mechanical pressure on the solids. The principle of equivalence of solids pressure resulting from mechanical pressure and that generated by flow resistance is the basis of the compression-permeability cell proposed by Ruth and utilized by Grace for detailed experimental analysis.[24,25,50]

The result of this work has been the determination of curves for point specific resistance vs. solids pressure, typical data reported by Grace being shown by Figure (11). It has been noted that for cakes built of particles above a certain size, five microns approximately, the specific resistance does not vary appreciably or if it does vary due to slight compressibility of the cake structure the Kozeny-Carman relationship, Equation (16), can describe the change of α with pressure. For materials of smaller size compressible cakes result in which the change of specific resistance with pressure becomes much greater than can be accounted for by the Kozeny-Carman equation based on changes in porosity.

Calculations for filtration of a slurry based on specific resistance data obtained by analysis of the filter cake in a compression-permeability cell depends on numerical integration of the data according to

$$\alpha_{av} = \frac{p - p_1}{\int_0^{p - p_1} \frac{dps}{\alpha}} \tag{22}$$

In integrating this expression from a lower limit of zero solids pressure at the cake surface to the maximum solids pressure to which the cake is subjected $(p - p_1)$, values of specific resistance are required corresponding to compression pressures approaching zero solids pressure.

No experimental data presented in the literature indicate the inital or surface specific resistance of a filter cake for which values are reported resulting from compression-permeability cell analysis, these measurements beginning at some minimum pressure. Tiller has pointed out the difficulties of integrating these data when values of specific resistance at low pressures are not available to guide extrapolation to a limiting value of specific resistance.[63] The investigation of Grace showed how analytical data were used to predict average specific resistance for filtrations at various pressures.[25] For the most compressible materials for which extensive results were published, in particular zinc sulfide B, fine silica, and Darco G-60, the calculated specific resistance values were considerably higher than measured specific resistance obtained during test filtrations. The results with talc C, for which one filtration only was reported, are an exception to this generalization. Grace extrapolated the reported data arithmetically to zero pressure according to the example shown in the appendix of the publication.[24] Kottwitz and Boylan report average specific resistance values integrated from compression-permeability cell data to be appreciably lower in every case analyzed compared to data taken in constant pressure filtrations.[37] Fitting the data to the exponential equation, $\alpha = \alpha_o p_s^n$, substitution into Equation (22) and subsequent integration from 0 to p yields the expression for average specific resis

$$\alpha_{av} = \alpha_o(1 - n)\ p^n \tag{22a}$$

An analysis of data reported by Grace indicates that a large number of calculated values of point specific resistance plotted vs. pressure on log-log coordinates result in formation of approximately linear relationships. This would lead to the supposition that the exponential relationship expressed in Equation (33) would lend itself to extrapolation. From the mathematical form it is necessary to limit the extrapolation to some pressure greater than zero since otherwise the specific resistance would be taken as zero at the cake surface. A lower limit of zero would be erroneous as a bed of deposited particles under negligible pressure stress at the cake-slurry interface would contain resistance of some finite magnitude due to the geometrical configuration of their arrangement. Tiller noted that a lower limit of pressure p_i must be utilized in integrations below which α is constant with pressure in calculations employing the logarithmic relationship.[62] 0.1 p.s.i. was selected as an arbitrary lower limit in calculations reported by Tiller.

The evaluation of average specific resistance from compression-permeability cell data is dependent upon a method of determining the lower limit, zero pressure value, of α in order to carry out the integration of Equation (22). Arithmetic extrapolation of the data reported by Grace for talc C is demonstrated by Figure (28) for the integration shown in Example 9. In the numerical integration illustrated in Example 9. lower magnitudes for initial values of α would result in greater values of the integral since the reciprocal of α is required by Equation (22).

In Figure (45) the estimated average specific resistance curves based on zinc sulfide A data reported by Grace are shown. Curve A represents the locus of experimental data from test filtrations reported by Grace. Curve B is estimated from compression-permeability cell data analyzed by numerical integration using arithmetic extrapolation.* Curve C is based on the closest fit of the data to the empirical power function relating α and p_s, Equation (33), integrating in Equation (22a) to zero initial pressure. Curve D is also based on the power function but the lower limit of integration is arbitrarily chosen at 0.1 p.s.i. with α considered constant below this pressure in a second part of the

* Calculations shown in Appendix VII.

integration.

Determination of average specific resistance from compression-permeability cell data is very sensitive to the method used to extrapolate data from the minimum of approximately one pound per square inch solids pressure to zero pressure as illustrated in Figure (45). Integrations by means of Equation (22) using data obtained by logarithmic extrapolation, curves C and D in Figure (45), lead to high values of predicted filtration resistance. It is also to be noted that experimental values of average specific resistance vs. pressure given by curve A depends on the validity of the assumptions from which the filtration equation was derived and on the degree to which equilibrium consolidation was attained in the course of the test filtrations (see Chapter II).

It is of interest from a technical standpoint as well as theoretical to develop data in conjuction with compression-permeability cell measurement which enable limiting values of porosity and specific resistance to be determined. The lowest pressures at which data were reported by Grace or Kottwitz and Boylan were in the neighborhood of one pound per square inch solids pressure.

The lowest mechanical pressure practical for compression-permeability cell measurement is dependent upon the permeability of the cake. If for example a tweleve inch filtrate head is required to obtain a flow rate great enough for accurate measurement this fixes the per cent pressure variation through the cake with respect to mechanical pressure on the piston as illustrated in Figure (10). Grace reported the raw data from which point specific resistance and porosity of talc were calculated at

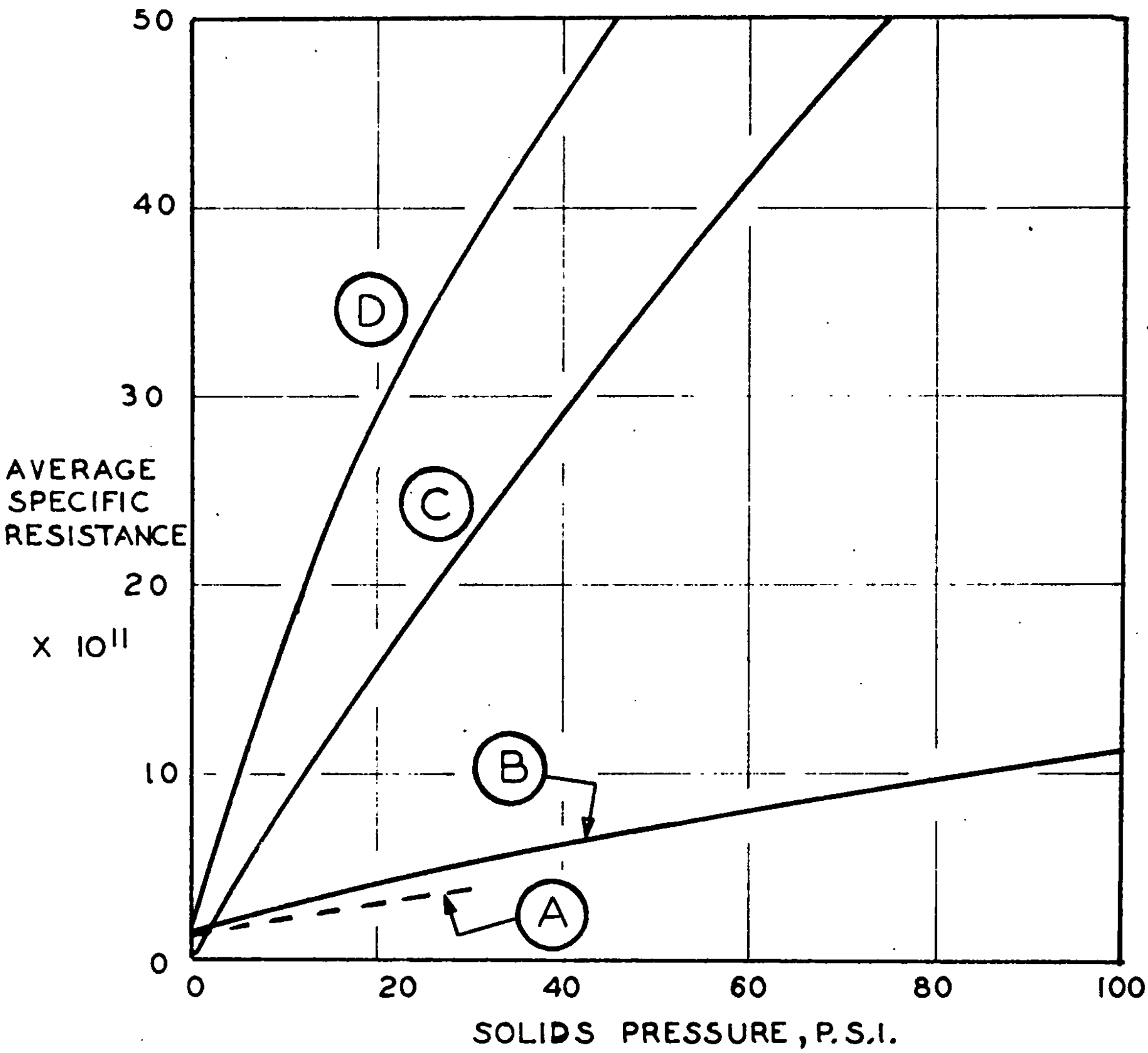

FIGURE 45.

SENSITIVITY OF CALCULATED AVERAGE SPECIFIC RESISTANCE DATA TO METHOD OF EXTRAPOLATION TO ZERO PRESSURE

1.10 p.s.i. following the procedure shown in Example 8. The filtrate head was 21.3 cm. or 0.302 p.s.i. assuming specific gravity of filtrate to be 1.0. For this example the solids pressure increased from the nominal 1.10 p.s.i. at the cake surface, the mechanical pressure, to 1.40 p.s.i. at the medium, and increase of 30% through the cake. For a compressible material an incremental specific resistance increase would possibly be considerable, corresponding to 30% solids pressure increase. The point specific resistance data for talc reported by Grace closely follows a logarithmic relationship with pressure as shown in Figure (11). From 1.10 p.s.i. to 1.40 p.s.i. α increases by 12% according to this data. It would be expected by this analysis that the errors introduced by pressure variation in the cake for compressible solids under these conditions would constitute a lower limit of test pressure below which the accuracy of the compression-permeability cell technique become doubtful. Extension of testing range of this device to lower pressures to permit precise extrapolation of data to zero pressure appears to be unlikely.

The Kozeny-Carman equation utilizing the value of 5.0 for the proportionality constant k was shown by the data of Grace to yield conservative results in relating the change in specific resistance with solids pressure for compressible materials, this departure being partially shown by the variability in calculted specific surface with pressure in Figure (16) for k = 5.0. Reference has been made to the fact that values of the empirical constant k have been found to vary widely when pressure drop was measured during flow at constant rate through packed beds of varying shape particles.[17] In a compressible filter cake it can be assumed that the factor k is a variable throughout the cake thickness and varies according to geometrical structures of the particles deposited and compressed to different forms. By this assumption as the cake surface is approached k takes on some finite value corresponding to the loose structure in cakes formed of fine particles at zero stress.

A plot made to examine the change in the Kozeny term $k\ S_0^2 / \rho_s$ at low pressures with experimentally determined porosities following the form of the Kozeny-Carman equation, Equation (16), is shown in Figure (46). Changes in surface area S_o and solids density ρ_s with change in stress can be assumed negligible in the absence of forces capable of particle deformation. The change in the term $k\ S_0^2 / \rho_s$ with pressure as measured experimentally reflects changes in properties influencing the value of k. Experimentally determined values of k in principle could be utilized to estimate initial values of specific resistance with knowledge of the magnitude of surface porosity with the upper limit of maximum porosity being the fraction of liquid by volume in the slurry. Experimental clarification is needed to relate slurry concentration to the true limiting value of porosity at the finite surface of the cake.

Hoffing and Lockhart described a simple permeability measuring device which could be adapted for use in measuring low pressure permeability.[32] A cake of known mass from a slurry to be examined in compression-permeability cell measurements would be deposited in a glass tube by means of settling. The average porosity and specific resistance would be observed at each step as a function of pressure during flow induced by a head of filtrate increased from very low values. The suggested apparatus is shown

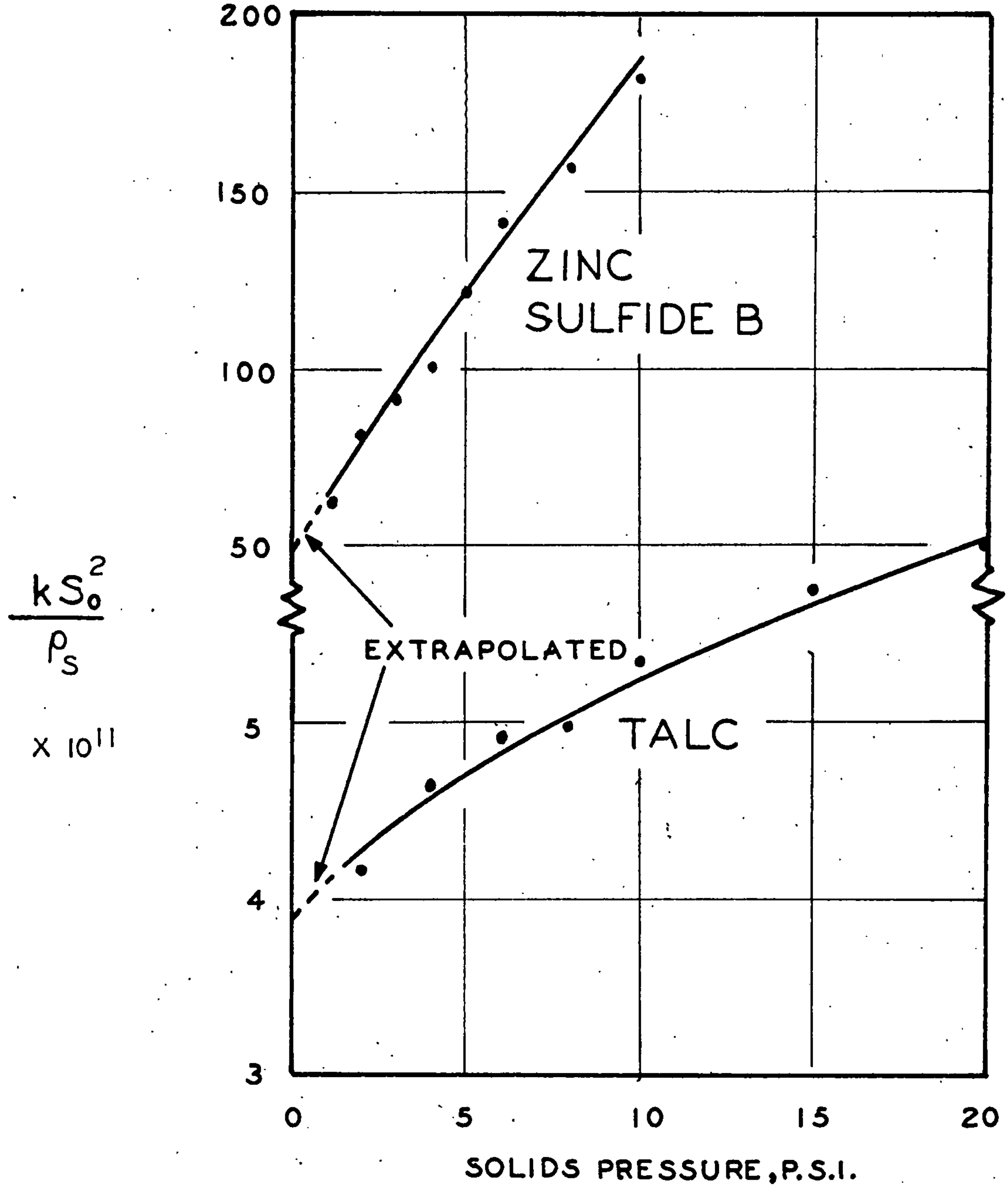

FIGURE 46.

EMPIRICAL KOZENY CONSTANT CALCULATED FROM COMPRESSION PERMEABILITY CELL DATA AS FUNCTION OF PRESSURE in Figure (47). Values of average porosity and average specific resistance approach the same finite value at zero solids pressure as will respective point values. Since the average values can be calculated at much lower pressures by permeability measurement alone, curves constructed from data obtained in both series of tests will converge on some finite value as illustrated by Figure (48). Such a series of tests in forming curves such as shown in Figure (48) would provide substantiating proof for the theory forming the basis of the fundamental equation of filtration.

The limiting pressure to which cake properties could be extrapolated would seem to be the minimum pressure stress under which a filter cake of the material would form. Considering the macroscopic case the pressure at the surface of a filter cake is a function of the change in kinetic energy of filtrate as it increases in velocity passing into the porous cake. In gravity settling by analogy the surface solids pressure of the settled mass is related to the cumulative conversion of kinetic energy of particles settling on its surface. Initial or surface porosity and specific resistance in the course of filtration would then be dependent upon instantaneous filtrate rate, relative gravities of solids and filtrate and slurry concentration if the hypothesis is valid.

In summary, mathematical treatment would indicate that integration of cake resistance data obtained by means of compression-permeability cell technique would lend itself to handling in a straight-forward manner, but the theory at present admits little rational treatment of data in the low pressure region below one to two pounds per square inch solids pressure. Suggested approaches to experimentally determine properties of compressible cakes at low pressures are discussed, these being the use of the Kozeny-Carman relationship for estimating initial specific resistance and simple permeability measurements to evaluate surface porosity.

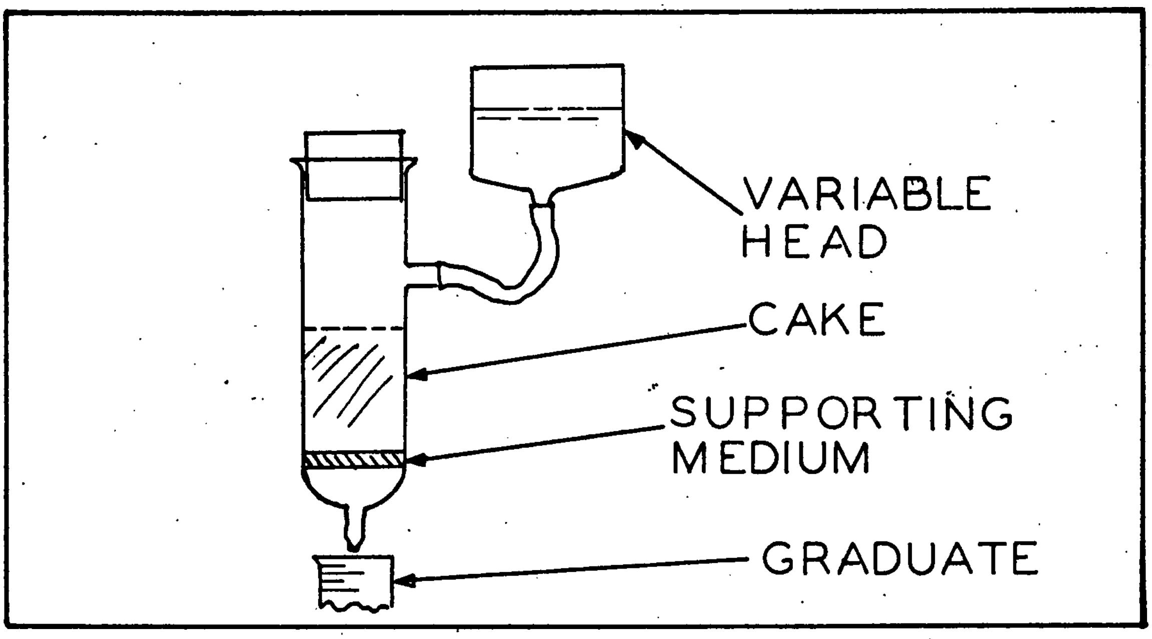

FIGURE 47.

PERMEABILITY APPARATUS

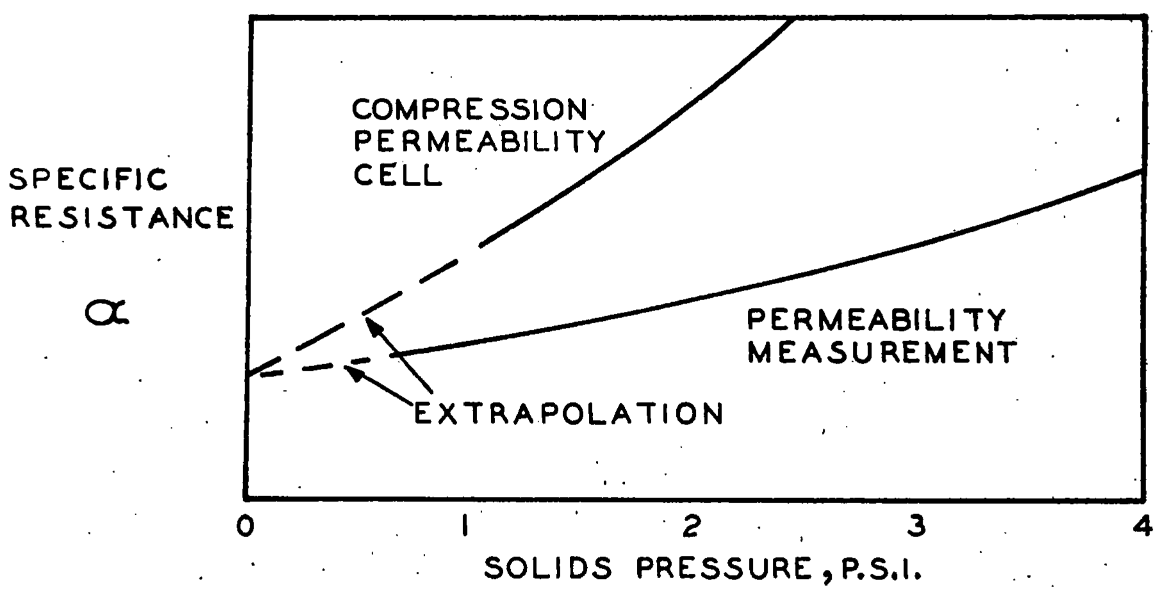

FIGURE 48.

METHOD FOR ESTIMATING SURFACE PROPERTIES
OF FILTER CAKE

BIBLIOGRAPHY

1. Arnell, J. C., Can. J. Research A26, 103 (1946)

2. Bell, G. R., and Hutto, F. B., Jr., "New Concepts in the Analysis of Rotary Precoat Filter Operation", Presented at Seattle A. I. Ch. E. meeting, June 1957

3. Bloomfield, A. J. V., J. Soc. Chem. Ind. 47, 325T (1928)

4. Bonilla, C. F., Trans. A. I. Ch. E. 34, 243 (1938)

5. Brownell, L. E., and Gudz, G. B., Chemical Engineering 152, 112 (September 1949)

6. Brownell, L. E., and Katz, D. L., Chem. Eng. Prog. 43, 537, 601, 703 (1947)

7. Bryden, C. L., and Dickey, G. D., "Theory and Practice of Filtration", Reinhold, New York (1946)

8. Carman, P. C., J. Soc. Chem. Ind. 52T, 208 (1933); 53T, 301 (1934)

9. Carman, P. C., Trans. Inst. Chem. Engrs. (London) 15, 158 (1937)

10. Carman, P. C., J. Soc. Chem. Ind. 57T, 225 (1938)

11. Carman, P. C., Trans. Inst. Chem. Engrs. (London) 16, 168 (1938)

12. Carman, P. C., Ind. Eng. Chem. 30, 1163 (1938); 31, 1047 (1938)

13. Carman, P. C., and Arnell, J. C., Can. J. Research A26, 128 (1948)

14. Carman, P. C., and Malherbe, P. L., J. Soc. Chem. Ind. 69, 134 (1950)

15. Chalmers, J. M., Elledge, L. R., and Porter, H. F., Chemical Engineering 63, 191 (June 1955)

16. Choudhury, A. P. R., and Dahlstrom, D. A., A. I. Ch. E. J. 3, 433 (1957)

17. Coulson, J. M., Trans. Inst. Chem. Engrs. (London) 27, 237 (1949)

18. Crone, H. G., and McKee, R. F., Brit. Coal Util. Res. Assn. 14, 329 (1950)

19. Cunningham, G. E., Broughton, G., and Kraybill, R. R., Ind. Eng. Chem. 46, 1196 (1954)

20. Dahlstrom, D. A., ''Scale-up Methods for Continuous Filtration Equipment'', Presented at International Symposium on the Scaling-up of Chemical Plants and Processes, Institution of Chemical Engineers, London, England, May 1957

21. Dahlstrom, D. A., and Nickolaus, N., Chem. Eng. Prog. 52, 87 (1956)

22. D'Arcy, H. P. G., ''Les Fontaines Publiques de la Ville de Dijon'', Victor Dalamont (1856)

23. Grace, H. P., Chem. Eng. Prog. 47, 497 (1951)

24. Grace, H. P., Chem. Eng. Prog. 49, 303 (1953)

25. Grace, H. P., Chem. Eng. Prog. 49, 367 (1953)

26. Grace, H. P., A. I. Ch. E. J. 2, 307 (1956)

27. Graton, L. C., and Fraser, H. J., J. Geology 43, 785 (1935)

28. Heertjes, P. M., Research (London) 3, 254 (1950)

29. Heertjes, P. M., and Haas, H. v. d., Rec. Trav. Chim. Pays-Bas 68, 361 (1949)

30. Hermans, P. H., and Bredee, H. L., J. Soc. Chim. Ind. 55T, 1 (1936)

31. Hobby, C., and Newhouse, A., ''An Integrated Set of Programs for Curve and Surface Fitting on Unequally Spaced Points'', Presented at Houston meeting of Association for Computing Machinery, June 1957

32. Hoffing, E. H., and Lockhart, F. J., Chem. Eng. Prog. 47, 3 (1951)

33. Holland, C. D., and Woodham, J. F., Petroleum Refiner 32, 149 (1953)

34. Hrubicek, J., Kolloid-Beihefte 53, 385 (1941), quoted by A. E. Scheidegger, ''The Physics of Flow Through Porous Media'', MacMillan, New York (1957)

35. Hutto, F. B., Jr., Chem. Eng. Prog. 53, 328 (1957)

36. Kobata, H. T., Leppla, P. W., and Neu, E. L., ''Laboratory Scale Precoat Test Leaf'', Presented at Seattle A. I. Ch. E. meeting, June 1957

37. Kottwitz, F. A., and Boylan, D. R., ''Prediction of Resistance in Constant Pressure Cake Filtration'', Presented at Seattle A. I. Ch. E. meeting, June 1957

38. Kozeny, J., Sitzer-Akad. Wiss. Wien, Math. Naturw. Klasse 136, IIa, 271 (1927)

39. Lamb, H., ''Hydrodynamics'', 6th ed., Cambridge University Press, London (1932)

40. Lea, F. M., and Nurse, R. W., ''Symposium on Particle Size Analysis'', supplement to Trans. Inst. Chem. Engrs. (London) 25, (1947)

41. Luke, C. D., ''Constant Pressure-Constant Rate Filtration'', Presented at Cleveland A. I. Ch. E. meeting, December 1952

42. McMillen, E. L., and Webber, H. A., Ind. Eng. Chem. 30, 708 (1938)

43. Mondria, H., Applied Science Research A2, 165 (1950)

44. Nelson, P. A., and Dahlstrom, D. A., Chem. Eng. Prog. 53, 320 (1957)

45. Opler, A., Ind. Eng. Chem. 45, 2621 (1953)

46. Reeves, E. J., Petroleum Processing 4, 885 (1949)

47. Rhodes, E. H., Ind. Eng. Chem. 26, 1331 (1934)

48. Rietema, K., Chemical Engineering Science 2, 88 (1953)

49. Ruth, B. F., Ind. Eng. Chem. 27, 708, 806 (1935)

50. Ruth, B. F., Ind. Eng. Chem. 38, 564 (1946)

51. Ruth, B. F., ''A Mechanism of Displacement Washing of Filter Cakes'', Presented at Cleveland A. I. Ch. E. meeting, December 1952

52. Ruth, B. F., and Kempe, L. L., Trans. A. I. Ch. E. 33, 34 (1937)

53. Scheidegger, A. E., ''Statistical Theory of Flow Through Porous Media'', Presented at Boston A. I. Ch. E. meeting, December 1956

54. Scheidegger, A. E., ''The Physics of Flow Through Porous Media'', MacMillan, New York (1957)

55. Sjenitzer, F., Trans. Inst. Chem. Engrs. (London) 33, 289 (1955)

56. Smith, E. G., Chem. Eng. Prog. 47, 545 (1951)

57. Souders, M., Chem. Eng. Prog. 52, 255 (1956)

58. Sperry, D. R., Ind. Eng. Chem. 36, 323 (1944)

59. Swearingen, J. S., Oil and Gas Journal 52, No. 7, 283 (1953)

60. Taylor, G. I., Proc. Royal Soc. (London) A219, 186 (1953)

61. Tiller, F. M., Chem. Eng. Prog. 49, 467 (1953)

62. Tiller, F. M., Chem. Eng. Prog. 51, 282 (1955)

63. Tiller, F. M., ''Variable Rate-Variable Pressure Filtration'', Presented at Boston A. I. Ch. E. meeting, December 1956; to be published in A. I. Ch. E. Journal

64. Von Rosenberg, D. U., A. I. Ch. E. J. 2, 55 (1956)

65. Walas, S. M., Trans. A. I. Ch. E. 42, 783 (1946)

66. Waterman, H. I., and van Gilse, J. P. M., J. Soc. Chem. Ind. 49T, 444, 483 (1930); 50T, 41, 95 (1931)

67. Wrotnowski, A. C., Chem. Eng. Prog. 53, 313 (1957)

68. Young, G. J., Trans. Amer. Inst. Min. Eng. 42, 752 (1911)

NOMENCLATURE

Roman

a	fraction of particle cross section in area contact with adjacent particle
A	area, sq.ft.
D	diameter, ft.
D_o	molecular diffusion coefficient, ft.^{2}/sec.
F	force, lb.force
g_c	proportionality constant relating force and mass, 32.2 ft.lb.mass/(lb.force)(sec.^{2})
h	height of fluid column, ft.
h_{av}	average height of fluid column, ft.
h_{cent}	height of fluid column above centroid of submerged surface, ft.
I	relative light intensity at phototube with suspension in sample cell
I_o	relative light intensity at phototube with suspending liquid in sample cell
k	dimensionless proportionality constant
K	constant term denoting combination of several constants grouped for convenience
L	thickness of filter cake, ft.
m	mass ratio of wet cake to dry cake, dimensionless
m_i	mass ratio of wet cake to dry cake at surface of cake, dimensionless
n	exponent in empirical logarithmic equation relating specific resistance in units ft./lb.mass to solids pressure, lb.force/sq.in.
N	nuetral stress in cavity of consolidometer, lb.force/sq.ft.
p	pressure, lb.force/sq.ft., unless noted as given in units lb.force/sq.in.
p_o	nominal filtration pressure as in vacuum filtration, units as in p

p_s solids pressure, units as given in p

p_x hydraulic pressure at distance x from surface af filter cake, units as given in p

p_1 hydraulic pressure at filter medium cake interface, units as given in p

q flow rate per unit area of filter cake or superficial velocity of flow through cake, cu.ft./(sq.ft.)(sec.)

q_i flow rate per unit area of filter cake at surface of cake, cu.ft./(sq.ft.)(sec.)

q_o flow rate of slurry liquid from slurry into cake per unit area of cake, cu.ft./(sq.ft.)(sec.)

q_x flow rate per unit area of filter cake at distance x from surface of filter cake, cu.ft./(sq.ft.)(sec.)

q_1 flow rate per unit area of filter cake through interface of filter cake and medium, cu.ft./(sq.ft.)(sec.)

r radius, ft.

r_o radius of capillary or circular conduit, ft.

R radius of filter drum or filter disc, ft.

R_H Hydraulic radius, ft.

R_m medium resistance, 1/ft.

Re Reynolds number, dimensionless

Re_{mod} modified Reynolds number, Carman

s weight fraction solids in slurry, dimensionless

S_o specific surface of solids deposited in bed or filter cake, sq.ft./cu.ft. deposited solids

u velocity of flow in a conduit at distance r from axis of conduit as in laminar flow, ft./sec.

U maximum velocity of flow in a conduit at axis, ft./sec.

v volume of filtrate per square foot, cu.ft./sq.ft.

v_{cycle} volume of filtrate per unit area per filtration cycle, cu.ft./sq.ft.

v_o volume of slurry liquid removed from slurry per unit area of cake, cu.ft./sq.ft.

V average velocity of flow in a conduit, as in a pipe, ft./sec.

V_b displaced volume of capillary or cake voids, cu.ft.

V_c volume of capillary or cake voids, cu.ft.

V_w volume of wash fluid, cu.ft.

w solids deposited in filter cake per unit area, lb.mass/sq.ft.

w_{max} solids deposited in filter cake at end of filtration cycle, lb.mass/sq.ft.

w_x solids deposited in differential thickness of filter cake at distance x from surface of cake, lb.mass/sq.ft.

W solids deposited in filter cake per unit time, as in continuous filtration, lb.mass/(sq.ft.)(sec.)

W_{av} weight fraction filtrate in total wash effluent

W_c weight fraction filtrate in total cake fluid

W_i instantaneous weight fraction filtrate in wash effluent

x distance from surface of filter cake, ft.

y distance from solid surface at which shear stress is acting due to flow of fluid, ft.

Greek

α specific resistance of deposited solids, ft./lb.mass

α_{av} average specific resistance of solids in filter cake, ft./lb.mass

α_o specific resistance at reference pressure of one lb.force/sq.in. in empirical expression relating specific resistance and solids pressure given in units lb.force/sq.in.

α_x specific resistance of solids at distance x from surface of filter cake, ft./lb.mass

β angle of submergence of drum or disc filter, degrees or radians; also, ratio of wash fluid volume to void volume, dimensionless

ϵ	porosity, or ratio of void volume to cake volume, dimensionless
ϵ_{av}	average cake porosity, dimensionless
ϵ_x	porosity of cake solids at distance x from surface of cake, dimensionless
θ	time, seconds, unless noted
μ	viscosity, lb. mass/(ft.)(sec.)
ρ	density of filtrate, lb.mass/cu.ft.
ρ_f	density of slurry, lb.mass/cu.ft.
ρ_s	density of solids, lb.mass/cu.ft.
ϕ	angle from axis of rotation in drum or disc filter subtending an arc on the periphery of the drum or disc
ω	rate of rotation of drum or disc filter, radians or degrees per second

Note: The nomenclature used here conforms to that agreed upon at a meeting of F. M. Tiller, H. P. Grace, B. F. Ruth, C. D. Luke, R. L. Ingmanson, C. D. Ulrich and others at the Cleveland meeting of the A. I. Ch. E. December 1952.

APPENDIX I

COMPRESSION-PERMEABILITY CELL DATA

Table VIII contains data taken from curves reported by Grace obtained in compression-permeability cell measurements on several materials.[24] These data form the basis of calculations performed in Chapters III, IV, and V. Part A of Table VIII is specific resistance data and Part B porosity data.

TABLE VIII

COMPRESSION-PERMEABILITY CELL DATA

Part A. Specific Resistance, ft./lb.mass (10^{10}), vs. Solids Pressure, lb.force/sq.in.

Solids Pressure	1	2	3	4	5	6	8	10	15	20
Carbonyl Iron E	0.95	1.75						1.78		
UT 238 Tungsten	0.60	0.69		0.73	0.76	0.78	0.80	0.81	0.86	0.91
Talc C	9.0	12.9	15.6	18.0	20.0	21.8	25.2	28.0	34.2	29.9
Kaolin (Al_2SO_4)		90		102		122	127	131	149	159
Darco B	3.20	4.00	4.62	5.20	5.62	6.08	6.71	7.32	8.4	9.9
Zinc Sulfide A	17.5	20.3	27.2	30.0	34.0	38.8	43.0	51	68	85
Zinc Sulfide B	85	151	205	270	315	382	481	595	810	1070
Calcium Carbonate (unflocculated)	7.6	9.3	10.1	10.9	11.3	11.8	12.1	12.6	13.1	13.8
Polystyrene Latex	2.8	17.5	56	110	190	245	305	380	470	540
Silica	50	110	180	260	340	410	610	800	1260	1950
Solka-Floc	.0025	.0048	.0070	.0093	.012	.014	.018	.023	.031	.045
Ilmenite	3.2	12.9	19.5	21.8	22.8	24.0	26.2	27.7	28.6	30.2
Titanium Dioxide R-110 (unflocc.)	31.0	39.7	42.5	49.0	50.5	54.0	59.5	63.0	71.0	78.0

TABLE VIII (CONT.)

COMPRESSION-PERMEABILITY CELL DATA

Part A. (Cont.)

Solids Pressure	40	60	80	100	200	400	600	800	1000	2000
Carbonyl Iron E				1.80		1.86		1.95	2.00	2.20
UT 238 Tungsten	0.96	1.02	1.16	1.28	1.87	2.85	3.8	4.7	5.8	10.3
Talc C	59.8	76.2	92.0	107	191	395	600	920	1250	4000
Kaolin (Al_2SO_4)	194	223	258	282	400	600	790	940	1060	
Darco B	15.0	19.6	24.5	30.6	75	200	380	600	890	3100
Zinc Sulfide A	159	240	334	435						
Zinc Sulfide B	2280	3430	5100	7300						
Calcium Carbonate (unflocculated)	15.5	17.8	19.4	21.0	29.0	43	59	75	91	
Polystyrene Latex	750	890	990	1100	1350	1750	1950	2020		
Silica	4680	7600	11600	14600	21500					
Solka-Floc	.090	0.140	0.190	0.260	0.800	3.05	5.1	15.5	26.0	150
Ilmenite	34.2	37.6	39.2	41.6	48	53	60	67	71	96
Titanium Dioxide R-110 (unflocc.)	96	104	120	134	171	198	211	240	272	

TABLE VIII (CONT.)

COMPRESSION-PERMEABILITY CELL DATA

Part B. Porosity vs. Solids Pressure, lb. force/sq.in.

Solids Pressure	1	2	3	4	5	6	8	10	15	20
Carbonyl Iron E	.46	.425						.425		
UT 238 Tungsten	.81	.805			.80			.798		.79
Talc C	.86	.825	.81	.80	.793	.785	.77	.765	.742	.735
Kaolin (Al_2SO_4)	.585	.570	.558	.55	.546	.542	.538	.53	.522	.515
Darco B	.852	.848	.84			.83		.825		
Zinc Sulfide A	.90	.89	.88	.875	.872	.87	.865	.86	.855	.85
Zinc Sulfide B	.90	.875	.86	.85	.845	.84	.83	.82		.79
Calcium Carbonate (unflocculated)	.78	.765	.76	.755	.752	.75	.745	.74	.735	.73
Polystyrene Latex	.90	.725	.65	.615	.58	.562	.541	.528	.512	.495
Silica	.975	.973	.972	.97	.966	.962	.958	.955	.95	.945
Solka-Floc	.84	.825	.815	.805	.80	.795	.778	.774	.763	.753
Ilmenite	.86	.71	.67	.655	.648	.643	.64	.638	.631	.625
Titanium Dioxide R-110 (unflocc.)	.78	.77	.76	.75	.745	.74	.735	.725	.71	.69

TABLE VIII (CONT.)

COMPRESSION-PERMEABILITY CELL DATA

Part B. (Cont.)

Solids Pressure	40	60	80	100	200	400	600	800	1000	2000
Carbonyl Iron E				.425		.425		.423	.421	.41
UT 238 Tungsten	.78	.77	.76	.75	.72	.685	.66	.645	.63	.585
Talc C	.78	.77	.76	.75	.72	.685	.66	.645	.63	.585
Kaolin (Al_2SO_4)	.495	.49	.48	.47	.442	.41	.38	.36	.35	
Darco B	.81	.801	.794	.788	.77	.743	.726	.713	.71	.675
Zinc Sulfide A	.835	.825	.82	.81						
Zinc Sulfide B	.765	.75	.735	.725						
Calcium Carbonate (unflocculated)	.715	.71	.71	.70	.675	.64	.61	.59	.57	
Polystyrene Latex	.475	.465	.460	.45	.43	.408	.39	.385		
Silica	.935	.928	.921	.908	.898					
Solka-Floc	.72	.697	.678	.665	.612	.545	.503	.47	.44	.372
Ilmenite	.612	.603	.598	.59	.58	.57	.562	.555	.55	.528
Titanium Dioxide R-110 (unflocc.)	.675	.672	.67	.66	.635	.61	.59	.575	.57	

APPENDIX II

CALCULATIONS DEMONSTRATING PRESSURE VARIATION WITH TIME ACROSS FILTER CAKE

Using compression-permeability cell data integrated for average specific resistance and average cake porosity presented in Part H. of Table XV and shown graphically in Figure (20), calculations performed for filtration of talc slurry at 5 p.s.i. constant pressure are given in Table IX. The results of the calculations are utilized in plotting Figure (29) for illustration of the change in cake pressure drop with time calculated for constant pressure filtration with constant medium resistance.

The calculation procedure follows the method presented for Example 10. Chapter III using the same slurry concentration (s = 0.10) and physical properties as given in Example 10.

TABLE IX

CALCULATIONS FOR TALC FILTRATION AT 5 P.S.I.

P_1	Δp	q	$\alpha_{av.}$	ϵ_{av}	m	v	θ
lb.force/sq.in.		cu.ft./(sq.ft.)(sec.)	ft./lb.mass			cu.ft./sq.ft.	seconds
5.0	0.0	2.32 (10^{-3})	0.32 (10^{11})	0.945	7.42	0.0000	0.00
4.0	1.0	1.85	0.60	0.911	4.83	0.00346	1.68
3.0	2.0	1.39	0.77	0.895	4.19	0.00808	4.63
2.0	3.0	0.926	0.91	0.885	3.88	0.01620	12.73
1.5	3.5	0.694	0.98	0.880	3.75	0.02391	22.43
1.0	4.0	0.463	1.03	0.876	3.64	0.03971	32.88
0.75	4.25	0.347	1.06	0.875	3.61	0.0550	71.5
0.60	4.40	0.278	1.08	0.874	3.59	0.0700	120.1
0.50	4.50	0.232	1.09	0.849	3.59	0.0849	179.0

APPENDIX III

CALCULATIONS FOR POROSITY DISTRIBUTION DURING FILTRATION OF KAOLIN AT 100 P.S.I.

The results of calculations, given in Table X, are based on average porosity and average specific resistance data calculated from compression-permeability cell data presented in Part F. of Table XV.

The physical properties of the slurry and filtrate used in the calculations are as follows:

μ = 0.001 lb.mass/(ft.)(sec.)

ρ = 62.4 lb.mass/cu.ft.

ρ_s = 163.5 lb.mass/cu.ft.

s = 0.05 mass fraction solids in slurry

R_m = 1.0 (10^{11}) reciprocal feet

The procedure outlined for Example 10., Chapter III, is followed in calculating filtration time θ corresponding to filtrate volume v and pressure drop Δp. Case thickness L is calculated by Equation (4b).

$$L = \frac{v\left(\frac{s\rho}{1 - ms}\right)}{\rho_s\,(1 - \epsilon_{av})} \qquad (4b)$$

The results of the calculations are shown in Part A. of Table X.

To plot Figure (30), values of porosity are calculated as a function of p_s and x using the procedure given in Chapter V and illustrated by Appendix VII. The calculations for the porosity-distance relationship are given in Part B. of Table X together with corresponding values of x/L and (L - x) used to construct Figures (31) and (32).

The porosity distance curve for $\triangle p$ = 100 p.s.i. (cake thickness L of infinite magnitude) is taken from calculations given in Part F. of Table XV.

TABLE X

CALCULATIONS FOR POROSITY DISTRIBUTION DURING FILTRATION OF KAOLIN

Part A. Filtration Calculation

P_1	Δp	q	α_{av}	v	θ	L
lb.force/sq.in.		cu.ft./(sq.ft.)(sec.)	ft./lb.mass	cu.ft./sq.ft.	minutes	inches
90	10	$4.173\ (10^{-3})$	$1.042(10^{12})$	$3.190\ (10^{-3})$	0.0123	0.0017
60	40	2.770	1.451	13.71	0.0630	0.0072
20	80	0.935	1.756	67.60	0.720	0.0353
10	90	0.464	1.840	161.5	3.01	0.0846
0	100	0.0	1.902	∞	∞	∞

TABLE X (CONT.)

CALCULATIONS FOR POROSITY DISTRIBUTION DURING FILTRATION OF KAOLIN

Part B. Solids Pressure-Porosity Distribution

p_s lb.force/sq.in.	$\int_0^{p_s} \frac{dp_s}{\alpha(1-\epsilon)}$ $\frac{(\text{lb.force})(\text{lb.mass})}{(\text{ft.})(\text{sq.in.})}$ (10^{-12})	x/L	x inches	L - x inches	
		p = 10 p.s.i.			
2	5.2	0.26	.0004	.0013	0.570
4	10.2	0.51	.0009	.0008	0.550
6	13.5	0.68	.0011	.0006	0.542
8	17.6	0.88	.0015	.0002	0.538
10	20.0	1.00	.0017		0.530
		p = 40 p.s.i.			
5	11.2	0.19	.0014	.0058	0.546
10	20.0	0.34	.0025	.0047	0.530
20	34.4	0.59	.0042	.0030	0.515
30	46.8	0.81	.0058	.0014	0.505
40	58.1	1.00	.0072		0.497
		p = 80 p.s.i.			
10	20.0	0.20	.0072	.0281	0.530
20	34.4	0.35	.0123	.0230	0.515
40	58.1	0.59	.0209	.0144	0.495
60	79.5	0.81	.0287	.0066	0.490
80	98.0	1.00	.0353		0.480
		p = 90 p.s.i.			
10	20.0	0.19	.0189	.0686	0.530
30	46.8	0.44	.0443	.0450	0.505
50	69.1	0.65	.0653	.0294	0.492
70	89.0	0.89	.0840	.0136	0.485
90	105.6	1.00	.0846		0.475

APPENDIX IV

CALCULATIONS FOR MASS RATIO OF WET TO DRY CAKE DURING FILTRATION AT 15 P.S.I.

Average specific resistance and average porosity data integrated from compression-permeability cell data for computations of Appendix VII are utilized in calculating time vs. filtrate volume for polystyrene latex, results being presented in Table XI, and for calcium carbonate, computations shown in Table XII. The procedure of Example 10., Chapter III, is employed in the calculations.

Figure (33) is obtained by plotting values of mass ratio of wet to dry cake m vs. values of time θ corresponding to the same pressure drop across the cake. The results given for talc in Table VI of Chapter III for filtration at 15 p.s.i. are used in addition to the results given in Tables XI and XII.

TABLE XI

CALCULATIONS FOR LATEX FILTRATION AT 15 P.S.I.

p_1	Δp	q	α_{av}	ϵ_{av}	m	v	θ
lb.force/sq.in.		cu.ft./(sq.ft.)(sec.)	ft./lb.mass			cu.ft./sq.ft.	seconds
15	0	6.960 (10^{-3})	0.14 (10^{11})	0.950	20.95	0.0000	0
14	1	6.485	0.20	0.934	15.85	0.0052	0.8
12	3	5.560	0.41	0.925	13.95	0.0110	1.7
10	5	4.637	0.70	0.921	13.25	0.0135	2.2
8	7	3.710	0.97	0.918	12.75	0.0178	3.3
6	9	2.780	1.25	0.915	12.30	0.0245	5.4
4	11	1.855	1.52	0.913	12.01	0.0376	11.1
2	13	0.927	1.77	0.911	11.76	0.0783	44.1
1	14	0.464	1.89	0.910	11.61	0.1539	166.5

Parameters

μ = 0.001 lb.mass/(ft.)(sec.)

ρ = 62.4 lb.mass/cu.ft.

ρ_s = 59.2 lb.mass/cu.ft.

s = 0.04 mass fraction solids in slurry

R_m = 1.0 (10^{10}) reciprocal feet

TABLE XII

CALCULATIONS FOR CALCIUM CARBONATE FILTRATION AT 15 P.S.I.

p_1	Δp	q	α_{av}	ϵ_{av}	m	v	θ
lb.force/sq.in.		cu.ft./(sq.ft.)(sec.)	ft./lb.mass			cu.ft./sq.ft.	seconds
15	0	6.960 (10^{-3})	0.59 (10^{11})	0.820	2.860	0.0000	0
14	1	6.485	0.70	0.782	2.475	0.0004	0.06
12	3	5.560	0.81	0.760	2.300	0.0013	0.21
10	5	4.637	0.89	0.752	2.241	0.0025	0.44
8	7	3.710	0.95	0.747	2.210	0.0036	0.70
6	9	2.780	1.00	0.743	2.185	0.0068	1.72
4	11	1.855	1.04	0.739	2.170	0.0121	4.09
2	13	0.927	1.07	0.737	2.153	0.0277	16.48
1	14	0.464	1.09	0.736	2.146	0.0592	69.38
0	15	0.000	1.10	0.735	2.140	∞	∞

Parameters

μ = 0.001 lb.mass/(ft.)(sec.)

ρ = 62.4 lb.mass/cu.ft.

ρ_s = 256 lb.mass/cu.ft.

s = 0.20 mass fraction solids in slurry

R_m = 1.0 (10^{10}) reciprocal feet

APPENDIX V

CALCULATIONS DEMONSTRATING DEVIATION FROM CONVENTIONAL FILTRATION EQUATION

The procedure of Example 10., Chapter III, is utilized to perform the calculations for filtration of polystyrene latex at 10 p.s.i. and talc C at 5 p.s.i. and 15 p.s.i. using integrated data given in Table XV in Appendix VII. Table XII contains the calculated results for filtration of latex at 10 p.s.i. The computations for filtration of talc at 5 p.s.i. are given in Table XI and for filtration of talc at 15 p.s.i. by Table VI.

TABLE XIII

CALCULATIONS FOR LATEX FILTRATION AT 10 P.S.I.

p_1	Δp	q	α_{av}	ϵ_{av}	m	v	$1/q$
lb.force/sq.in.		cu.ft./(sq.ft.)(sec.)	ft./lb.mass			cu.ft./sq.ft.	(sq.ft.)(sec.)/cu.ft.
10	0	4.637 (10^{-3})	0.14 (10^{11})	0.950	20.45	0.000	216
9	1	4.185	0.20	0.934	15.85	0.008	239
8	2	3.708	0.30	0.928	14.55	0.014	270
7	3	3.250	0.41	0.925	13.95	0.019	308
6	4	2.781	0.54	0.923	13.60	0.023	360
5	5	2.320	0.70	0.921	13.25	0.027	431
4	6	1.855	0.83	0.920	13.05	0.035	540
3	7	1.391	0.97	0.918	12.75	0.047	718
2	8	0.928	1.11	0.917	12.60	0.072	1079
1	9	0.464	1.25	0.915	12.30	0.147	2160

Parameters

μ = 0.001 lb.mass/(ft.)(sec.)

ρ = 62.4 lb.mass/cu.ft.

ρ_s = 59.2 lb.mass/cu.ft.

s = 0.04 mass fraction solids in slurry

R_m = 1.0 (10^{10}) reciprocal feet

APPENDIX VI

POROSITY VARIATION - RESULTS OF NUMERICAL ANALYSIS OF GRACE DATA

Compression-permeability cell data taken from the publications of Grace are tabulated in Appendix I. Portions of this data, that reported for eleven materials up to 100 p.s.i., were fitted by a least squares equation using a numerical procedure based on orthogonal polynomials adapted for high speed numerical computation by Newhouse and Hobby.[31] The cited numerical procedure, using a program written for the I B M 650 system, produces an equation in the form of a power series from dependent variable data points selected in uneven increments.

Porosity vs. solids pressure data tend to approximate a straight line in many cases when plotted on semi-log coordinates. For this reason equations were fitted to data in the relationship

$$\epsilon = f(\log p_s) = a_o + a_1 \log p_s + a_2(\log p_s)^2 + a_3(\log p_s)^3 + a_4(\log p_s)^4$$

The object of the analysis was to obtain numerical values of $\left[-\alpha(1-\epsilon)\frac{d\epsilon}{dps}\right]$ vs. p_s. To facilitate calculation of these terms, the numerical procedure was modified to differentiate the least squares equation and punch out values of $\frac{d\epsilon}{d\log p_s}$ vs. p_s. Table XIV contains tabulated values of this differential. By mathematical conversion $\frac{d\epsilon}{dp_s}$ is obtained and is also given in Table XIV. Data from Appendix I corresponding to each material and pressure are used to calculate the terms $\left[-\alpha(1-\epsilon)\frac{d\epsilon}{dps}\right]$ which are plotted in Figure (41).

TABLE XIV

POROSITY VARIATION - RESULTS OF NUMERICAL ANALYSIS OF GRACE DATA

$d\epsilon / d \log p_s$

Pressure (p.s.i.)	2	4	6	8	10	15	20	40	60	80	100
Solka Floc	.0559	.0639	.0700	.0751	.0796	.0888	.0946	.1188	.1348	.1476	.1584
Talc C	.0996	.0898	.0870	.0865	.0868	.0894	.0926	.1056	.1167	.1262	.1345
Silica	.0135	.0216	.0266	.0303	.0330	.0377	.0407	.0460	.0475	.0477	.0423
Latex	.4662	.3011	.2273	.1838	.1550	.1127	.0899	.0563	.0485	.0473	.0482
Kaolin (Al_2SO_4)	.0561	.0529	.0517	.0514	.0514	.0525	.0540	.0609	.0675	.0734	.0789
Calcium Carbonate (unflocc.)	.0402	.0393	.0375	.0361	.0352	.0343	.0345	.0399	.0473	.0550	.0625
Zinc Sulfide B	.0781	.0743	.0765	.0794	.0823	.0882	.0926	.1017	.1048	.1052	.1045
Darco B	.0283	.0288	.0285	.0283	.0282	.0287	.0292	.0352	.0413	.0472	.0528
Zinc Sulfide A	.0413	.0343	.0338	.0349	.0363	.0404	.0442	.0556	.0632	.0687	.0730
Tungsten	.0144	.0086	.0098	.0125	.0156	.0231	.0299	.0503	.0644	.0752	.0839
Ilmenite	.3080	.1162	.0555	.0306	.0201	.0163	.0227	.0529	.0697	.0767	.0775

TABLE XIV (CONT.)

POROSITY VARIATION - RESULTS OF NUMERICAL ANALYSIS OF GRACE DATA

$d\epsilon / dp_s$

Pressure (p.s.i.)	2	4	6	8	10	15	20	40	60	80	100
Solka Floc	.1214	.0693	.0506	.0407	.0345	.0258	.0205	.0129	.0097	.0080	.0069
Talc C	.2162	.0974	.0629	.0469	.0377	.0259	.0201	.0115	.0085	.0068	.0058
Silica	.0293	.0234	.0192	.0164	.0143	.0109	.0088	.0050	.0034	.0026	.0021
Latex	1.0121	.3267	.1643	.0996	.0673	.0327	.0195	.0061	.0035	.0026	.0021
Kaolin (Al_2SO_4)	.1218	.0574	.0374	.0279	.0223	.0152	.0117	.0066	.0049	.0040	.0034
Calcium Carbonate (unflocc.)	.0873	.0426	.0271	.0196	.0153	.0099	.0075	.0043	.0034	.0030	.0027
Zinc Sulfide B	.1695	.0806	.0553	.0430	.0357	.0256	.0201	.0010	.0076	.0057	.0045
Darco B	.0614	.0312	.0206	.0153	.0122	.0083	.0064	.0038	.0030	.0026	.0023
Zinc Sulfide A	.0896	.0372	.0244	.0189	.0158	.0117	.0096	.0060	.0046	.0037	.0032
Tungsten	.0312	.0093	.0071	.0068	.0068	.0067	.0065	.0055	.0047	.0041	.0036
Ilmenite	.4713	.1261	.0401	.0166	.0087	.0047	.0049	.0057	.0050	.0042	.0034

multiply by 0.1

TABLE XIV (CONT.)

POROSITY VARIATION - RESULTS OF NUMERICAL ANALYSIS OF GRACE DATA

$$\left[-\alpha\,(1-\epsilon)\,\frac{d\epsilon}{dps}\right]$$

Pressure (p.s.i.)	2	4	6	8	10	15	20	40	60	80	100
Solka Floc	1018	1260	1450	1575	1760		2280	3250	4110	4900	6000
Talc C	488	350	295	272	223	221	213	200	200	204	211
Silica	87	183	299	430	516	686	943	1520	1860	2380	2820
Latex	474	1530	1715	1540	1200		660	240	167	139	127
Kaolin (Al_2SO_4)	472	263	209	164	137	108	90	58	51	49	46
Calcium Carbonate (unflocc.)	190	114	80	60	50	39	28	19	18	17	17
Zinc Sulfide B	320	325	337	351	382	405	424	588	652	770	906
Darco B	374	263	213	177	156	126	117	108	117	131	149
Zinc Sulfide A	200	139	123	110	112	115	122	157	192	223	265
Tungsten	420	133	111	109	111	118	124	116	110	114	115
Ilmenite	1760	990	343	157	87	43	55	75	93	66	58

APPENDIX VII

POROSITY VARIATION CALCULATIONS

Compression-permeability cell data of Appendix I provide the basis for calculating porosity-distance curves for the following materials, results of which are given in Table XV:

Part A. Solka-Floc at 100 p.s.i.

Part B. Silica at 100 p.s.i.

Part C. Zinc Sulfide B at 100 p.s.i.

Part D. Calcium Carbonate (flocculated) at 100 p.s.i.

Part E. Calcium Carbonate (flocculated) at 350 p.s.i.

Part F. Kaolin (Al_2SO_4) at 100 p.s.i.

Part G. Polystyrene Latex at 100 p.s.i.

Part H. Talc C at 100 p.s.i.

Part I. Zinc Sulfide A at 100 p.s.i.

The computations yield values of x/L vs. p_s and the corresponding values of ϵ vs. x/L are plotted in Figures (42), (43), and (44), these results based on 100 p.s.i. pressure differential. Calculations for calcium carbonate at 350 p.s.i. are given in Part E. for comparison to the experimental curve of Grace for this material in Figure (40).[24]

Columns (2) and (3) contain point values of specific resistance and porosity corresponding to solids pressure in column (1). Zero pressure values are obtained by graphical extrapolation of experimental points at higher pressures as demonstrated for talc in Figure (28). Integration of the experimental data is accomplished conveniently by taking points from the smoothed extrapolated curves and numerically integrating by Simpson's rule as illustrated by Example 9. The proportionate cake thickness x/L corresponding to solids pressure of column (1) and point porosity in column (3) is calculated from the integrals by Equation (80b).

Calculations given in Appendices II, III, IV, and V for filtration of calcium carbonate, latex, kaolin, and talc C require average specific resistance and average porosity data. To provide data for these calculations one additional integration can be made with the data utilized for investigating porosity variation to obtain average specific resistance by Equation (22) and average porosity by Equation (82). The additional calculations are included for convenience in Parts D., F., G., and H. of Table XV.

TABLE XV

POROSITY VARIATION CALCULATIONS

Part A. Solka Floc

p_s lb.force/sq.in.	α ft./lb.mass (10^8)	ϵ	$\int_0^{p_s} \frac{dp_s}{\alpha(1-\epsilon)}$ $\frac{\text{(lb.mass)(lb.force)}}{\text{(ft.)(sq.in.)}}$ (10^{-8})	x/L
0	0.5	0.853	0	0
2	4.7	0.827	73.1	0.50
6	13.8	0.789	98.1	0.67
14	30.9	0.763	114.9	0.78
22	48.0	0.750	123.4	0.84
30	66.0	0.736	128.9	0.88
70	155	0.687	142.0	0.97
90	228	0.672	145.3	0.99
100	260	0.665	146.6	1.00

TABLE XV (CONT.)

POROSITY VARIATION CALCULATIONS

Part B. Silica

p_s lb.force/sq.in.	α ft./lb.mass (10^{12})	ϵ	$\int_0^{p_s} \frac{dp_s}{\alpha(1-\epsilon)}$ $\frac{(\text{lb.mass})(\text{lb.force})}{(\text{ft.})(\text{sq.in.})}(10^{-12})$	x/L
0	0.16	0.979	0	0.00
2	1.10	0.972	21.2	0.65
6	4.10	0.963	27.1	0.83
14	12.06	0.951	29.7	0.91
22	21.1	0.943	30.7	0.94
30	31.7	0.939	31.2	0.96
70	96.8	0.925	32.2	0.99
90	133	0.914	32.5	0.995
100	146	0.908	32.6	1.000

TABLE XV (CONT.)

POROSITY VARIATION CALCULATIONS

Part C. Zinc Sulfide B

p_s lb.force/sq.in.	α ft./lb.mass (10^{12})	ϵ	$\int_0^{p_s} \frac{dp_s}{\alpha(1-\epsilon)}$ $\frac{\text{(lb.mass)(lb.force)}}{\text{(ft.)(sq.in.)}}$ (10^{-12})	x/L
0	0.35	0.935	0	0
2	1.49	0.872	28.1	0.45
6	3.74	0.839	39.5	0.63
14	7.70	0.807	47.6	0.76
22	12.0	0.785	51.7	0.83
30	16.2	0.772	54.3	0.87
70	42.2	0.745	60.5	0.97
100	73.0	0.725	62.4	1.00

TABLE XV (CONT.)

POROSITY VARIATION CALCULATIONS

Part D. Calcium Carbonate (flocculated) at 100 P.S.I.

p_s lb.force/sq.in.	α ft./lb.mass (10^{11})	ϵ	$\int_0^{p_s} \frac{dp_s}{\alpha(1-\epsilon)}$	$\int_0^{p_s} \frac{dp_s}{\alpha}$	x/L	α_{av} ft./lb.mass (10^{11})	ϵ_{av}
			$\frac{(\text{lb.mass})(\text{lb.force})}{(\text{ft.})(\text{sq.in.})}$	(10^{-11})			
0	0.59	0.820	0	0	0	0.59	0.820
2	0.93	0.765	12.50	2.68	0.05	0.75	0.786
6	1.18	0.750	27.9	6.43	0.12	0.93	0.770
12	1.28	0.738	46.9	11.29	0.20	1.06	0.759
16	1.32	0.734	58.5	14.36	0.25	1.11	0.754
32	1.49	0.724	100.5	25.7	0.43	1.24	0.744
48	1.63	0.718	137.3	36.0	0.59	1.33	0.738
64	1.80	0.713	169.7	45.2	0.73	1.42	0.734
80	1.94	0.710	199.4	53.7	0.85	1.49	0.731
100	2.10	0.707	233.6	63.7	1.00	1.57	0.727

TABLE XV (CONT.)

POROSITY VARIATION CALCULATIONS

Part E. Calcium Carbonate (flocculated) at 350 P.S.I.

p_s lb.force/sq.in.	α ft./lb.mass (10^{11})	ϵ	$\int_0^{p_s} \frac{dp_s}{\alpha(1-\epsilon)}$ $\frac{\text{(lb.mass)(lb.force)}}{\text{(ft.)(sq.in.)}}$ (10^{-11})	x/L
0	0.59	0.820	0	0
2	0.93	0.765	12.50	0.04
6	1.18	0.750	27.9	0.08
12	1.28	0.738	46.9	0.14
16	1.32	0.734	58.5	0.18
32	1.49	0.724	100.5	0.31
48	1.63	0.718	137.3	0.42
64	1.80	0.713	169.7	0.52
80	1.94	0.710	199.4	0.61
150	2.49	0.690	291.0	0.88
350	3.99	0.649	329.0	1.00

TABLE XV (CONT.)

POROSITY VARIATION CALCULATIONS

Part F. Kaolin (Al_2SO_4)

p_s lb.force/sq.in.	α ft./lb.mass (10^{12})	ϵ	$\int_0^{p_s} \frac{dp_s}{\alpha(1-\epsilon)}$ $\frac{\text{(lb.mass)(lb.force)}}{\text{(ft.)(sq.in.)}}$	$\int_0^{p_s} \frac{dp_s}{\alpha}$ (10^{-12})	x/L	α_{av} ft./lb.mass (10^{12})	ϵ_{av}
0	0.75	0.620	0	0	0	0.75	0.620
4	1.02	0.550	10.8	4.44	0.10	0.90	0.587
8	1.27	0.538	18.3	7.89	0.17	1.01	0.570
16	1.51	0.520	30.7	13.7	0.29	1.17	0.554
24	1.65	0.507	41.0	18.8	0.39	1.28	0.542
32	1.80	0.500	49.7	23.7	0.47	1.35	0.532
40	1.98	0.495	57.7	27.5	0.55	1.45	0.523
80	2.56	0.480	92.8	45.2	0.88	1.77	0.513
100	2.82	0.470	105.5	52.6	1.00	1.90	0.504

TABLE XV (CONT.)

POROSITY VARIATION CALCULATIONS

Part G. Polystyrene Latex

P_s lb.force/sq.in.	α ft./lb.mass (10^{11})	ϵ	$\int_0^{p_s} \frac{dp_s}{\alpha(1-\epsilon)}$ $\frac{(\text{lb.mass})(\text{lb.force})}{(\text{ft.})(\text{sq.in.})}$	$\int_0^{p_s} \frac{dp_s}{\alpha}$ (10^{-11})	x/L	α_{av} ft./lb.mass (10^{11})	ϵ_{av}
0	0.14	0.950	0	0	0	0.14	0.950
1	0.28	0.900	76.5	4.96	0.75	0.20	0.935
4	11.0	0.615	99.2	8.17	0.975	0.49	0.918
10	38.0	0.528	99.8	8.19	0.98	1.22	0.917
20	54.0	0.495	100.0	8.23	0.985	2.44	0.917
100	110	0.450	101.7		1.000		

TABLE XV (CONT.)

POROSITY VARIATION CALCULATIONS

Part H. Talc C

p_s lb.force/sq.in.	α ft./lb.mass (10^{11})	ϵ	$\int_0^{p_s} \frac{dp_s}{\alpha(1-\epsilon)}$ $\frac{\text{(lb.mass)(lb.force)}}{\text{(ft.)(sq.in.)}}$	$\int_0^{p_s} \frac{dp_s}{\alpha}$ (10^{-11})	x/L	α_{av} ft./lb.mass (10^{11})	ϵ_{av}
0	0.32	0.945	0	0	0	0.32	0.945
2	1.29	0.825	24.62	2.58	0.12	0.77	0.895
6	2.18	0.785	36.51	4.89	0.23	1.23	0.866
10	2.80	0.765	43.61	6.50	0.31	1.54	0.851
14	3.39	0.740	48.86	7.79	0.37	1.80	0.841
18	3.75	0.738	53.20	8.90	0.43	2.02	0.833
50	6.75	0.70	75.2	15.1	0.72	3.31	0.799
100	10.7	0.66	93.4	20.9	1.00	4.79	0.777

TABLE XV (CONT.)

POROSITY VARIATION CALCULATIONS

Part I. Zinc Sulfide A

p_s Lb. Force/sq.in.	α Ft./lb. mass (10^{11})	ϵ	$\int_0^{p_s} \frac{dp_s}{\alpha(1-\epsilon)}$ $\frac{\text{(Lb. mass)(lb. force)}}{\text{(ft.)(sq.in.)}}$ (10^{-11})	x/L
0	1.60	0.916	0	0
2	2.18	0.888	10.9	0.17
6	3.56	0.867	22.5	0.35
14	6.50	0.856	34.1	0.54
22	9.20	0.848	41.0	0.65
30	12.0	0.842	45.9	0.72
70	28.6	0.827	58.8	0.92
100	43.5	0.810	63.5	1.00

APPENDIX VIII

NUMERICAL PROCEDURE FOR ROTARY DRUM FILTRATION CALCULATIONS

Solutions for the rate of filtration with continuous drum filters are obtainable by trial and error approximation when conditions of variable static head, variable cake pressure drop, and constant medium resistance are to be met. Stepwise solution along the drum contour is necessary to determine rates, time, and filtrate volume at intervals in order to approximate the magnitude of static head.

The procedure outlined is based on simultaneous solution of Equations (18a) and (87), finding values of q and Δp_c satisfying the expressions for fixed values of v. Approximate solutions are obtained as follows:

1. Select incremental increase in filtrate volume, Δv.
2. Find q which satisfies Equations (18a) and (87) for some $p_c = p_o + p_s - p_1$, obtaining p_s by approximation of time O by the expression

$$\theta = \int \frac{dv}{q} \tag{25}$$

Note: The trapezoidal rule is convenient for this purpose, where

$$\theta = \frac{\Delta v}{2} \left(\frac{1}{q_{previous}} + \frac{1}{q_{trial}} \right)$$

When sufficient number of terms are calculated, the time θ to the specific increments of filtrate volume can be calculated more exactly by numerical integration procedures such as Simpson's rule.

3. Repeat approximation by increasing v by an additional increment until accumulated time, $\Sigma\Delta\theta$, equals the time of submergence of a differential section of area in passing through the slurry in one cycle of rotation.

Illustration of the method is given for filtration of talc slurry in Appendix IX. Machine computations using the procedure outlined can be made by programing α_{av} and ϵ_{av} as functions of Δp_c by least squares equations obtained through fitting data to polynomial coefficients as outlined in Appendix X. Calculations are initiated by a first trial Δp_c inserted with data and convergence is insured by averaging successive values of q and Δp_c until the difference in consecutive terms is reduced to a value less than a desired minimum.

APPENDIX IX

CALCULATIONS FOR ROTARY DRUM FILTRATION OF TEN PER CENT TALC SLURRY AT 5 P.S.I. WITH EIGHT FOOT DIAMETER DRUM

Calculations are given for continuous filtration of ten weight per cent talc slurry in water with an eight foot diameter drum filter using cake property data published by Grace.[25] Solid and liquid properties used in the calculations are the same as given in Example 10. Figure (37) contains the plotted results of calculations obtained by three methods: (a) exact treatment for variable static head in curve A, (b) Ruth equation with variable static head in curve B, and (c) exact constant pressure calculation with integrated static head correction in curve C. In addition, the Ruth equation with average static head correction to pressure was solved for the conditions of filtration.

Final filtrate volume for the calculations are as follows:

Method	Filtrate Volume per Square Foot of Emerging Surface
Exact procedure, variable static head	0.0520 cubic feet
Exact procedure, average static head	0.0497
Ruth equation, variable static head	0.0449
Ruth equation, average static head	0.0491

The results of calculations using the four procedures show close agreement between values of filtrate volume computed with average static head correction to the pressure differential and variable static head for this example. The Ruth equation with variable static head and average static head correction both yielded less estimated filtrate volume per cycle than the exact equations by a maximum of only 14%.

In performing the calculations for filtrate volume vs. time of submergence, power series expressions were fitted to average specific resistance and average porosity data vs. cake pressure differential using the procedure of Appendix X. The power series equations derived are

$$\alpha_{av} = 0.310 + 0.314\,\Delta p_c - 0.044\,\Delta p_c^{\,2} + 0.00275\,\Delta p_c^{\,3}$$

$$\epsilon_{av} = 0.945 + 0.0340\,\Delta p_c + 0.00530\,\Delta p_c^{\,2} - 0.000302\,\Delta p_c^{\,3}$$

from data taken from Figure (20)

p_1	ϵ_{av}	α_{av}
0	0.945	0.32
2	0.895	0.77
4	0.876	1.03
6	0.866	1.23
8	0.858	1.40

The equations for variable static head with cake pressure drop variable were solved by trial and error using the procedure of Appendix VIII with the solutions shown in Table XVI, Part A. Simpson's rule was used to check values of θ calculated by accumulated trapezoidal rule approximations with good agreement being indicated.

Equations for constant pressure filtration with static pressure added as a constant correction term, Equation (29), were solved by the procedure of Example 10. and the results are given in Table XVI, Part B.

The Ruth equation for variable static head, Equation (88), was solved at four values of ϕ for comparison of the rate of filtrate production with that predicted using the exact expressions, the results plotted in Figure (38) shown in Table XVI, Part C.

TABLE XVI

CALCULATIONS FOR ROTARY DRUM FILTRATION OF TEN PER CENT TALC SLURRY AT 5 P.S.I. WITH EIGHT FOOT DIAMETER DRUM

Part A. Exact Equations with Variable Static Head

v	q	Δp_c	p_s	p_1	$\theta_{trap.}$	$\theta_{Simpson}$
cu.ft./sq.ft.	cu.ft./(sq.ft.)(sec.)	p. s. i.			seconds	
0.000	2.314 (10^{-3})	0.00	0.00	5.00	0.0	0.0
0.006	1.619	1.71	0.21	3.49	3.2	
0.012	1.219	2.84	0.47	2.62	7.5	
0.018	0.960	3.71	0.77	2.06	13.1	
0.024	0.810	4.34	1.09	1.75	19.9	19.9
0.030	0.700	4.81	1.32	1.51	27.9	
0.036	0.608	5.09	1.39	1.31	37.1	37.7
0.042	0.525	5.10	1.23	1.13	47.7	
0.048	0.426	4.79	0.70	0.92	60.5	60.5
0.052	0.361	4.22	0.00	0.78	72.0	

Part B. Exact Equations with Average Static Head

v	q	Δp_c	p_s	p_1	θ
cu.ft./sq.ft.	cu.ft./(sq.ft.)(sec.)	p. s. i.			seconds
0.000	2.530 (10^{-3})	0.00	0.45	5.45	0.0
0.003	1.868	1.43		4.03	1.3
0.009	1.404	2.43		3.03	5.0
0.017	0.940	3.43		2.03	12.3
0.026	0.708	3.93		1.53	22.5
0.041	0.476	4.43		1.03	50.5
0.057	0.360	4.68		0.78	88.4

Part C. Ruth Equation with Variable Static Head

θ	ϕ	v
seconds	radians	cu.ft./sq.ft.
20	0.698	0.0239
47	1.640	0.0397
72	2.510	0.0449

APPENDIX X

LEAST SQUARES CURVE FITTING USING ORTHOGONAL POLYNOMIALS

The mathematical theory and derivation of orthogonal polynomials are described in standard texts on numerical methods of calculus. Applications of curve fitting by means of orthogonal polynomials in this work were met in Example 11. of Chapter III and in numerical computation for rotary drum filtration in Chapter IV. The procedure used to fit an equation to m vs. θ data for numerical differentiation in Example 11. will be demonstrated.

The procedure used is as follows:

1. Selection of number of data point to be fitted and degree of equation: a third degree equation was used to fit a least squares polynomial series of four terms to five data points. To use orthogonal polynomials conveniently by hand calculation the points are evenly spaced in the dependent variable and total to an odd number. From Figure (33) dm/dθ is seen to become effectively constant after θ = 0.1 minutes after which the derivative is essentially zero. Because of the rapid rate of change of m vs. θ in the initial part of the curve it will be more accurate to divide the curve into two portions. Five values will be taken between zero and 0.04 minutes spaced 0.01 minutes apart and five values between 0.04 and 0.12 minutes in 0.02 minute increments.

t	θ	m	θ	m
-2	0.00	7.42	0.04	3.24
-1	0.01	4.40	0.06	3.13
0	0.02	3.61	0.08	3.02
1	0.03	3.36	0.10	3.01
2	0.04	3.24	0.12	3.00

The terms t designate the finite points to which the polynomials are fitted, the expressions for t in terms of θ being

1st set of points $t = 100\,\theta - 2$

2nd set of points $t = 50\,\theta - 4$

The third degree polynomial least squares equation fitted to the data points has the form

$$m = f(t) = a_o p_o(t) + a_1 p_1(t) + a_2 p_2(t) + a_3 p_3(t)$$

and the polynomials p_n are given by

$p_o(t) = 1$ $\quad p_1(t) = t/2$ $\quad p_2(t) = 1/2(t^2 - 2)$

$p_3(t) = 1/6(5t^3 - 17t)$

2. The coefficients a_n are calculated from the table derived from the mathematical form for the polynomial expression

t	p_o	p_1	p_2	p_3
-2	1	-1	1	-1
-1	1	-0.5	-0.5	2
0	1	0	-1	0
1	1	0.5	-0.5	-2
2	1	1	1	1
γ	5	2.5	3.5	10

where $a_n = \dfrac{\Sigma f(t)^t p_n{}^t}{\gamma}$ from data values of f(t) yielding for the first set of points the expression

$$m = 4.41 - 1.88\,p_1(t) + 0.91\,p_2(t) - 0.21\,p_3(t)$$

3. The above expression for m in terms of t can be converted to m in terms of θ by substituting the expression $t = 100\,\theta - 2$ in the polynomial terms. Since the differential is required the computations are simplified if the polynomial expression is differentiated before substitution, differentiating $m = f(t)$ in the form $dm/d\theta = (dm/dt)(dt/d\theta)$

resulting in the expression

$$\frac{dm}{d\theta} = \frac{a_1}{2} + a_2t + \frac{a_3}{6}(15t^2 - 17)\ 100 = \frac{-1.88}{2} + 0.91\ (100\theta - 2)$$

$$- \frac{0.21}{6}\ (150000\ \theta^2 - 6000\ \theta + 43)\ 100 = -427 + 30100\ \theta - 525000\ \theta^2$$

using $dt/d\theta = 100$.

Evaluation of the differential expression results in

θ	$dm/d\theta$	m (calculated)
0.00	-427	7.41
0.01	-178	4.48
0.02	- 35	3.50
0.03	- 3	3.44
0.04	- 62	3.23
minutes	1/minutes	

The values of the differential are divided by 60 to obtain consistent units of time in seconds for the computations illustrated in Example 11.

4. By similar treatment an equation is fitted to the second set of data points resulting in (the third degree term becoming negligible)

$$\frac{dm}{d\theta} = \frac{d}{dt}\ 3.08 - 0.12\ p_1(t) + 0.04\ p_2(t)\ \frac{d}{d\theta}\ (50\ \theta - 4) = -11 + 1000\ \theta$$

θ	$dm/d\theta$
0.04	-7
0.06	-5
0.08	-3
0.10	-1
0.12	0

The error in fitting an equation to a set of points is magnified when the differential of the expression is taken as may be seen above in the table of results for the first set of points. While the points are well approximated by the least squares expression, the differential terms are observed not to decrease regularly as would be indicated by the curve in Figure (33). More accurate differentials can be obtained for a given point in such a curve by differentiating a polynomial expression fitted to a curve in which the point being examined is intermediate.